Detailed Case Studies

11 Detailed Case Studies

Tareq Abuimara, Attila Kopányi, Jean Rouleau, Ye Kang, Andrew Sonta, Ghadeer Derbas, Quan Jin, William O'Brien, Burak Gunay, Juan Sebastián Carrizo, Viktor Bukovszki, András Reith, Louis Gosselin, Jenny Zhou, Thomas Dougherty, Rishee Jain, Karsten Voss, Tugcin Kirant Mitic and Holger Wallbaum

Summary

In this chapter, we will unite the theory and the practice of occupant-centric design through an analysis of seven unique case study buildings. The case studies are diverse in several ways, including geographic location, type, size, and project phase. We will offer our key insights drawn from qualitative and quantitative analysis in order to support researchers and industry practitioners alike.

11.1 Introduction

In this chapter, we demonstrate the real-world application of the occupant-centric design methods and principles developed and presented in the previous chapters of this book. We provide an analysis of seven unique case study buildings that demonstrate how occupant-centric design can assist in developing better designs that suit occupants' needs and preferences while meeting clients' needs and energy targets. The selected case studies demonstrate alternative methods and approaches for considering occupant behavior and occupant-related assumptions throughout the building design process. These real-world examples illustrate the strengths and shortcomings of current occupant modeling approaches and assumptions in the design process. The case studies also provide examples of various qualitative and quantitative research approaches to evaluate both technical and nontechnical aspects of occupant modeling and representation. Our analysis involves simulation, field studies, surveys, and interviews with design stakeholders and occupants.

We selected the case studies in this chapter based on the following criteria: (1) authors' access to information about the cases, (2) breadth of design/construction phases represented among the cases, and (3) usability of analysis outcomes for advancing occupant modeling approaches during building design. The case studies are diverse in terms of project phase,

DOI: 10.1201/9781003176985-11

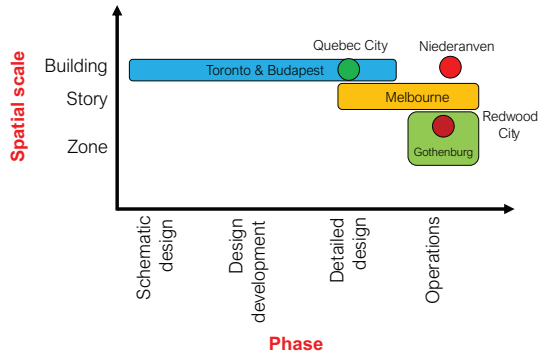

Figure 11.1 A conceptual diagram illustrating the range of the case studies with regards to project phase and spatial scale.

Figure 11.2 Geographical distribution of the case studies.

location/climate zone, building type and size, and analysis approach. Collectively, our analysis of the selected case studies covers approximately the whole life cycle of a building, including design, construction, and operation (see Figures 11.1 and 11.2).

In the Toronto and Budapest case studies (Case Studies 1 and 2), we demonstrate alternative methods of representing occupants during design (see also Chapter 3). In the Quebec City, Melbourne, Redwood City, Niederanven, and Gothenburg case studies (Case Studies 3–7), we focus on post-occupancy conditions, aiming to evaluate design approaches and provide recommendations for occupant-centric design and operation. The seven case studies are summarized in Table 11.1.

Table 11.1 Summary of the seven case studies

Case study	*Location (Köppen climate classification)*	*Building size and type*	*Project phase*	*Case study objectives*
Case Study 1: Toronto	Toronto, Canada (Dfa, humid continental)	Mid-rise office building	Design	• Document occupant modeling approaches during design • Develop a method for handling occupant-related uncertainty during design
Case Study 2: E-co-housing	Budapest, Hungary (Dfb, warm summer continental)	Mid-rise multi-unit residential building	Design & construction	• Explore and leverage synergies between people and the built environment in all dimensions of sustainability • Bridge qualitative participatory co-design methods and simulation for higher fidelity energy models
Case Study 3: Cité Verte	Quebec City, Canada (Dfb, warm summer continental)	Mid-rise multi-unit residential building	Post-occupancy	• Evaluate the feasibility of low-energy buildings • Assess the impact of occupants on achieving low-energy goals
Case Study 4: Gillies Hall	Melbourne, Australia (Cfb, temperate oceanic)	Six-story student residence	Post-occupancy	• Assess occupants' comfort and well-being as well as energy saving potentials from passive house strategies when coupled with performance-based modeling • Assess the benefits of deploying low-cost sensing techniques in passive house design

Table 11.1 Continued

Case study	*Location (Köppen climate classification)*	*Building size and type*	*Project phase*	*Case study objectives*
Case Study 5: Stanford Redwood City	Redwood City, USA (Csb, dry-summer subtropical/ Mediterranean)	Mid-rise office building	Post-occupancy	• Optimize building layouts to maximize occupants' productivity and collaboration while achieving energy efficiency
Case Study 6: Goblet Lavandier & Associésa headquarter	Niederanven, Luxembourg (Cfb, temperate oceanic climate)	Mid-rise office building	Post-occupancy	• Derive occupant-centric rules for optimal exterior shading design
Case Study 7: Samhällsbyggnad 1	Gothenburg, Sweden (Cfb, marine west coast)	Institutional office building	Post-occupancy	• Enhance indoor environmental quality (IEQ) and energy savings potential based on an evaluation of occupants' satisfaction in energy efficient buildings

11.2 Case Study 1: Toronto, Canada

Tareq Abuimara, William O'Brien, Burak Gunay, Juan Sebastián Carrizo

11.2.1 Summary

This case study is a mid-rise office building located in Toronto, Canada. The analysis of this case study includes implementing alternative methods for occupant considerations during building design (as detailed in Chapter 3). The occupant-centric analysis of this case study building covers the entire design phase of the building and aims to document the current practices of occupant modeling throughout the simulation-aided building design process and investigate possible improved approaches. The analysis included documenting occupant-related design assumptions and the implications of these assumptions on design outcomes.

The analysis was performed using qualitative (workshop and interviews) and quantitative (simulation-based investigation) approaches. The qualitative analysis included documenting occupant modeling approaches and assumptions through the analysis of design documents and interviewing

design stakeholders of the case study. The quantitative analysis was a simulation-based investigation to assess occupant assumptions and propose alternative approaches for modeling occupants and quantifying their impact on design decisions. The simulation-based investigation included occupant-centric parametric analysis, design optimization, and comfort analysis.

The findings of the qualitative analysis indicated the absence of a standardized and consistent occupant assumptions sharing mechanisms among design stakeholders. Further, these findings indicated that the adoption of an integrated design process (IDP) could have assisted in avoiding discrepancies among design disciplines.

The findings of the quantitative simulation-based investigation indicated that occupant assumptions are influential in terms of selecting optimal energy conservation measures (ECMs) and determining optimal design solutions. Additionally, the occupant-centric comfort analysis indicated the need to consider comfort at the occupant and building zone level rather than at the building level.

Overall, the findings of this case study analysis can contribute to occupant-centric building design by providing insights to building designers on how to handle occupant-related uncertainty throughout the simulation-aided building design process. Additionally, the findings can inform relevant building codes and standards on advancing requirements to improve the quality of assumptions and efficiently manage occupant-related uncertainty.

11.2.2 Building Description

The Toronto building is a mid-rise commercial building located in Liberty Village to the west of downtown Toronto, Canada. The building consists of four similar office floors, a retail ground floor, and two levels of underground parking. The building has a gross floor area of 7,940 m^2 (including the underground parking). The building is in ASHRAE climate zone 6A (cold-humid) with overcast cold winters and hot-humid summers.

The above grade floors were constructed using mass timber and nail laminated timber (NLT) panels, and the main design objective was to create a building that is sustainable, aesthetically pleasing, and cost-effective by returning to the use of heavy timber. Figure 11.3 shows the building shortly after construction and Table 11.2 summarizes key performance specifications.

11.2.3 Methodology

In this study, both qualitative and quantitative data collection and analysis approaches were used as described in the sections below.

Figure 11.3 Toronto case study building.

Table 11.2 Toronto case study description

1.1.1. *Item*	*Description*
Typical office floor area	1,728 m^2
HVAC	Rooftop package unit with zone level variable air volume (VAV) reheat Hydronic baseboard heating
Cooling coefficient of performance (COP)	3.5
Boiler (space heating)	Type: Condensing boiler Fuel: Natural gas Nominal thermal efficiency = 0.9
Heat recovery	Air-to-air heat exchanger Sensible effectiveness at 100% heating /cooling airflow = 70% Sensible effectiveness at 75% heating/cooling airflow = 85%
Outdoor air minimum flow rate	0.000435 $m^3/s.m^2$
Windows	U-factor = 1.9 $W/m^2 \cdot K$; SHGC = 0.33 WWR (overall) = 46.5% WWR (south) = 85% WWR (north) = 12% WWR (east) = 41% WWR (west) = 41%
Walls	U-value = 0.245 $W/m^2 \cdot K$

11.2.3.1 Qualitative Analysis

The qualitative analysis sought to document occupant assumptions and occupant modeling approaches throughout the case study building's design process. In brief, the process included semi-structured interviews about current practices with four key design stakeholders: the owner representative,

the architect, the mechanical engineer, and the energy modeler. First, written questionnaires were sent to each stakeholder, with each questionnaire customized to the stakeholder's scope of work and design objectives. Then, questionnaire responses were analyzed qualitatively, and the findings were used as the basis for a set of interview questions. Next, interviews were conducted to obtain depth and clarification. Finally, all the questionnaire and interview responses were analyzed qualitatively, and conclusions were drawn.

11.2.3.2 Quantitative Analysis

The quantitative analysis took the form of a simulation-based investigation that included a parametric analysis, optimization study, and comfort study. For this purpose, an energy model for a typical office floor of the case study building was created using EnergyPlus (see Figure 11.4). Custom scripts in MATLAB were used to automate simulations. Each step of analysis is described below.

11.2.3.2.1 OCCUPANT-CENTRIC PARAMETRIC ANALYSIS

The first step of the simulation-based investigation was to use a parametric analysis to evaluate the impact of occupant assumptions on the ranking

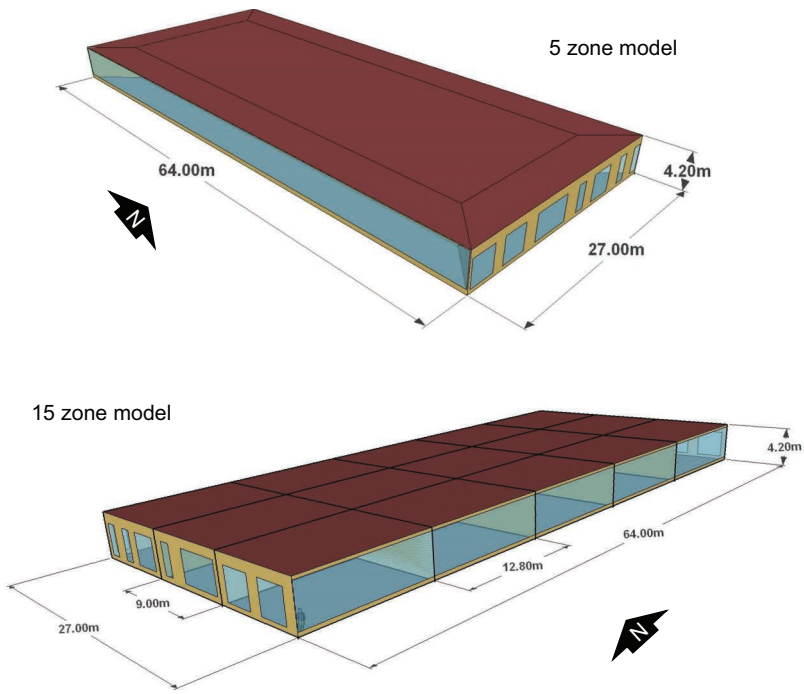

Figure 11.4 The EnergyPlus model used for simulation-based investigation.

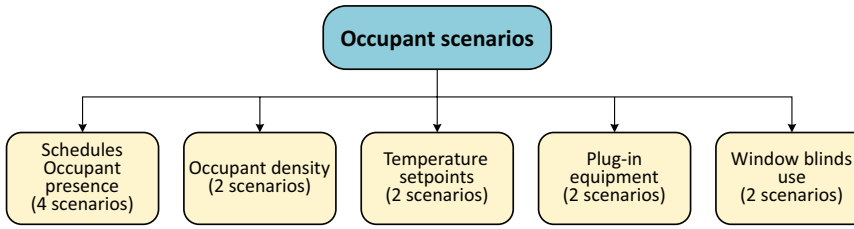

Figure 11.5 Occupant scenarios used in parametric analysis.

Table 11.3 List of design parameters/energy conservation measures used in the parametric analysis

Systems-related parameters	**Envelope-related parameters**
Cooling COP	Window-to-wall ratio (WWR)
Water boiler efficiency	Window properties (U-factor & SHGC)
Lighting power density (LPD)	Wall insulation
Plug-in equipment loads	Roof insulation
Water pumps efficiency	Air infiltration
ERV efficiency	

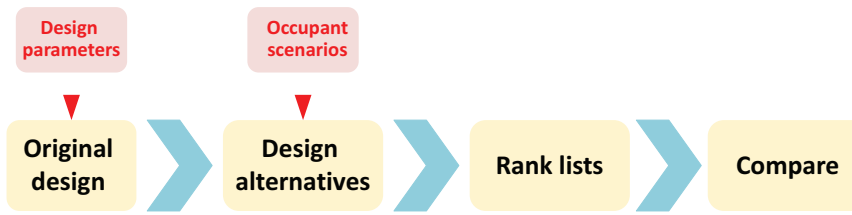

Figure 11.6 The parametric analysis workflow.

and the saving potential of energy conservation measures (ECMs)/design parameters (DPs). The case study model was simulated using a parametric analysis and EnergyPlus under 12 occupant scenarios (see Figure 11.5).

In the parametric analysis, 12 ECMs and DPs were considered, as shown in Table 11.3. Multiple values for each ECM/DP were used. The simulation workflow is shown in Figure 11.6.

11.2.3.2.2 OCCUPANT-CENTRIC DESIGN OPTIMIZATION

The second phase of the simulation-based investigation was an optimization study. The objective of the study was to evaluate the impact of occupant

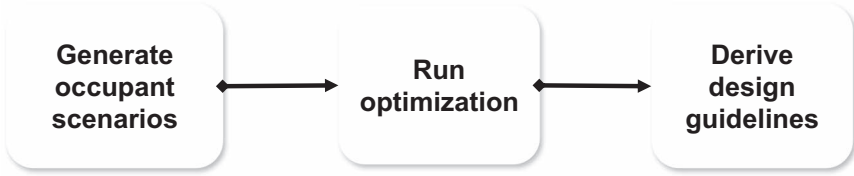

Figure 11.7 The three-step approach followed in the optimization study.

assumptions on the outcomes of building design optimization. The optimization study was performed following the three-step approach, as shown in Figure 11.7.

Step 1 was generating occupant scenarios by using multiple occupant presence scenarios and varying the relationship between occupant presence schedules and lighting and equipment schedules. Four different occupant presence schedules were used: default (as per ASHRAE Standard 90.1), low occupancy (40% occupancy at the highest), morning peak (90% morning and 40% in afternoons), and afternoon peak (40% morning and 90% in afternoons). For each occupancy schedule, four altered lighting and equipment schedules were generated. A total of 64 occupant scenarios were created (4 occupancy × 4 lighting × 4 equipment).

Step 2 was to run the optimization using the genetic algorithm (GA) in MATLAB. The objective function was set to minimize the HVAC energy use intensity (kWh/m^2). A penalty was applied to the objective function for design solutions that have unsatisfactory comfort conditions (i.e., more than 300 unmet hours). Ten different ECMs/DPs were considered in the optimization including WWR, window material, and exterior shading (overhangs and sidefins).

Finally, Step 3 was training decision trees using MATLAB "*fitctree*" function. Decision trees are a useful method to visualize the optimization outcomes and derive occupant-centric design parameters selection rules.

11.2.3.2.3 OCCUPANT COMFORT ANALYSIS

The comfort analysis was focused on investigating the impact of occupants' spatial distributions on comfort and energy performance of the building. To this end, the following steps were followed:

1 The building typical floor model zoning was adjusted to have 15 thermal zones instead of five (see Figure 11.8). The intention was to have a more realistic zoning strategy that included a variety of zone orientations

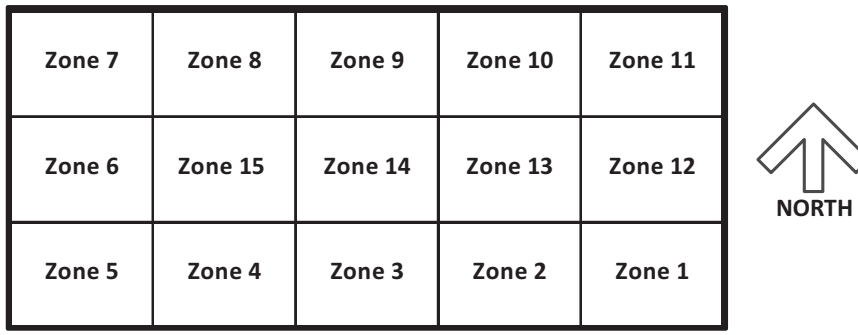

Figure 11.8 Case study model plan demonstrating thermal zones and their orientations.

(south-facing, north-facing, east-facing, west-facing, core, and corner offices). Further, the model HVAC equipment and flow rates (air and water) were hard-sized based on a sizing run using default ASHRAE Standard 90.1 values for occupant density and schedules. The equipment hard-sizing was done to mimic reality, as real buildings' equipment has preset maximum capacities.

2 Seventy-five occupant distribution scenarios (ODSs) were created for the use in simulations. An ODS refers to the distribution of building occupants across building zones. The same total number of occupants was maintained in all the ODSs. The ODSs were generated by sampling from uniformly distributed large population using a custom script in the programming language R.

3 The hard-sized model was simulated in EnergyPlus under the 75 ODSs. A MATLAB custom script was used to automate the process.

4 The simulation was repeated with the demand-controlled ventilation (DCV) to evaluate the impact of using building adaptive technologies (e.g., DCV) on comfort and energy performance.

Several performance metrics were evaluated in this analysis. For energy use, energy use intensity (EUI) was used, as it is a commonly used metric in the architecture, engineering, and construction (AEC) industry. For comfort, unmet hours, as defined by ASHRAE Standard 90.1, were used. However, a limitation of unmet hours is that it does not consider the number of occupants who suffer from discomfort. Thus, a new comfort metric was developed for this study. The new thermal comfort metric is called occupant discomfort hours (ODH). ODH indicates the annual share of each occupant at a given zone of discomfort hours. Further details about this metric and how it is calculated are available in Abuimara *et al.* (2021).

11.2.4 Results and Discussion

11.2.4.1 Design Process Documentation

The design process documentation was classified and summarized under four main groups of findings: (a) type and source of occupant assumptions during design, (b) design workflow, (c) communicating occupant-related assumptions, and (d) challenges and limitations throughout the design process. Each group of findings is described in turn below.

11.2.4.1.1 TYPE AND SOURCE OF OCCUPANT ASSUMPTIONS DURING DESIGN

The Toronto building was designed without a specific target tenant; instead, the client had a general vision of the total number of occupants the building would host. Due to the lack of specific information about occupants, the architect sourced occupant assumptions from Ontario Building Code (OBC). The OBC occupant density of 20 m^2/person was used by the architect's in-house energy modeling using Sefaira software. The mechanical engineer used conservative occupant assumptions for designing and sizing the mechanical equipment. It is common practice among HVAC designers to size HVAC equipment to supply the highest expected heating and cooling loads (Djunaedy *et al*., 2011).

The energy modeler was somewhat involved early in the design process in a design charrette. At this early phase, the energy modeler used the ASHRAE Standard 90.1 values for occupant density, lighting power density (LPD), and equipment power density (EPD) for creating an energy model of the building. Once the design development phase started and the energy modeler was reengaged, several of the original assumptions had to be refined to align with the current design (e.g., the LPD was adjusted based on the selected lighting fixtures, from 8 to 3.9 W/m^2).

Overall, the design team's occupant assumptions were sourced from codes and standards, including, for example, OBC, NECB, and ASHRAE Standard 90.1. Additionally, some assumptions (e.g., the mechanical engineer's) were based on experience.

Sourcing occupant assumptions from codes and standards or from experience can limit or narrow occupant representation during building design. In particular, occupant assumptions in codes and standards (densities and schedules) tend to be conservative and outdated, as many were developed in 1980s and based on a small set of data (Abushakra *et al*., 2004).

11.2.4.1.2 DESIGN WORKFLOW

Initially, this building's design process was intended to be an integrated design process, as all design stakeholders participated in a design charrette early in the design process. However, as the design progressed, the process became characterized by a traditional design process, where different

design stakeholders performed their tasks independently at different times throughout the process. For example, although the energy modeler was involved in the early design charrette, they were not involved again until late in the design development phase when most of the critical design decisions (e.g., type of HVAC system) had already been made. This intermittent or delayed involvement of energy modelers is typically driven by the client's unwillingness and/or misunderstanding of the role of energy modeling during the design process (Oliveira and Marco, 2018).

Additionally, the energy modeling scope was not integrated into other scopes, such as the mechanical engineering scope (e.g., HVAC selection and sizing). The HVAC system type was selected and designed by the mechanical engineer using their conservative occupant assumptions, and then the equipment sizing was handed to the energy modeler who performed energy modeling using their own occupant assumptions. This inconsistency of occupant assumptions may have led to suboptimal design decisions and/or missed design opportunities.

11.2.4.1.3 COMMUNICATING OCCUPANT-RELATED ASSUMPTIONS

The Toronto building's design team members reported that they communicated through regular phone calls, emails, and bi-weekly meetings. Drawings, reports, and computer models were shared. No specific information-sharing platform or mechanism was reported.

Although the design team members reported that they communicated regularly, a deeper investigation of the design documents and models (along with information obtained during the interviews) revealed discrepancies in some of the basic occupant assumptions made and used by different design stakeholders, as shown in Figure 11.9.

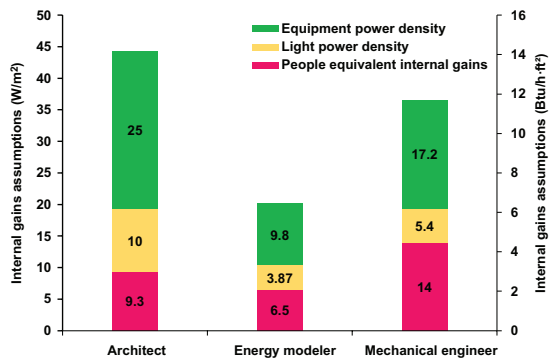

Figure 11.9 Assumptions made by the different design team members of the Toronto case study building.

The lack of information-sharing mechanisms may have led to these discrepancies in assumptions and constitutes a fundamental issue in the design process. Effective communication throughout the design process is widely recognized as fundamental for successful building design (Arditi and Gunaydin, 2002).

11.2.4.1.4 CHALLENGES AND LIMITATIONS THROUGHOUT THE DESIGN PROCESS

One of the major challenges that the Toronto building designers faced was time, including the time each team member was involved in the design process and the time assigned to complete the design task. The former is typically out of a design team's control, as it is determined by the project owner. The latter is a common practice in the AEC industry, where a specific timeline is assigned to design tasks. For example, in the case of the Toronto building, the modeler was hired to perform the main modeling scope late in the process when they had limited impact on design outcomes because all critical design decisions had already been made and approved by the owner.

Another major challenge the Toronto building design team faced was the cost limitation of the project (capital cost and added engineering costs). For example, when asked why adaptive ventilation technologies were not considered, the mechanical engineer reported that cost was the main driver for selecting HVAC and any additional technologies were not considered by the owner.

11.2.4.2 Occupant-Centric Parametric Analysis Results

The first phase of the quantitative analysis was an occupant-centric parametric analysis. Figure 11.10 presents the results of the parametric analysis under different occupant scenarios. Overall, the results presented in Figure 11.10 indicated that occupant scenarios affect the energy-saving potential of ECMs/DPs. Some ECMs/DPs such as implementing DCV were sensitive to occupant scenarios and demonstrated drastic changes in energy savings potential (1%–12%). However, ECMs/DPs such as increasing wall and roof thermal resistance (i.e., R-value) demonstrated robustness to changing occupant scenarios, as the energy saving potential was only moderately affected (6%–8%). The energy-savings potential of adjusting the WWR also demonstrated moderate sensitivity to changing occupant scenarios (2%–6%).

The results shown in Figure 11.10 also demonstrated the insensitivity of some ECMs/DPs, such as cooling COP, to occupant presence. According to the results, the ECMs/DPs saving potential was highly sensitive to assumptions about temperature setpoints. Further, the results indicated the impact of plug-in equipment assumptions on the energy-saving potential of different ECMs/DPs. These variable sensitivities of ECMs/DPs to occupant scenarios point to the importance of occupant assumptions during building design. In other words, variable sensitivities to occupant scenarios affect design decisions of selecting ECMs/DPs.

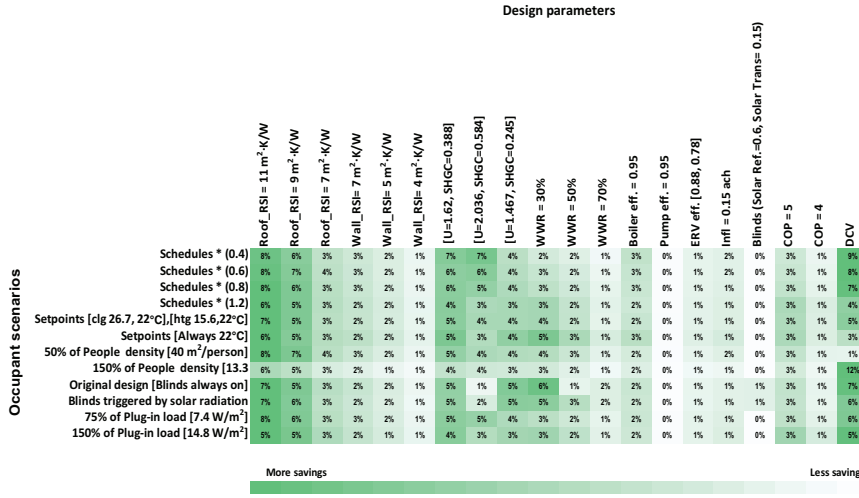

Figure 11.10 Design parameters' ranking and energy use savings under multiple occupant scenarios.

Overall, the parametric analysis results highlight the impact that occupant assumptions have on the savings and ranking of ECMs/DPs. Likewise, the results emphasize the importance of accurately considering occupant assumptions during the building design process and support the use of more occupant-centric parametric analysis when selecting ECMs/DPs.

11.2.4.3 Occupant-Centric Design Optimization Results

The second step of the quantitative analysis was occupant-centric design optimization. The design optimization was performed under 64 occupant scenarios. Figure 11.11 presents the results of the 64 optimization runs where GA was used to search for optimal design solutions. Overall, Figure 11.11 demonstrates that occupant scenarios had a substantial impact on the outcomes of the 64 optimization runs. The results also indicated that even with the same occupancy scenario, varying lighting and plug-in equipment schedules can impact the HVAC energy use intensity significantly and lead to different optimal design solutions. The box plots in Figure 11.11 show that the median of the cost function fluctuated drastically with different occupant scenarios. Figure 11.11 also indicates that there were several outlier solutions outside the interquartile but no outliers on the lower side of the population, which means that there were many poor design solutions but few optimal and semi-optimal solutions. This result offers the insight to building designers that considering families of optimal and near-optimal solutions offers flexibility in choosing ECMs/DPs that better suit each project constraint (e.g., budget, time).

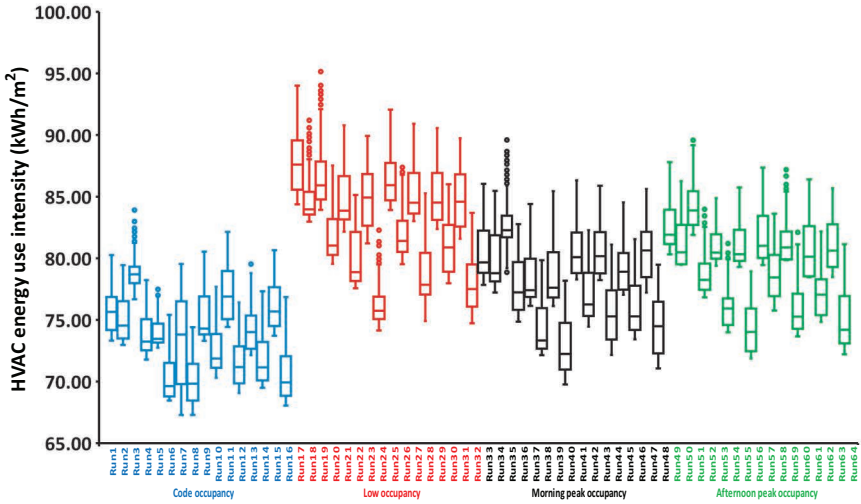

Figure 11.11 Optimization results for the 64 different occupant scenarios.

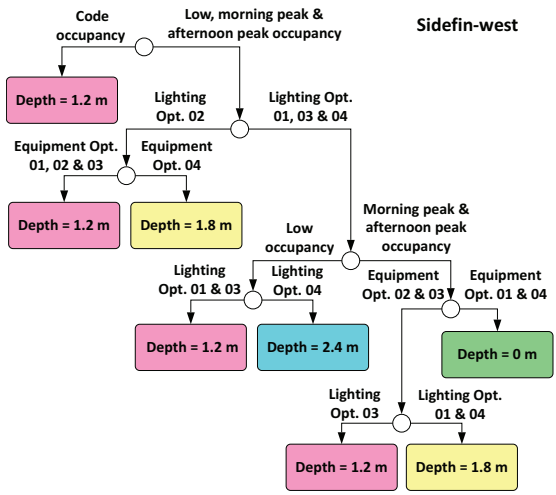

Figure 11.12 Example classification tree demonstrating sensitivity to occupant assumptions.

Decision trees were used to better understand and visualize the final results of the optimization. Figures 11.12 and 11.13 are examples of the decision trees that were trained using the 64 optimization runs results. Figure 11.12 represents a case were the DP (i.e., size of window sidefin shading on west-facing windows) was highly sensitive to occupant assumptions.

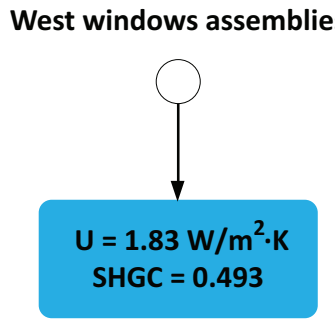

Figure 11.13 Example classification tree demonstrating robust design parameter to occupant assumptions.

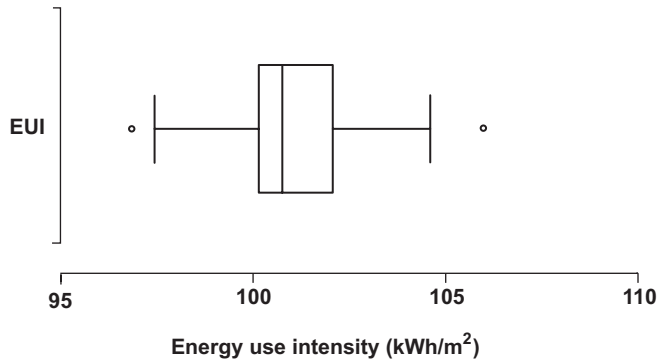

Figure 11.14 EUI of the 75 simulations.

Figure 11.13 demonstrates an example of a DP (i.e., window U-factor and SHGC) that is robust to occupant scenarios. Decision trees are very useful in occupant-centric design optimization, as they can assist designers in classifying and grouping ECMs/DPs based on their sensitivity to occupant scenarios.

11.2.4.4 Occupant-Centric Comfort Analysis Results

The third phase of the quantitative analysis was evaluating the impact of occupants' distributions scenarios (ODS) on comfort and energy performance. The case study building was simulated under 75 ODSs.

Overall, the results indicated that occupants' spatial distributions had a high impact on comfort and a moderate impact on energy use. Figure 11.14 demonstrates the range of EUI reported from the 75 simulations. It is evident

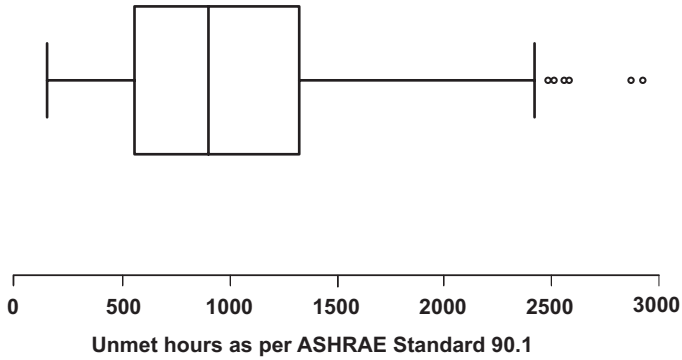

Figure 11.15 Unmet hours as per ASHRAE Standard 90.1 under multiple occupant distribution scenarios.

that ODSs were modestly influential on energy use, as EUI experienced changes in the range of 5–10 kWh/m^2/yr. The hard-sized HVAC equipment and flow rates likely contributed to limiting the changes in EUI.

On another front, Figure 11.15 presents the range of the unmet hours as per ASHRAE Standard 90.1 for the 75 simulation runs. The ODSs had a substantial impact on the number of unmet hours (i.e., thermal comfort). The unmet hours ranged from 150 unmet hours with the standard code ODS (i.e., homogeneous occupants' distribution across building zones) to about 3,000 unmet hours with some extreme ODSs where some zones were overpopulated.

To evaluate comfort at zone and occupant level, overheating and overcooling ODH were reported. Figure 11.16 presents the overheating ODH. It is clear from Figure 11.16 that different zones had different values of ODH. Further, the zones that were south- and west-facing and core zones (zones 1–5 and zones 13–15; see Figure 11.16) experienced a wider range of ODH. South-facing zones had a higher WWR (85%) and were subject to longer periods of direct solar gains compared to the east- and north-facing zones. The high WWR made south-facing zones more likely to experience overheating, especially with the increased internal gains from occupants. Core zones are also generally known to experience overheating, as they have minimal heat exchange with surrounding zones and the effect of infiltration is negligible. In the Toronto building, the wide range of ODH in south-facing, west-facing, and core zones indicates sensitivity to occupant distributions, where the higher the occupant density, the more discomfort levels will be in a given zone.

Figure 11.17 demonstrates the reported overcooling hours for the different building zones. Generally, overcooling ODH was not reported to be substantially sensitive to ODSs, as the highest overcooling ODH was observed

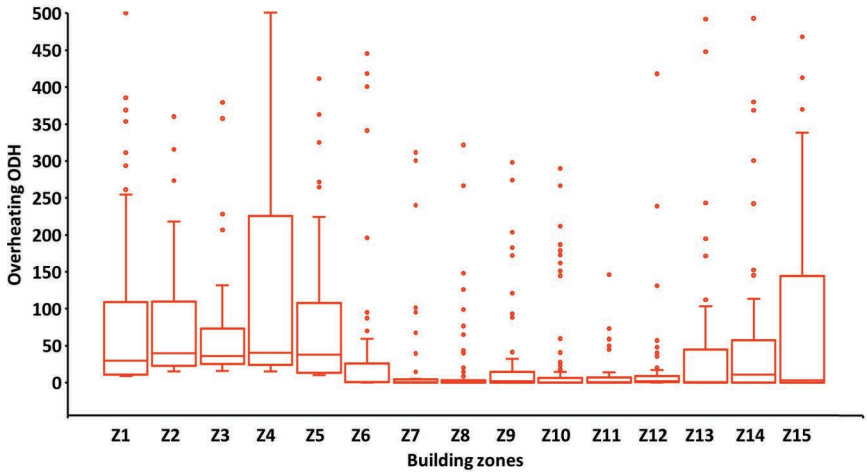

Figure 11.16 Overheating occupant discomfort hours (ODH) (Zones 13–15 are core zones).

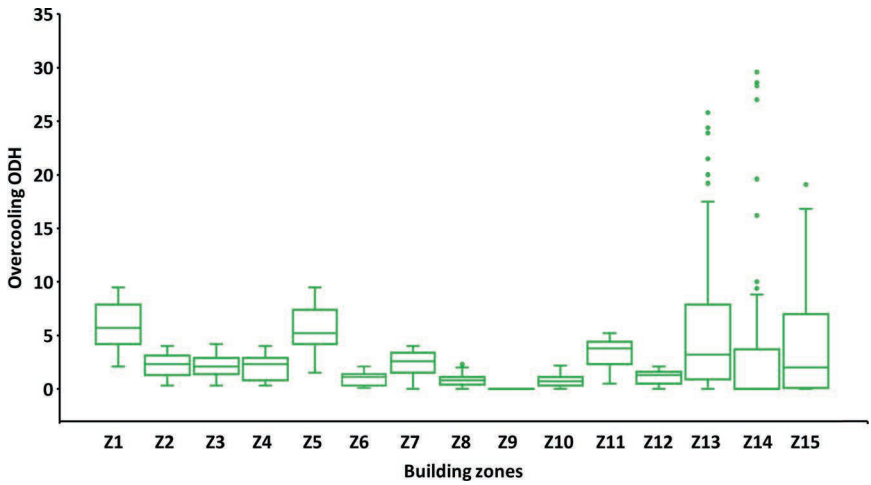

Figure 11.17 Overcooling occupant discomfort hours (ODH) (Zones 13–15 are core zones).

in core zones 13, 14, and 15. Upon further investigation, these core zones were found to be under-occupied (only one or two occupants) and surrounded by zones that were also under-occupied.

The simulations under the 75 ODSs were repeated with DCV enabled; then, the results were compared to the previous run results. Figure 11.18 presents the EUI results for both simulations under the 75 ODSs with and

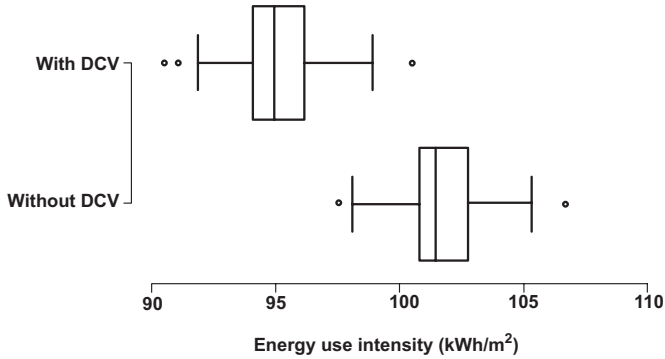

Figure 11.18 EUI with and without demand-controlled ventilation (DCV) under the 75 ODSs.

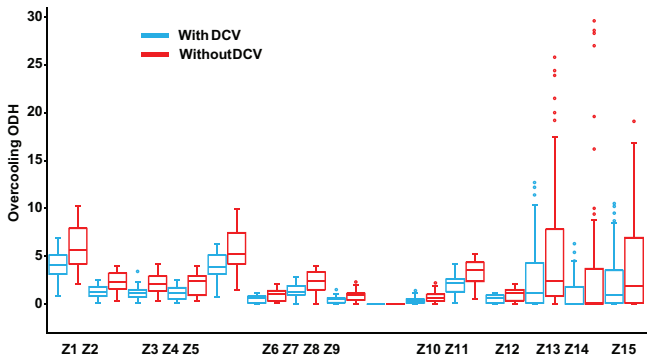

Figure 11.19 Overcooling ODH with and without DCV (Zones 13–15 are core zones).

without DCV. Incorporating DCV was beneficial in terms of saving energy; however, it demonstrated a similar range of sensitivity to ODSs.

Figure 11.19 demonstrates a comparison between the overcooling ODH with and without DCV. The results indicated that deploying DCV was beneficial in reducing overcooling ODH by about 50%. Using DCV also reduced the unnecessary ventilation of under/unoccupied zones.

11.2.5 Concluding Remarks

To summarize, this occupant-centric documentation and analysis of the Toronto case study building design process included: (1) interviews with four design stakeholders (owner, architect, mechanical engineer, and energy modeler) and (2) a simulation-based investigation, including an occupant-centric

parametric analysis, an occupant-centric optimization, and a comfort study that analyzed the impact of occupants' spatial distributions across the building on comfort and energy performance.

The findings of the building design process documentation (via interviews) indicated that occupant-related assumptions were not a primary design input that influenced design outcomes. The design team typically sourced occupant assumptions from codes and standards and from their experience. Additionally, their design practice lacked an effective communication mechanism, which may have been responsible for discrepancies between occupant-related assumptions.

The simulation-based investigation indicated that occupant assumptions can be critical for selecting ECMs/DPs as well as influential on design outcomes (i.e., different occupant assumptions can lead to different optimal solutions). An evaluation of the impact of ODSs on building performance revealed that ODSs can yield different comfort and energy performance. Overall, the analysis indicated that in order to achieve more accurate design predictions and reach optimal design solutions, occupants and occupant assumptions should be given more attention during the design process in terms of consistency and accuracy of assumptions. In addition, designs should be evaluated using alternative occupant scenarios to predict building performance and inform design decisions.

11.3 Case Study 2: Budapest, Hungary

Attila Kopányi, Viktor Bukovszki, András Reith

11.3.1 Summary

An apartment building with 27 units, a community hall, and a shared laundry room will be constructed in downtown Budapest, Hungary, as part of the E-co-housing project. This case study demonstrates a method to create occupancy schedules based on use-pattern extraction through participatory design (also referred to as *co-design*), which refers to making design decisions through a problem-oriented mutual learning process involving occupants and architects. The two main research questions were therefore as follows: (1) How can a participatory design methodology be integrated into the building energy modeling workflow? (2) Does integrating participatory design result in significant differences in energy demand outputs compared to standard modeling workflows?

To assess the possibility of acquiring additional information regarding occupancy behavior from the participatory design process, occupancy schedules for the building energy simulations were created based on focus group interviews. The energy modeling outcomes using these co-design schedules were compared to those applying schedules from national guidelines. A difference of over 10% heating energy use intensity (EUI) was found

in the apartments, and a difference of between 46% and 86% in heating EUI was found in the community hall. This difference is achieved through the differentiation between the use of living and common areas and between active and passive occupancy.

11.3.2 Building Description

E-co-housing is an experimental building for a novel social housing policy spearheaded by the 14th district of Budapest, developed as part of a UIA (Urban Innovative Actions) research project by the same name. The main goals of the project are to provide methods and evidence of just, sustainable transition in housing and to inform policymakers of how a holistic approach to sustainable housing development offers a financially viable, environmentally friendly, and socially sensitive alternative to alleviate housing poverty. As part of the project, an apartment building with 27 units and two common areas (i.e., community hall and laundry room), with a total floor area of 1,950 m^2 will be constructed in downtown Budapest, Hungary by 2022 (see Figures 11.20 and 11.21). Hungary is in a warm summer continental climate zone, and the building itself will be in a dense urban area characterized by perimeter blocks with attached buildings. The building has four stories, divided into two detached tracts connected by a network of suspended corridors. This arrangement separates an inner courtyard and a larger backyard from the street. The estate is legally owned by the municipality, with the apartments rented out at a subsidized rate to residents who live in housing poverty.

The E-co-housing project follows a combination of the co-housing model, zero-energy building principles, and continuous occupant engagement with

Figure 11.20 3D model of E-co-housing.

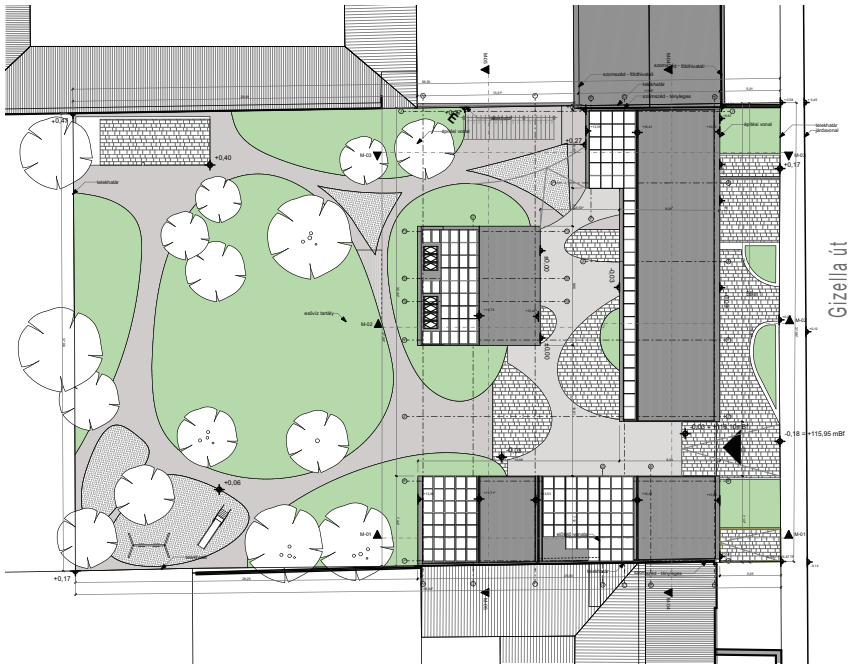

Figure 11.21 Site plan of E-co-housing (ABUD Mérnökiroda Kft, 2020).

the objective of minimizing operational expenditures to achieve a viable business model for affordable housing. In practice, this model entails a wide range of shared facilities, a strong community development program, collaborative facility management, and predictable and minimized energy demand and load curves. To that end, an initial energy simulation conducted during the design phase by the design team predicted an EUI of 54.7 kWh/m^2, while the heating and cooling EUI were 6.9 and 10.6 kWh/m^2, respectively. This simulation was based on standard Hungarian engineering practice, which uses standard occupancy data from conventional buildings. However, relying on standard data neglects two occupant behavior-centric challenges:

1 a demographically varied occupant pool of people living in housing poverty, and
2 a range of unconventionally used rooms and facilities.

The first challenge stems from the building project's goal to create a support network of occupants built on a synergistic occupant pool. This pool includes single, elderly, disabled, family, student, and social worker tenants.

The heterogeneity of expected occupants means that there is a challenge in accurately estimating when and how different apartments and shared facilities will be used, which in turn decreases confidence in projections for energy demand and load curves. This effect is critical since a core tenet of the business model is to have a reliable and predictable reduction of operational expenditures.

The second challenge is that the co-housing model translates to shared facilities with unconventional occupancy patterns. For example, the project includes a 107 m^2 community hall, and a 20 m^2 shared laundry room. The energy demand of these spaces is not insignificant, and their use will highly depend on the simultaneity of diverse occupant motivations, which adds an extra layer of uncertainty to predicting building operation.

In response to these two challenges, a co-design process involving occupants in the building's architectural design was conducted. This process provided an opportunity to access specific occupancy data, which can be used to simulate shared facilities and account for occupant heterogeneity.

The aim of the present case study is to showcase how these challenges/opportunities were addressed during the design phase of the project—in particular, how co-design was leveraged to navigate the complexities related to occupant behavior.

11.3.3 Methodology

This case study methodology followed an alteration of the standard simulation approach to include participatory or co-design (see Figure 11.22). The role of participatory design in this approach was to produce simulation-ready occupancy schedules, thus adding new data-collection and new data-preprocessing steps. The design steps were as follows: (1) defined and organized focus groups representative of potential building occupants, (2) interviewed focus group members during a design workshop to understand their daily routines, (3) aggregated daily routines for overall occupancy schedules, and (4) translated the schedules using occupant metadata. This exercise deviated from standard occupancy schedules by providing metadata to differentiate occupancy patterns of different social groups and by detailing activities that constituted occupancy. The research questions were addressed by using the new occupancy schedules together with a selection of standard schedules in the same building energy modeling (BEM) engine and comparing the outputs.

11.3.3.1 Participatory Design

The participatory design process consisted of three design workshops with a focus group (n=16). To approximate the future building occupants as much as possible, the municipality recruited focus group participants from among a pool of residents who were already tenants in municipal social housing.

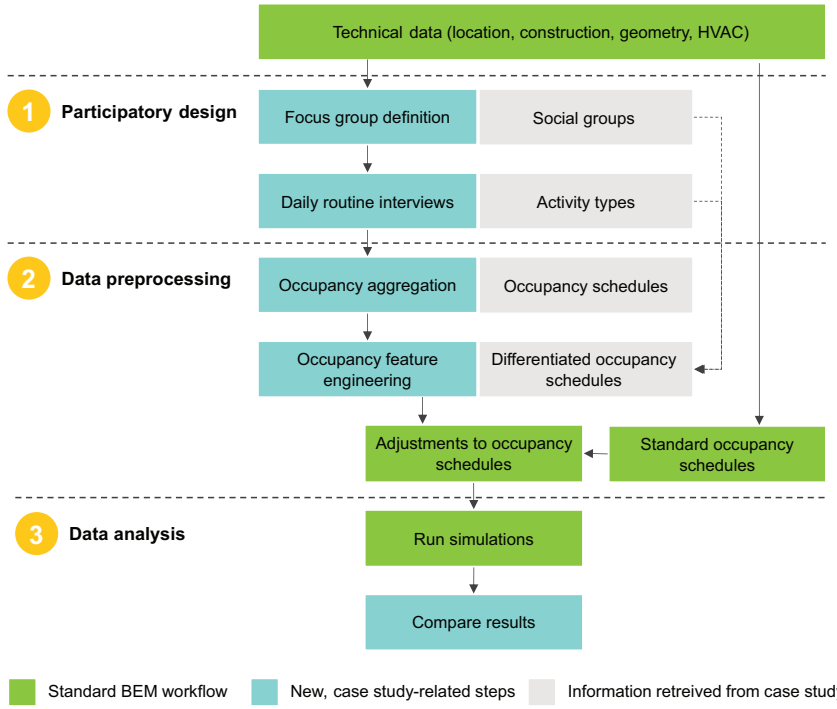

Figure 11.22 Case study design in the context of the standard BEM pipeline.

The residents were joined by a group of social workers, co-housing experts, and architects from the E-co-housing consortium. The former "target" group (n_t=8) and the latter "expert" group (n_e=8) together formed the final focus group. To fulfill the project goals of synergistic housing community composition, this focus group was selected to provide a mix of age, sex, family status (single, couple, etc.), education level, and employment status were selected (see Table 11.4). The age distribution among the focus group participants represented the national average, and the sex balance was roughly equal (male = 7, female = 9). Compared to the national average, family and employment status were more evenly distributed, while the education level of the target group was lower. During the workshops, participants used pseudonyms (used throughout this case study).

The information relevant to occupancy patterns was collected in the second workshop, where the focus group was partially present (n_t = 8, 100%; n_e = 3, 38%). This workshop focused on individual habits and behaviors and, to a lesser extent, specific design solutions. Each respondent drew up their individual daily routine chart for typical weekdays at an hourly resolution (see Figure 11.23), differentiating between four activity categories: sleeping, work/activities outside the house, at-home leisure, and at-home chores. This

Table 11.4 Composition of the focus group, row-by-row for: age, sex, family status, education, employment status

Between 18 and 30			*Between 30 and 65*			*Older than 65*		
Female			Male					
Single	Couple		Single parent	Family with fewer than 3 children		Family with 3 or more children		
Elementary	Vocational		Other secondary	Post-secondary education				
Unemployed	Seasonal	Part-time	Full-time	Self-employed		Retired		

Darker colors indicate a larger cohort population, where each row shows proportions independently.

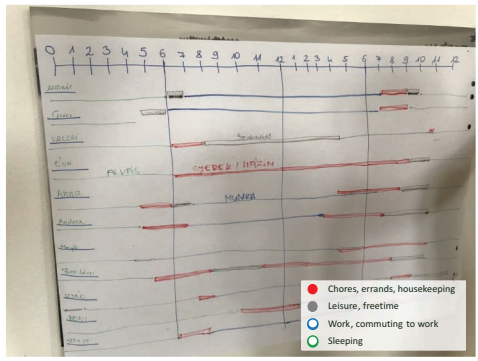

Figure 11.23 Registering of daily routines during participatory design workshop #2. Participants' activities were color-coded per hour (scale on top) as a Gantt chart.

level of differentiation and resolution was necessary for architectural design and served as a pre-processing logic for occupancy schedules.

The occupancy schedules were generated through the aggregation of daily routine schedules. The aggregation method in each case involved taking the mean of responses. Two types of occupancy schedules were created: (1) a general schedule and (2) an active vs. passive occupancy schedule. For the general schedule, all activity types except for work were included equally. Separate active and passive occupancy schedules were generated by considering only chores and leisure activities for the former and sleeping for the latter. In the context of this case study, active and passive occupancy were differentiated in terms of occupant heat load.

11.3.3.2 Building Energy Modeling

To evaluate the impact of using the occupancy schedule created based on the co-design methodology, a BEM was created using EnergyPlus 9.2 and simulated applying different occupancy schedules. Along with the occupancy schedule

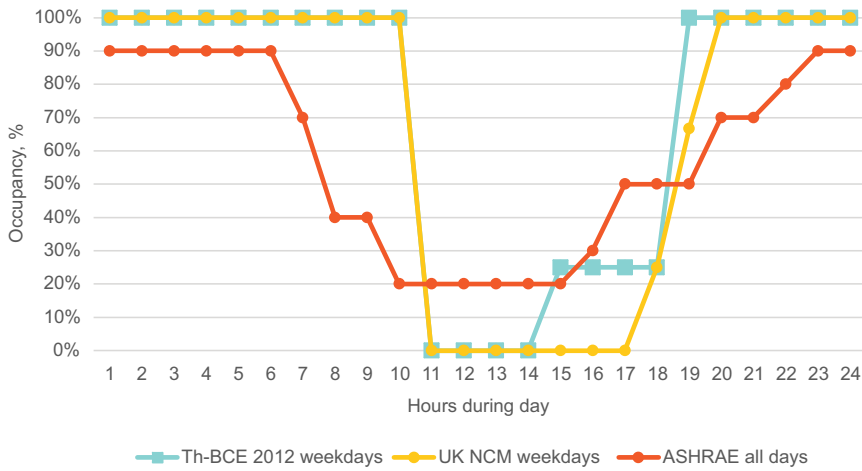

Figure 11.24 Residential occupancy schedules based on different standards.

created using co-design approaches, three other schedules from national guidelines and standards were used, as described in the paragraphs that follow.

Based on a review of the available standards and guidelines of European countries, the authors only found hourly occupancy schedules for residential buildings in the French Th-BCE 2012 (2012) and the UK NCM Database (2018); therefore, only these were used in the study as European schedules. The residential occupancy schedule provided by ASHRAE Standard 90.1 (2019) was applied as well, as it is widely recognized and used in the energy modeling industry worldwide.

The residential occupancy profiles provided by these three standards are shown in Figure 11.24. Notably, ASHRAE uses the same schedule for all days, and in the Th-BCE 2012 and the UK NCM guidelines, the weekend occupant schedule is 100% throughout the whole period. The Th-BCE 2012 standard weekday values are averages, as it has a different profile for Wednesdays. The UK standard provides occupancy schedules on room level. Since in the created BEM each apartment represented one thermal zone, the room-level schedules had to be aggregated into an apartment-level profile. This aggregation was accomplished by assuming the number of occupants for each area based on its function.

In the BEM, 3.88 W/m^2 equipment power density was used with an average 66% diversity, while the lighting power density was assumed to be 2 W/m^2.

11.3.3.3 Occupant Heat Load Profile of the Living Areas

Using the schedules from the co-design process, it was possible to differentiate between active and passive occupancy when creating the hourly occupancy

heat load profile for the living areas (i.e., private apartments). This profile was calculated as a weighted average of the active and passive heat loads, where the weighting factors were the probabilities of the active and passive occupancy based on the focus group interview results (see Equation 11.1).

$$q_{\text{Co-design}} = p_a \cdot q_a + p_p \cdot q_p \tag{11.1}$$

where:
$q_{\text{Co-design}}$: occupant heat load in the living areas, W/person
p_a: probability of active occupancy
q_a: heat load of active occupant, W/person
p_p: probability of passive occupancy
q_p: heat load of passive occupant, W/person

When calculating the heat load used in the co-design schedule, a 72 W/person heat load was used for each passive occupant, corresponding to the heat load of an average person while sleeping, as per the ASHRAE 55-2010. When considering active occupancy, 100 W/person was assumed, corresponding to the metabolic rate of a seated, relaxed person (International Organization for Standardization, 2006).

When determining the heat load profile based on the Th-BCE 2012, UK NCM, and ASHRAE occupancy schedules, no differentiation was possible regarding active and passive occupancy; therefore, the schedule value was always multiplied by 100 W/person, including during the nighttime.

11.3.3.4 Occupant Schedule and Heat Load Profile of the Common Areas

Since participants were not asked about their weekend habits during the co-design focus group workshops, information about weekend occupancy was not available. Therefore, in the co-design schedules for the living areas (i.e., private apartments) and common areas (i.e., community hall and laundry room), the same weekend occupancy was used (as in the case of the Th-BCE 2012 and UK NCM standards, i.e., a constant value of 100%).

The co-design schedule of the common areas was created using assumptions regarding the probability that an occupant will use the common rooms for either chores/work or leisure. The assumed probability values are summarized in Table 11.5. The overall probability (at each hour) of the common area usage was then determined as the average of the probability values of the respondents. The occupancy ratio values were then determined proportionately to the probability values, with 100% occupancy assigned to the highest probability value.

In case of the Th-BCE 2012 and UK NCM standards, no specific guidelines were given for the occupancy of common areas; therefore, the same schedules were used for the living areas. The ASHRAE standard provided

Table 11.5 Assumed probability values for the occupancy of the common areas

	Community hall	*Laundry room*
Probability of using the area for chores or work	10%	10%
Probability of using the area for leisure	50%	50%

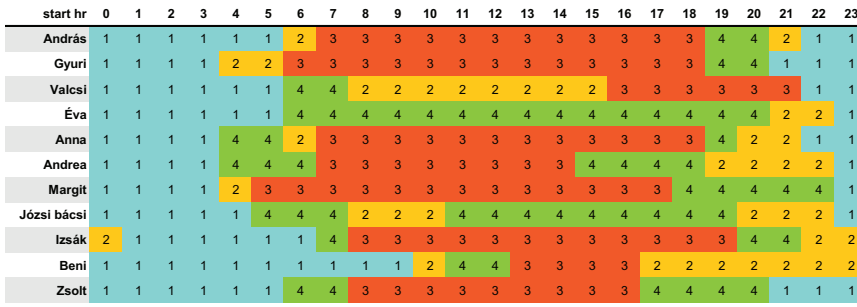

Figure 11.25 Daily routine charts. Activities were coded as 1=sleeping, 2=at-home leisure 3=away, 4=at-home chores.

the same occupancy profile for common areas in residential buildings as for the living areas. When determining the occupant heat load based on the schedules for the common areas, the 100 W/person metabolic rate used in all standards was used for co-design calculations.

11.3.4 Results

The E-co-housing case study results are presented below as follows: first, the daily routine charts drawn at the design workshop #2; then, the general, active-passive, and shared facility occupancy schedules; finally, a comparison of the simulation outcomes following the three selected standards.

11.3.4.1 Co-Design Daily Routines

Daily routines were broken down by activity type, as shown in Figure 11.25. The average times for key activities included waking up at 5h43; leaving the house at 8h53; arriving home at 18h20; and going to sleep at 22h38. Notably, 4 out of 11 respondents spent all their morning hours at home, and two stayed at home all day. These respondents explained their sporadic occupancy patterns mostly by their employment status. For instance, four respondents were self-employed, unemployed, seasonally employed, and a pensioner. Also, many respondents reported temporary, short-term, and

volatile employment conditions, overtime working, multiple workplaces, and seasonal jobs. On average, respondents spent seven hours sleeping, roughly eight hours out of the house, around 5.33 hours spending free time at home, and the remaining 3.5 hours doing chores. Regarding differences in sex, female respondents slept over 1.5 hours less than male respondents, but almost two hours more being active at home than male respondents. Differences in age and family status yielded no discernible patterns in occupancy.

11.3.4.2 Co-Design Occupancy Schedules

Overall occupancy of the apartment units (Figure 11.26) dropped from 100% to around 40% between 4h00 and 8h00 and rose to 100% between 16h00 and 22h00. The schedules plateaued in the morning hours until noon, with some movement in the afternoon.

However, not all occupancies were the same from an energy perspective. The active and passive occupancies were equal at around 5h00 and 22h00, respectively. Between these two points, more people were awake than sleeping. Sleep times varied from 20h00 to midnight, and wake times ranged between 3h00 and 10h00. This means that there was a passive occupancy component in the schedule for about 58% of the day. Likewise, active occupancy clearly showed a morning and evening peak at 6h00 and 19h00, respectively. In between those times, most but not all occupancy was active.

Time spent on active, at-home daily activities in the common areas took away from time spent on the same activities in private apartments. This pattern was shown by a truncated inverted trajectory of common hall occupancy versus apartment occupancy (see Figure 11.27). As the share of passive occupancy in overall occupancy increased, people spent more time in their apartments than in the community hall. The laundry room occupancy is flatter, with minor peaks at 9h00 and 21h00, compared to the plateau

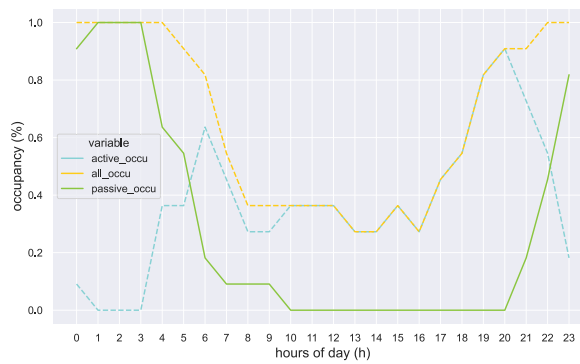

Figure 11.26 Daily occupancy by the level of activity. All occupancy is the sum of active and passive occupancies.

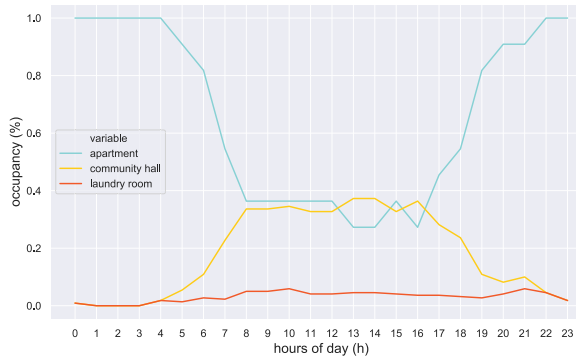

Figure 11.27 Daily occupancy in private apartments vs. common areas (community hall and laundry room).

between 8h00 and 16h00 for the community hall. This flattening is due to the smaller overall assumed coefficients, and the peaks can be explained by a higher prevalence of chores (in the case of the laundry room).

11.3.4.3 Occupant Heat Load Profiles

The daily occupant heat load profiles based on the analyzed standards and the co-design workshop results are summarized in Figure 11.28. Due to the application of a lower heat load for occupants during night hours, the co-design heat load profile shows generally lower values during this time. The root mean squared error (RMSE) between the co-design occupant weekday heat load profile and the other profiles for the living areas is summarized in Table 11.6. The heat load profile based on the ASHRAE occupant schedule shows the highest similarity to the co-design profile.

In the case of the common areas, the occupant heat load profiles showed significant differences. The co-design heat load profiles of the community hall and the laundry room showed higher values during daytime, which reflects the assumption that occupants are more likely to use these areas during this period.

11.3.4.4 Impact on Energy Modeling Outputs

The heating EUI, cooling EUI, and total EUI of the living areas modeled using the co-design occupancy schedule were 6.0, 12.4, and 66.1 kWh/m^2, respectively. The comparison of these values with the outcomes of applying the other analyzed occupancy schedules is shown in Figure 11.29. The largest deviation can be seen in the heating EUI, followed by the cooling EUI, while the total EUI shows a very small difference, <1%. The heating

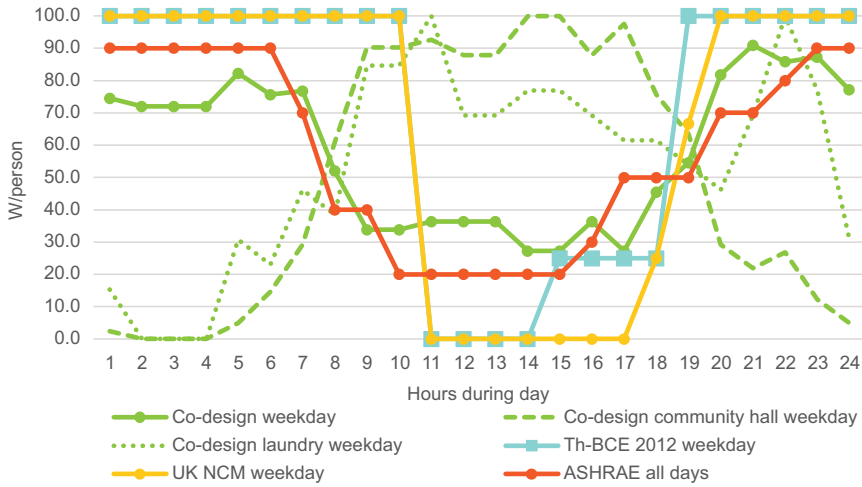

Figure 11.28 Occupant heat load profiles used in the analysis. Different profiles were created for the living areas, the community hall, and the laundry room in the co-design methodology; for the other schedules, the same profile was used in every zone. The weekend heat profile was a constant 100 W/person in the co-design, Th-BCE 2012, and UK NCM cases; for ASHRAE, the same heat profile was applied for each day.

Table 11.6 RMSE between the co-design weekday heat load profile and the other analyzed occupant load profiles of the living areas

	Th-BCE 2012	*UK NCM*	*ASHRAE*
RMSE, W/person	31.7	33.6	13.2

consumption was predicted to be lower and the cooling consumption higher based on the Th-BCE 2012 and UK NCM standards; in case of ASHRAE, the results were the opposite.

In the community hall, when considering the co-design schedule, the cooling EUI was 119.5 kWh/m^2, the heating EUI was very low (only 0.42 kWh/m^2), and the total EUI was 125.7 kWh/m^2. The comparison between the heating, cooling, and total EUI applying different schedules is shown in Figure 11.30. All energy results were predicted to be lower in the Th-BCE 2012, UK NCM, and ASHRAE cases.

Figure 11.31 depicts the differences in the heating and total EUI of the laundry room using different occupancy schedules (no cooling system was designed for the laundry room). Figure 11.31 shows a similar pattern, with larger differences regarding the heating EUI. Both the heating and total

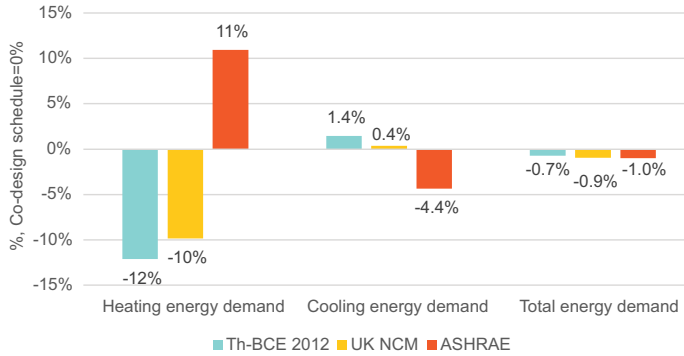

Figure 11.29 Heating, cooling, and total EUI of the living areas modeled with different occupancy schedules. The reference points are the results based on co-design schedule.

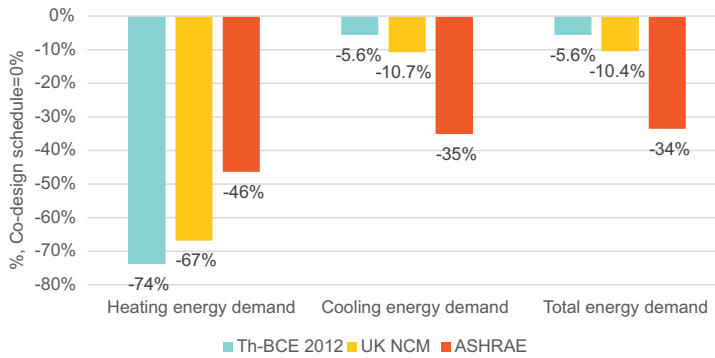

Figure 11.30 Heating, cooling, and total EUI of the community hall modeled with different occupancy schedules.

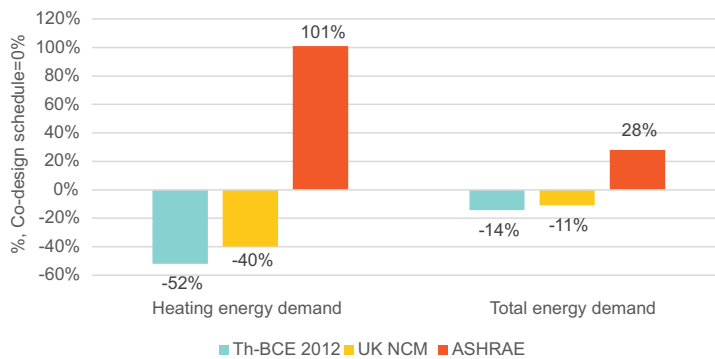

Figure 11.31 Heating and total EUIs of the laundry room modeled with different occupancy schedules.

EUI were predicted to be lower based on the Th-BCE 2012 and UK NCM standards; in case of ASHRAE, the results were the opposite.

11.3.5 Discussion

In the living areas, the difference in the heating and cooling EUI can be attributed to the disparity in the average occupant heat loads (see Figure 11.32). When applying the Th-BCE 2012 and UK NCM standards, the average heat load was slightly higher; yet, when applying the ASHRAE standard, it was lower. This discrepancy could be due to the heating EUI being lower and the cooling EUI higher in the case of the Th-BCE 2012 and UK NCM standards, while the opposite was true for the ASHRAE standard. In the living areas, the heating and cooling EUIs represented only a small part of the total EUI. The large differences in the heating and cooling EUIs compared to the total EUI might be explained by the occupant heat load, which directly affects the heating and cooling demand.

In the community hall, the cooling constituted the largest share of the total demand, hence the difference in the total demand; the cooling demand showed a similar pattern. The heating consumption was very low in all cases, which could have caused larger differences.

The difference in the cooling EUI of the community hall when applying different schedules can be explained by the variation in the daily profile of the occupant heat loads. As shown in Figure 11.33, the co-design-based occupant heat load increased during the daytime and significantly contributes to the rise in cooling demand in the community hall on a typical summer day. Yet, the occupant load profile based on the ASHRAE standard showed a decrease during the day, causing the cooling EUI to remain at almost a constant value throughout the day.

Moreover, in the laundry room, only the heating and total energy EUIs could be analyzed since no cooling was designed for this space. The

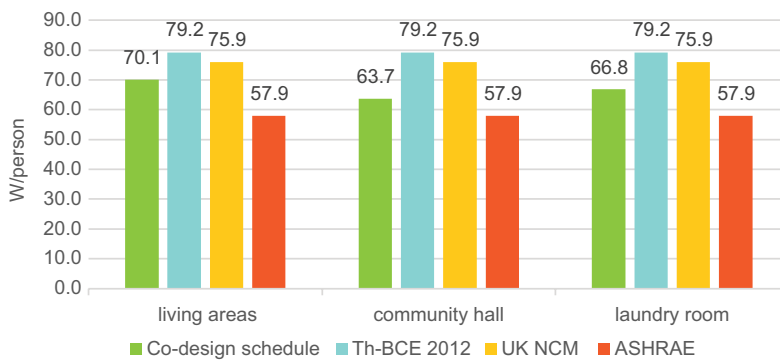

Figure 11.32 Average occupant heat load values in the three analyzed areas: living areas, community hall, and laundry room.

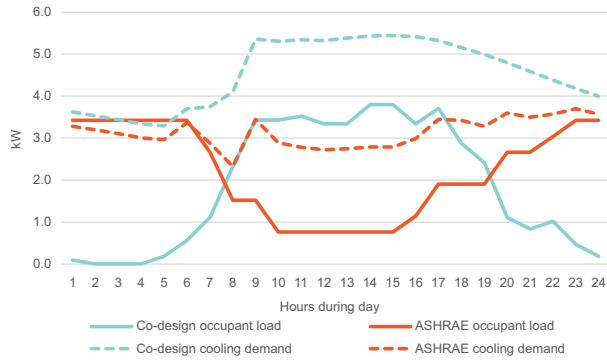

Figure 11.33 The occupant heat loads and the cooling energy demand of the community hall using the co-design schedules and ASHRAE standard, considering a typical summer day.

difference in the heating EUI of the analyzed models can be explained by the changes in the occupant heat loads. All the models resulted in lower heating consumption while having higher occupant heat loads.

Limitations of this case study stem from: (1) uncertainties in BEM, (2) assumptions made prior to modeling, and (3) the co-design methodology. In the case of BEMs based on the Th-BCE 2012 and UK NCM standards, the occupancy schedule of the living areas was used for the common rooms as well, assuming an energy modeler would follow a similar path. While this approach is purely speculative, it draws attention to the uncertainties designers face because of a lack of accurate model inputs. Also, the results were limited to weekday analyses only, as weekend schedules were not collected during the focus groups. This case study was likewise limited to analyzing the effect of changing the occupancy schedule only, whereas other sources of internal heat gains (e.g., equipment, lighting) may have been relevant as well. Additionally, in certain cases, the analyzed energy demands had very low absolute values, such as the heating demand in the laundry room and the community hall.

Regarding assumptions, the occupancy of these rooms was based on assumptions about the proportion of chore/leisure time that would be spent there. These assumptions, however, were not informed by focus group interviews. Furthermore, the calculations did not consider the facilities provided by the rooms, nor the number of people living in the building. Both factors heavily influenced common room occupancy. The comparison of these results may have been less insightful as a result.

Finally, the co-design process used in this project was intended to support architects, not BEM. Weekend schedules were thus not collected, and the focus group included only a limited sample size of people currently living in housing poverty. Retrieving occupancy schedules during co-design

is time-consuming, and so future larger studies should consider a more streamlined method.

11.3.6 Concluding Remarks

In this case study, participatory design was used as a tool for constructing more detailed and more accurate occupancy schedules compared to schedules from the three selected standards. Overall, between 13.2 and 33.6 W/person differences in heat load profiles were observed compared to standard occupancy schedules. While these differences did not translate to significant differences in overall energy EUI, it yielded over 10% heating EUI difference in apartments and between 46% and 86% heating EUI difference in the community hall. The difference in the EUI was achieved through the differentiation of active and passive occupancy and the ability to tell exactly how people are using the building beyond simply occupying it. Forecasting how occupants use the building could especially be significant for predicting occupancy in shared facilities and common areas, which are prevalent features of co-housing.

This case study analysis also showed that people living in social housing occupy buildings differently than standards predict (albeit this claim could be specific to this case study), potentially due to higher volatility in their employment schedules. The employment schedules for this study's participants were closer to the standard "9-to-5" work schedule for male occupants and less so for female occupants, but further research is required to explore the association between sex, work schedules, and occupancy patterns to understand how social housing occupancy may be distinct from conventional residential buildings. Overall, this study's findings suggest that participatory design may be a viable tool to depart from generic standards toward higher specificity in BEM as well as a valid research method to explore different factors of occupancy, which could potentially contribute to development of more inclusive standards in the field.

11.4 Case Study 3: Quebec City, Canada

Jean Rouleau, Louis Gosselin

11.4.1 Summary

In the mid-2010s, a 40-unit, four-story social housing building called *Les Habitations Trentino* was constructed in Quebec City, Canada (lat. 46.78°N, lon. 71.29°W), in an eco-neighborhood called La Cité Verte. The climate in Quebec City is characterized by significant variations throughout the year: cold and snowy winters (HDD18 = 4,843°C-day), and relatively warm, humid summers. The stakeholders wanted to reach a high level of energy performance for this building. During the design phase, building performance

simulations (BPS) and life-cycle analyses were performed to test different options to inform the decision-making process.

A partnership with the Chaire industrielle de recherche sur la construction écoresponsable en bois (CIRCERB) from Université Laval was established to analyze the behavior of this case study building. Researchers from Université Laval analyzed the energy performance of the building from the beginning of operation and found that occupants had a strong influence on the energy performance of the building. The researchers also found a substantial energy performance gap for this building, where the energy demand that was predicted prior to construction differed from the actual demand.

The objectives of the present case study analysis were thus (1) to explain the reasons behind this energy performance gap and assess if it was caused by an inaccurate representation of the occupants in simulation, and (2) to develop a method to assess the full influence of occupants on the performance of multi-unit residential buildings (MURBs). The analysis also aimed to find appropriate ways to incorporate occupant behavior into BPS to improve the design of MURBs and reduce the energy performance gap. Studied occupant behavior included occupancy, space heating, hot water and electricity consumption, setpoint temperatures, and the use of operable windows for ventilation. In brief, the study found that the performance gap was mainly caused by differences between the assumptions regarding occupants in the BPS and the actual occupant behavior observed in the building.

11.4.2 Building Description

Construction of *Les Habitations Trentino* took place in 2015 (see Figure 11.34). Although pre-construction BPS assumed a building population of 125 people, the total number of occupants in 2016 was 90. Energy bills for heat and electricity are included in the lease. The floor area of each unit varies between 70 and 80 m^2. The window-to-wall ratio (WWR) is 16%, with operable triple-glazed windows. A special feature of the building is that part of it was constructed with a cross-laminated timber (CLT) system, and a light-framed wall system was used for the other side. The thermal resistance (RSI value) of the opaque portion of the envelope is 6.32 m^2K/W for both construction systems. The air tightness of the envelope was measured to be 0.6 ACH at 50 Pa.

Heating is provided by a biomass-based district heating system. Each apartment is equipped with three or four hot water radiators. The energy supply for producing domestic hot water comes from the district heating network. A 100% fresh air ventilation strategy is used. Each dwelling has a switch to turn the mechanical ventilation on or off (with a heat recovery ventilator (HRV) efficiency of 85%). No mechanical cooling was installed.

Building data have been collected since the beginning of building occupancy (i.e., October 2015). Data on the consumption of electricity, domestic hot water, and heating is collected. Indoor temperature and humidity,

Figure 11.34 Picture of the building and floor plan.

window openings, mechanical ventilation control, and exhaust fan operation (kitchen hood, dryer, bathroom fan) are also monitored for some units. Overall, more than 500 data points are monitored, with, for the most part, an acquisition every 10 minutes.

At the building level, the annual EUI of the heating, electricity, and domestic hot water (DHW) in 2018 was 38.4, 48.1, and 51.3 kWh/m^2, respectively, for a total EUI of 137.8 kWh/m^2. These figures are a significant improvement compared to the typical total EUI observed for this type of building in Quebec, i.e., 250 kWh/m^2 (Whitmore and Pineau, 2021). The improvement is mostly due to the quality of the envelope that contributes to reducing the heating needs. Monitoring of the building from 2015 to 2020 showed that the annual energy consumption for heating and DHW was consistent over time, but electricity consumption increased over the last few years.

Figure 11.35 presents the annual EUI of all dwellings in the case study building, ranked from the lowest to the highest consumers. The most striking element of this figure is the large variation of energy consumption from one dwelling to another, despite their similar features. The EUI varied by a factor of 11 from 23.2 to 267.3 kWh/m^2 across dwellings. Very weak correlations between the DHW consumption and the number of occupants in

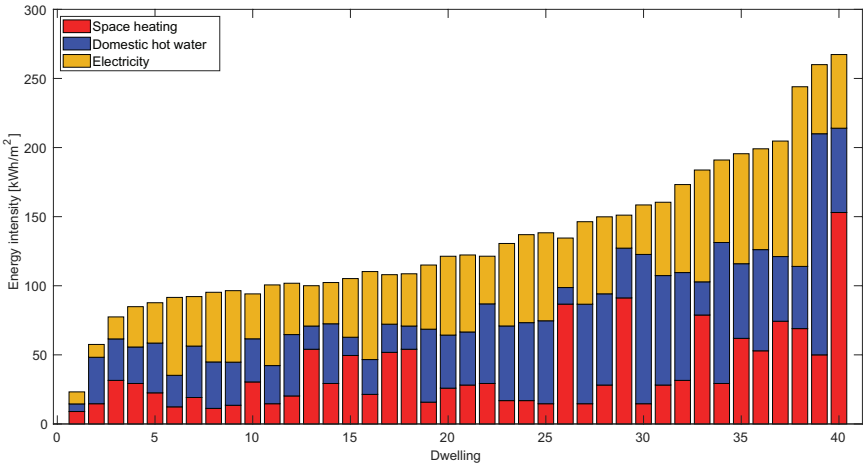

Figure 11.35 Annual energy intensity in each dwelling in 2018.

each dwelling and between the space-heating demand and the floor level were noted, but other factors such as orientation, construction system, etc., did not explain the variability of the EUI (Rouleau *et al.*, 2018). In fact, most of the observed variance appeared to be due to differences in occupant behavior.

Thermal comfort during summer was also studied. A portion of the dwellings exhibited overheating (Rouleau and Gosselin, 2018), with an indoor temperature above the limit provided by the adaptive comfort model of ASHRAE Standard 55. In other units, the indoor temperature stayed within the limits of acceptable conditions. Once again, most of the variability was linked to occupant behavior.

11.4.3 Methodology

Since this analysis had two distinct objectives, the methodology was divided into two sections: one to evaluate the impact of occupant behavior on the energy performance gap and the other to develop a novel occupant behavior model. Details of the methodology are provided below.

11.4.3.1 Occupant Behavior Assumptions during Design

During the design phase of the building, BPS was performed to assess the impact of different design options in terms of construction costs and energy savings. Different envelope assemblies were simulated with the Passive House Planning Package (PHPP) software (Feist, 2012), leading to the design previously presented above, which offered a good trade-off between cost

and energy performance. In these simulations, occupants were accounted for by static schedules that relied on fixed assumptions regarding occupancy, heating setpoint, etc. These were the default schedules supplied by the PHPP software.

For the purposes of this study, the PHPP model was examined thoroughly, and the assumptions of the initial energy model were compared to the monitored data. This step allowed for the identification of inaccurate assumptions. The initial energy model was modified to account for divergences between the model and the actual building. Changes in the total energy use predicted by the model were tracked as those changes were applied.

11.4.3.2 Occupant Behavior Simulation Model Development

A versatile integrated occupant behavior model was developed. To develop the model, existing models that simulated different facets of occupant behavior were adapted and assembled. The unified model provided sets of possible coherent schedules that served as inputs for the BPS.

The main requirements for the model were:

- *Integrated several facets of occupant behavior*: The model should provide schedules for the most influential types of occupant behavior with respect to energy consumption and thermal comfort (occupancy, electricity consumption, DHW consumption, heating setpoint, window opening).
- *Ensured coherence between sub-models*: The model should provide schedules that are coherent with one another. For example, if the occupancy schedule indicates that no one is present, the DHW and electricity consumption should be adapted accordingly.
- *Provided high time and space resolution*: The model should provide representative schedules at the level of a single dwelling. It should provide daily or yearly schedules, with a time step that could be as small as 10 minutes.
- *Replicated observed variance*: The model should generate schedules that properly match the observed unit-to-unit variance, as well as the day-to-day variability observed in the dwellings. The model should be probabilistic: two different runs lead to two different sets of schedules, both of which would still be within the observed variance for each type of occupant behavior.

For the occupancy, electricity, and domestic hot water sub-models, modifications were made to existing models to account for various factors. First, models were created using data from foreign countries (United Kingdom and USA); then, adjustments were made so the models better represented behaviors observed in Canada (Rouleau *et al*., 2019). Another modification was to add a "diversity" factor that was randomly assigned to each simulated

dwelling to ensure that the dwellings had diverging behaviors (i.e., that the simulated occupant profiles were different between households) so the full range of observed occupant behaviors was reproduced. Finally, the sub-models communicated with each other to make sure that the generated schedules for occupancy, electricity, and hot water were coherent with one another. The methodology to develop each sub-model is described below.

11.4.3.2.1 OCCUPANCY

The daily occupancy profiles generator developed by Richardson *et al.* (2008) was used as the basis for the model. The generator assigned the number of active occupants (i.e., present and not sleeping) in the simulated dwelling at a 10-minute frequency. Occupancy schedules were generated and then forwarded to other sub-models.

11.4.3.2.2 ELECTRICITY CONSUMPTION

Richardson *et al.* (2008) model was also used to generate schedules for the use of electric appliances (Richardson *et al.*, 2010). Another model was also used for the usage of artificial lighting (Armstrong *et al.*, 2009).

11.4.3.2.3 DOMESTIC HOT WATER CONSUMPTION

The domestic hot water sub-model used the yearly DHW event schedule generator developed by the National Renewable Energy Laboratory (NREL) in the United States (Hendron *et al.*, 2010). The hourly NREL model was adjusted so it would fit with the desired time resolution of 10 minutes.

11.4.3.2.4 HEATING SETPOINT

A probability distribution function that copied the distribution found in Canadian houses (National Resources Canada, 2011) was used to assign the heating setpoint of the heating system. The setpoint was treated as a static parameter that remains constant throughout the year.

11.4.3.2.5 WINDOW OPENING

The state of the windows (opened/closed) was calculated based on the outdoor and indoor temperatures using a logit equation to estimate the probability of window opening (when closed) and window closure (when opened). This equation was developed with the monitored data from the case study building. The equations that calculated the states were based on coefficients that varied for each simulated dwelling. Unit-to-unit variance was thus ensured.

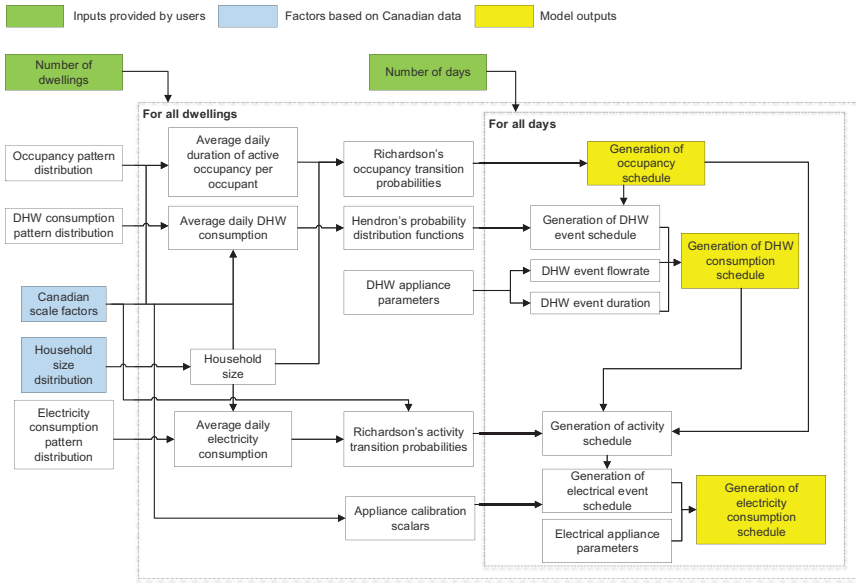

Figure 11.36 Architecture of the occupant behavior model showing the relationship between all sub-models.

More details on these occupant behavior models are available in Rouleau *et al.* (2019) and Rouleau and Gosselin (2020). The interactions between these different sub-models are presented in Figure 11.36.

Since the occupant behavior model described above could generate many different schedules that were representative of possible occupants, it offered the possibility to run Monte Carlo simulations. For this type of simulation, a large number of schedules can be created by running the model repeatedly. Then, these different schedules can be introduced into BPS tools. The results of this procedure will be probability distributions for important model outputs (e.g., energy consumption, thermal comfort, overheating, peak demand). These distributions can indicate the likeliness of achieving a certain level of performance while considering the full extent of possible occupant behaviors.

The abovementioned approach can also be used to size HVAC equipment. For instance, the methodology was used to study the sizing of hot water systems. The case study building's hot water consumption was simulated 100 times with the occupant behavior model. These 100 building consumption profiles were forwarded to a numerical model of a hot water system to find the optimal size of the system (storage water tank volume and heating capacity of the system). If an instantaneous water heater had been installed in the building, the methodology predicted that the ideal heating capacity

for the building ranged between 192 and 497 kW, depending on how much hot water the occupants in the building use. On the other hand, with a water tank of 2,000 L, the ideal heating capacity was between 33 and 77 kW.

11.4.4 Results and Discussion

The results of the case study analysis are presented and discussed in the sections below.

11.4.4.1 Occupant Behavior Assumptions during Design

According to these prior-to-construction simulations, the predicted annual heating EUI was 16.6 kWh/m^2 and the annual total EUI (summation of heating, electricity, and DHW) was 74.3 kWh/m^2. As shown in Figure 11.37, these values departed significantly from the actual average energy consumption observed in the building.

The assumptions of the initial energy model and the measurements were compared and analyzed to explain the discrepancies. Three notable sources of discrepancies were:

i *Window opening*: The original model did not include window opening during the heating season. However, it was observed that windows were opened 9.4% of the time during the heating season, and so the infiltration rate of the building was adjusted to include this behavior. The relatively high rate of window openings obviously increased the heating demand compared to predictions.
ii *Heating setpoint*: The heating setpoint was originally assumed to be 20°C. In practice, the actual temperature in the units tended to be much higher, around 23.9°C, which again increased heat consumption compared to predictions.
iii *Domestic hot water*: A daily consumption of 25 L/person was assumed, but the measured consumption was much higher, around 58.3 L/person.

Other changes applied to the energy model following the monitoring of the building included (continued from the list above): (iv) using the "true" weather data, (v) modifying the HRV efficiency from 85 (expected value by the HRV supplier) to 70 (estimated value from monitored data), (vi) reducing the building population from 125 to 90 people, (vii) considering the internal heat gains generated from the hot water recirculation loop, and (viii) using the "true" electricity demand. Implementing these changes in the original energy model achieved simulation predictions much closer to measurements, thus reducing the performance gap. As shown in Figure 11.37, changes in the model were applied cumulatively.

This exercise illustrated the challenge of making accurate assumptions about occupant behavior prior to construction. At the same time, the study

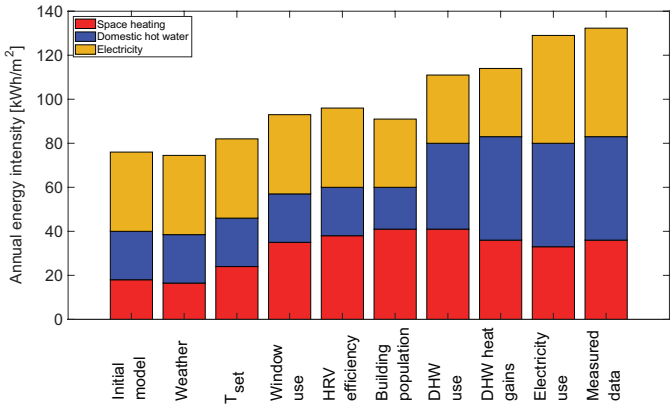

Figure 11.37 Revisiting assumptions related to occupant behavior to close the energy gap between predictions and measurements.

revealed the significant impact that these assumptions might have on energy predictions and, potentially, on design choices. In addition, the BPS used during the actual design phase only accounted for the "average occupant" and did not consider the full spectrum of possible occupants (as highlighted in Figure 11.35). Thus, there is a need to develop an integrated model encompassing the different facets and inherent variability of occupant behavior as well as design methods to exploit these kinds of models.

11.4.4.2 Occupant Behavior Simulation Method

The results presented in this section include the simulation outputs of an energy model of a single dwelling located in the case study building. Monitoring data were used to calibrate this numerical model to make sure the simulations adequately reflected the real building in terms of annual heating demand and thermal comfort. A total of 1,000 annual occupant profiles were then generated and provided to the dwelling model to generate probability distributions for the heating demand, total energy use, and thermal comfort (for more details, see Rouleau *et al.*, 2019). This approach is useful for assessing the robustness of the building design for use by different occupants.

The average annual heating EUI across the 1,000 simulations was 36.6 kWh/m^2 with an average total EUI of 110.2 kWh/m^2 when adding hot water and electricity use. In terms of thermal comfort, a mean value of 2,429 hours per year was deemed as not comfortable according to ASHRAE 55 (ASHRAE, 2017). Figure 11.38 provides the overall distribution observed from all simulations for the three performance indicators and illustrates the wide range of possible building outputs. For example, the heating EUI in the simulated dwelling went from 10 to 150 kWh/m^2 depending on which

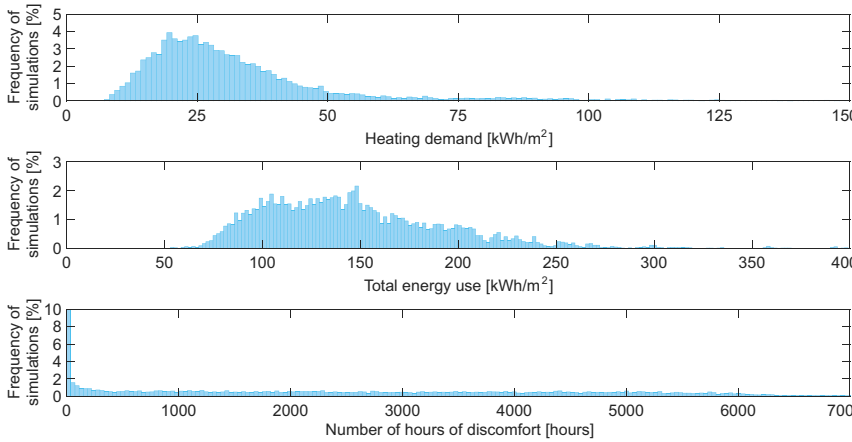

Figure 11.38 Projected distribution of various energy performance indicators depending on occupant behavior.

occupant profile was used. Note that in the monitored building, the space heating demand per dwelling ranged from 13 to 146 kWh/m^2, which was similar to the range obtained with the simulations. The same result was true for thermal comfort. On the one hand, there were multiple profiles that had close to zero hours of thermal discomfort. On the other hand, some profiles endured uncomfortable conditions for most of the year. The large range of energy consumption and thermal comfort conditions displayed in Figure 11.38 was similar to that observed in the actual dwellings.

For the three distributions shown in Figure 11.38, an important proportion of the simulations was located near the bottom boundary of the distribution where the contribution of each unit was small. This means that the overall energy consumption of the case study building was not as driven by the consumption of the majority of people in the dwellings as it was (at least to some extent) by its highest-consuming households. For instance, the average heating EUI in the biggest 15% of consumers was 77.4 kWh/m^2 versus 29.4 kWh/m^2 for the remaining 85% of households. This difference suggests that the current building design is sensitive to high levels of energy demand for certain types of behavior.

The distributions shown in Figure 11.38 were obtained for a single dwelling at the level at which a high diversity of behaviors was expected, which translated to a widespread of possible energy demands and thermal comfort. When more units were considered simultaneously (i.e., when the sample size increased), extreme behaviors canceled out and the variability of possible energy intensity and comfort level was reduced. This result suggests that large MURBs should be more robust in terms of energy performance with respect to occupant behavior.

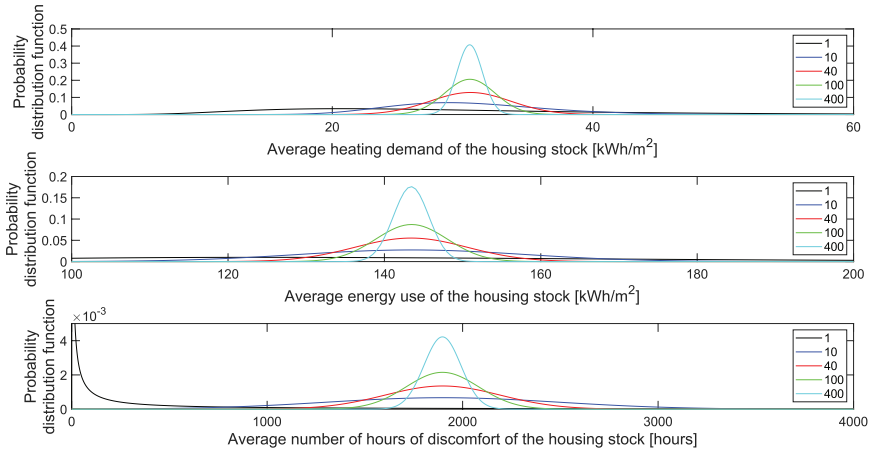

Figure 11.39 Impact of the number of units on the probability distribution of possible energy consumption, space heating consumption, and discomfort.

The energy and comfort distributions obtained from housing stocks of 1, 10, 40, 100, and 400 dwellings were considered. For each of these housing stock sizes, 10,000 combinations were randomly chosen from the simulations of the dwelling under different occupant behavior. The resulting distributions are displayed in Figure 11.39. The widest probability distribution function on each subplot corresponds to the distribution for a one-dwelling housing stock, and then the distributions become narrower as the housing stock increases, where the most cramped distribution is for a 400-dwelling housing stock. The case study building has 40 dwellings, and so the distribution projects that the annual heating EUI should be between 25 and 45 kWh/m^2, which is roughly what was observed year after year.

To improve the energy robustness of the building, it will be important to evaluate the reasons behind its high sensitivity to occupant behavior. In Figure 11.40, the outputs of each simulation are represented in multiple grids of 30 × 30 pixels. The color of a pixel conveys the average value of an aspect of occupant behavior for all simulations located within the pixel. For example, for simulated households with a heating demand between 75 and 100 kWh/m^2, the average frequency of opened windows is approximately 50% of the time.

At this point, the heatmaps were only produced for the actual building design, but the methodology can be applied to future building designs. Different configurations of building designs can be tested to assess their robustness regarding occupant behavior. One might envision robust design optimization, where the design is optimized not for a single occupant behavior profile but for various profiles to ensure that its high level of energy

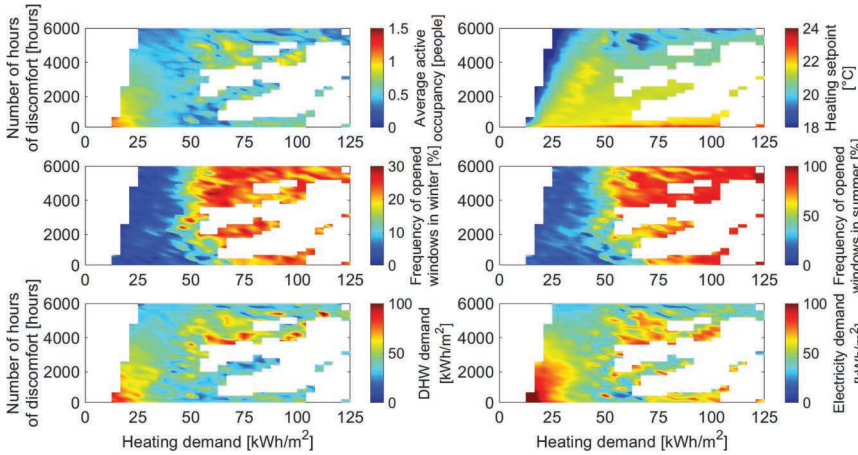

Figure 11.40 Heatmaps representing the influence of various aspects of occupant behavior on the heating demand and comfort performance of the building.

performance is sustained for the full array of possible occupant behaviors. Parametric-based studies are also possible, where designers can change values for a specific parameter (e.g., WWR) in the building model to see the changes in the distributions for the energy performance.

Robust design assessment offers additional information that can be provided to the building stakeholders with the generation of probability distributions. As discussed, typical pre-construction simulations yield only a single value of expected heating demand (or peak demand, thermal comfort, etc.). While this single expected value can be useful when comparing different designs, it regularly differs from reality; its predictive value is minimal. Generating probability distributions helps in that regard by providing a full range of possible outputs, which gives stakeholders a better idea of the range of performance that the building might exhibit.

Robust design assessment can also help building designers and owners identify behaviors that can drive up energy consumptions and to understand how the building responds to such behaviors. In this case study analysis, for instance, high window opening rates during the heating season were found to increase the heating EUI up to 100 kWh/m^2. If designers are not satisfied with this level of consumption, they could target designs that yield better performance with high window opening frequency (e.g., decrease WWR, increase mechanical ventilation rate to decrease the use of windows, inform occupants).

11.4.5 Concluding Remarks

This case study analysis demonstrated the significant influence that occupants can have on the energy performance of their dwellings. It is also

another example of the much-discussed energy performance gap (i.e., actual energy consumption differs from projected energy consumption during the design phase of the building). This analysis showed that the energy performance gap in this case study building was mainly caused by a misrepresentation of occupants in the energy simulations. Occupant behavior is a highly uncertain parameter, especially in residential buildings where behaviors change from one household to another; it is practically impossible to accurately forecast this variable in the simulations used to design a building.

For these reasons, multiple occupant behavior profiles are recommended when designing buildings. This method can be used to guide the decision-making process during the design phase. For example, the method can be applied to energy simulations with different levels of insulation or different WWRs, and the resulting probability distributions can be observed for energy consumption. In addition to considering the most likely or average value of energy consumption, the designer could also consider the possibilities of achieving extreme values depending on how occupants use the building systems

11.5 Case Study 4: Melbourne, Australia

Ye Kang, Jenny Zhou

11.5.1 Summary

This case study building was the first large-scale timber structure built to Passivhaus standard in the southern hemisphere. This case study analysis evaluated the interactional behavior between occupants and the building, multi-story student accommodation. Design specifications and in situ performance were compared to identify misalignments in three occupant-centric variables: presence profile, interaction with electrical appliances and lighting, and thermal comfort. Compared to a fixed value defined by the Passivhaus simulation model, the actual occupant presence varied significantly between in-semester and semester break, between weekdays and weekends, and between private rooms and shared spaces. The simulation underestimated the use of electrical appliances and lighting and overlooked its time dependency. The building also suffered from overheating problems that had not been identified in the design stage. The result of this study can contribute to a deeper understanding of human behavior and thermal comfort in Passivhaus buildings. The measured data can also help to refine the parameter setting for human factor variables in the future occupant-centric design.

11.5.2 Building Description

The case study building (see Figures 11.41–11.43) is a Passivhaus-certified six-story student accommodation building that is located in the mild temperate climate zone of Melbourne, Australia. The PH building has a gross floor area

Figure 11.41 Photograph of the building exterior.

Figure 11.42 Photograph of the studio room.

Figure 11.43 Photograph of a communal space.

Table 11.7 Thermal transmittances (U-value) and total areas of the Melbourne building envelope

Components	*Average U-value (W/m^2 K)*	*Total area (m^2)*
Wall system	0.308	2,814
Roof system	0.135	1,139
Ground floor system	0.843	1,009
Window	1.322	1,010

of ~5,200 m^2 that includes 150 independent studio rooms and various communal spaces. Each studio consists of a bedroom, an open-plan living/kitchen area, and a bathroom. The living/kitchen area is outfitted with a range of electrical appliances (cooktop, microwave, fridge, etc.). The communal spaces contain recreation rooms, communal kitchens, and a laundry room.

The building is of lightweight structure, with external walls and roofs built from cross-laminated timber (CLT) and a ground floor built from concrete panels. Rockwool and rigid foam insulation and triple-glazed windows were used to improve the thermal performance of the building envelope. The characteristics of the building envelope are summarized in Table 11.7. The building is equipped with three mechanical ventilation equipment with heat recovery (MVHR) units. The building management system (BMS) modulates air dampers to adjust the ventilation rate of the studios. The damper position remains in minimum mode (3.5 L/s) when the studio is vacant, and it adjusts to the max mode (10 L/s) and boost mode (25 L/s) based on the signal from the room key and bathroom light, respectively. When the average temperature of the floor exceeds 25°C for 10 minutes, the BMS will also activate the boost mode for the entire floor. The MVHR units are equipped with thermal batteries (via hot water) to provide tempered outdoor air to the student accommodations; the building has no active cooling systems. The building was occupied in February 2019.

11.5.3 Methodology

This section is arranged into three different sub-sections: (1) model and input variables, (2) in situ performance data collection and (3) TM52 method for overheating assessment, to address the objectives of this analysis.

11.5.3.1 Model and Input Variables

The Passive House Planning Package (PHPP) Version 9 simulation tool was used during the design stage to predict the building performance. PHPP is the only authorized software in the Australian context for PH certification (Australian Passive House Association, 2021). Similar to other building energy simulation tools, the PHPP is built upon energy conservation

principles and heat balance equations, but it models the entire building as one single zone and generates simulation results on a monthly basis owing to the limitation of the spreadsheet computing environment (Passive House Institute, 2015).

The simulation required a range of inputs from weather data to building service equipment. This work focused on three occupant-centric variables:

- *Presence profile*: The occupancy fraction (i.e., percentage of time that a space is occupied) was used to describe the presence profile. In the PHPP simulation, the indoor spaces were assumed to be occupied all the time with the occupancy fraction of 1.
- *Interaction with electrical appliances and lighting*: The energy demand was calculated from three variables; power rate, use frequency, and the total number of occupants (Eq. 1) (Passive House Institute, 2015). The PHPP manual (Passive House Institute, 2015) provided default settings for the first two variables (Table 11.8), and the last parameter was estimated based on the building use: one occupant per studio and eight additional residents for building management. The simulation was unable to capture the time variance of the appliance and lighting use because the PHPP applies a "per year" rate to the power rate or use frequency.

$$E_{el} = V_{\text{Norm}} \cdot h \cdot G \tag{11.2}$$

  where
  V_{Norm} is the power use of the appliance or lighting;
  h is the use frequency of the appliance or lighting;
  G is the total number of occupants.

- *Thermal comfort*: The PHPP applies overheating frequency (i.e., the percentage of time that the indoor temperature is above 25°C) to evaluate the thermal comfort of the building (Passive House Institute, 2015). When the annual overheating frequency exceeds 10%, the space is classified as overheating. To simplify the calculation, the PHPP database only specifies monthly average temperatures (Table 11.9) and a fixed

Table 11.8 The power rate and use frequency of electrical appliances and lighting

	Power rate	*Use frequency*
Dishwashing	0.8 kWh/use	65 use/(person-year)
Refrigerator	0.78 kWh/person-day	365 days/year
Cooktop	0.22 kWh/use	500 use/(person-year)
Television	80 W	1.5 hours/(person-year)
Small appliances	0.14 kWh/person-year	365 days/year
Lighting	10 W	8 hours/(person-year)

Table 11.9 Monthly average outdoor air temperature in Melbourne in the southern hemisphere

	January	*February*	*March*	*April*	*May*	*June*	*July*	*August*	*September*	*October*	*November*	*December*
T (°C)	20.6	20.8	19.0	15.8	13.0	10.7	10.1	11.0	12.7	14.6	17.1	18.8

Data were extracted from the PHPP database (Passive House Institute, 2015).

daily temperature swing (10°C). The PHPP evaluation completed for the case study building identified an overheating frequency of 6%, which meant there were no overheating concerns in the design stage.

In this case study analysis, the simulation results from these three occupant-centric variables are compared to in situ performance data to evaluate the interactional behavior between occupants and the multi-story student accommodation built to the Passivhaus standard.

11.5.3.2 In Situ Performance Data Collection

The building management system (BMS) and a wireless sensing platform were applied to collect in situ data for eight months from August 2019 to March 2020. The BMS recorded the energy use of the case study building and exterior temperature on an hourly basis. The indoor temperature and carbon dioxide (CO_2) concentration of indoor spaces were detected every 30 seconds using the wireless sensing platform. The monitoring devices were calibrated against standard reference instruments and displayed the accuracy of ±0.6°C for temperature and ±11 ppm for CO_2 concentration. Before the final data analysis and visualization, the sensor data were aggregated to hourly intervals to facilitate the comparison. Permission was granted to access 12 spaces in the building for device installation (Table 11.10). The 12 spaces spread over three floors and covered both studio rooms and communal spaces. Data collected by the BMS and the sensing platform were applied to pursue the three occupant-centric variables, as described below.

- *Presence profile:* The CO_2 concentration of indoor spaces recorded by the sensor nodes was used to determine the occupancy status and to generate the presence profiles. When the hourly CO_2 concentration

Table 11.10 The indoor monitoring stations and room characteristics

Room number	*Floor*	*Room type*	*Window orientation*
103	1	Communal	Northwest
108	1	Communal	Northwest
309	3	Studio	Northwest
314	3	Studio	Southwest
324	3	Studio	Southeast
327	3	Studio	Northeast
332	3	Communal	Northwest
609	6	Studio	Northwest
614	6	Studio	Southwest
624	6	Studio	Southeast
627	6	Studio	Northeast
632	6	Communal	Northwest

exceeded 550 ppm, the space was considered occupied. The 550 ppm was a cut-off value obtained from a four-day dataset measured during the Christmas holiday. It should be noted that this is a simplified approach as the indoor CO_2 concentration could be influenced by window operation and occupant behaviors. CO_2-based dynamic occupancy detection algorithms could further improve the accuracy of the outcomes.

- *Interactions with electrical appliances and lighting*: The BMS system disaggregated the energy use data of the case building into plug load, lighting, and other building service functions. The human interaction with electrical appliances and lighting was inferred from the BMS energy breakdown data.
- *Thermal comfort:* Considering the limitation of the fixed benchmark (25°C) in the PHPP tool (Fletcher *et al*., 2017), the TM52 method (Chartered Institution of Building Services Engineers, 2013), an adaptive method derived from EN 15251 (CEN, 2007), was applied in this study to assess the overheating risk of the building. The TM52 method is further detailed in the following section.

11.5.3.3 TM52 Method for Overheating Assessment

The TM52 method defines three criteria for overheating assessment. All three criteria, listed below, are associated with the exceedance (ΔT), which refers to the difference (rounded to the nearest integer) between the operative temperature of the indoor space and the TM52 benchmark. A space is classified as overheated when it fails any two out of three criteria specified by the TM52 approach.

- Criterion 1: Hours of exceedance, H_e, should not exceed 3% of the occupied hours ($H_e \leq 3\%$). H_e represents the total number of hours that the ΔT is greater than 0°C between November and March (typical non-heating season in the southern hemisphere).
- Criterion 2: Daily weighted exceedance, W_e, should be no more than 6°C-hours in any one day ($W_e \leq 6$°C-h). W_e refers to the hours when the indoor temperature is above the benchmark ($\Delta T \geq 1$°C) during occupied hours, weighted by a factor that is a function dependent on how many degrees the benchmark has been exceeded (Equation 11.3).

$$W_e = \sum (h_e \times W_F), \tag{11.3}$$

  where the weighting factor $W_F = 0$ if $\Delta T \leq 0$°C; otherwise, $W_F = \Delta T$, and h_e is the number of hours when $W_F = \Delta T$.
- Criterion 3: Maximum exceedance, max_ΔT, should be less than or equal to 4°C (max_$\Delta T \leq 4$°C). The max_ΔT represents the highest value of exceedance.

The determination of the exceedance (ΔT) and the TM52 benchmark (T_{ben}) is based on the exponentially weighted running mean outdoor temperature (T_{rm}) (Equations 11.4–11.6).

$$\Delta T = T_{op} - T_{ben} \tag{11.4}$$

$$T_{ben} = 0.33T_{rm} + 21.8 \tag{11.5}$$

$$T_{rm} = \begin{pmatrix} T_{out-1} + 0.8T_{out-2} + 0.6T_{out-3} + 0.5T_{out-4} + 0.4T_{out-5} \\ + 0.3T_{out-6} + 0.2T_{out-7}) / 3.8 \end{pmatrix} \tag{11.6}$$

where,

T_{op} is the operative temperature of the indoor space, considering the thermal uniformity of the case study building, indoor air temperature (T_{in}) is a reasonable approximation for operative temperature (T_{op}) (Tabatabaei Sameni *et al*., 2015).

T_{ben} is the benchmark.

T_{rm} is the exponentially weighted running mean outdoor temperature.

T_{out-1}, T_{out-2}, T_{out-3}, T_{out-4}, T_{out-5}, T_{out-6}, and T_{out-6} are the daily mean external temperature for the previous day, the day before, and so on.

11.5.4 Results and Discussion

A range of analyses was conducted to evaluate the interactional behavior between occupants and the case study building. The results are broken down into four sub-sections: (1) occupant presence, (2) use of electrical appliances and lighting, (3) thermal comfort, and (4) recommendations to improve the PHPP software. Each is discussed in turn below.

11.5.4.1 Occupant Presence

Figure 11.44 shows the occupancy fraction of the studio rooms (marked as orange) and communal spaces (marked as blue) of the case building. The occupancy data were disaggregated by in-semester/semester break and weekday/weekend designations. In contrast to the default setting in the PHPP tool (i.e., the building was assumed to be always occupied), the actual occupancy fraction of the measured spaces fluctuated.

There were significant differences between in-semester and semester break occupancy. The studio rooms had occupancy fractions ranging from 0.32 to 0.79 (with an average of 0.56) during the semester, but the values were decreased to 0.03–0.09 (with an average of 0.07) during the break. Similarly, the off-peak occupancy fraction (0.01–0.68, with an average of 0.35) was much lower than the in-semester values (0.01–0.18, with an average of 0.10) in communal spaces. The decrease in occupancy fraction during the semester break could be attributed to the increased vacancy in student accommodation during the semester break.

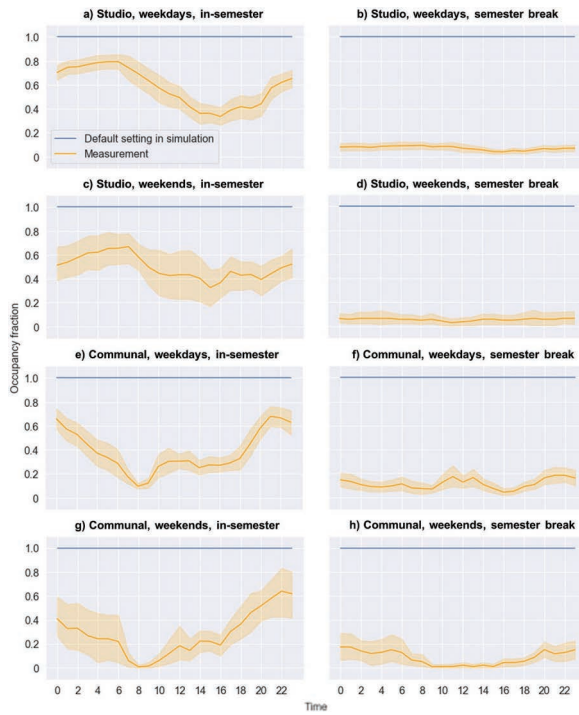

Figure 11.44 Measured occupancy fraction of the studio rooms on (a) weekdays, in-semester, (b) weekdays, semester break, (c) weekends, in-semester and (d) weekends, semester break, and communal spaces on (e) weekdays, in-semester, (f) weekdays, semester break, (g) weekends, in-semester, and (h) weekends, semester break. The uncertainty bounds represent the standard deviation. Semester: August 2019 to November 2019, March 2020; Semester break: December 2019 to February 2020.

The occupancy schedules also varied between weekdays and weekends during the semester. In studio rooms, a slight reduction in occupancy fraction could be found on weekends (0.32–0.67, with an average of 0.50; Figure 11.44c) compared to weekdays (0.34–0.79, with an average of 0.58; Figure 11.44a). A similar trend could be observed in communal spaces (0. 10–0.68, with an average of 0.38 for weekdays; Figure 11.44e; 0.01–0.64, with an average of 0.28 for weekends; Figure 11.41g). The decreasing occupancy fraction on weekends could be associated with the fact that the students had more opportunities to attend off-campus activities during this period and thus left their studios for a considerable amount of time. Considering the constantly low occupancy fraction (<0.2) of the case study building during the semester break, no discernible discrepancy in occupancy profiles could be discovered between weekdays and weekends.

The discrepancy in occupancy profiles between studio rooms and communal spaces also needs to be considered. During the weekdays of the semester (Figure 11.44a), the studios displayed the highest occupancy fraction (ranging between 0.7 and 0.79) between 00h00 (midnight) and 6h00 because most occupants preferred to stay in the studio and sleep during this period. Then, the values reduced significantly until 16h00 (occupancy fraction of 0.34), likely because students woke up and left their studios to attend various courses and activities.

After 16h00, people began to return to their studios and the occupancy fraction increased to 0.65 at 23h00. In contrast, a significant reduction of the occupancy fraction could be found from 0.66 to 0.10 between 00h00 and 8h00 in communal spaces (Figure 11.44e), as individuals left communal spaces and returned to their studios for sleeping. After that, the value rose to 0.30 at 11h00 and then fluctuated between 0.25 and 0.31 until 18h00. In the evening, as individuals entered the communal spaces for entertainment and group activities, the occupancy fraction escalated again and reached the maximum value (0.68) at 21h00. Later, the value declined until 23h00. The discrepancy in occupancy profiles between studio and communal spaces could also be observed on weekends of the semester and during the semester break.

11.5.4.2 Use of Electrical Appliances and Lighting

Figure 11.45 shows the power density of electrical appliances and lighting. Similar to occupancy profiles, the on-site data related to electrical appliances were categorized by in-semester/semester break and by weekday/weekend. In comparison to the default settings in the PHPP tool (1.9 W/m^2 for electrical appliances; 0.1 W/m^2 for lighting), the measured power density of electrical appliances and lighting ranged from 1.0 to 5.5 W/m^2 (an average of 2.7 W/m^2) and from 0 to 2.9 W/m^2 (an average of 1.7 W/m^2), respectively.

As expected, the power density of electrical appliances and lighting was much higher during the semester as compared to the semester break. Electrical appliances in-semester value (2.6–5.5 W/m^2, with an average of 3.6 W/m^2) was approximately three times the off-peak data (1.0–1.8 W/m^2, with an average of 1.3 W/m^2). A similar trend was observed for lighting, the case study building required 0.5–2.9 W/m^2 (with an average of 2.1 W/m^2) for lighting during the semester, and the power density was reduced to 0–2.1 W/m^2 (with an average of 1.0 W/m^2) during the break. The significant reduction in power density during the semester break could be attributed to the increased vacancy, as mentioned in the previous section.

The variation in the power density of the electrical appliances could also be observed between weekdays and weekends during the semester. The power density of the electrical appliances decreased from 3.6 to 2.7 W/m^2 between 00h00 and 5h00 (Figure 11.45a) as individuals stopped using electrical appliances and fell asleep. When students woke up, the value

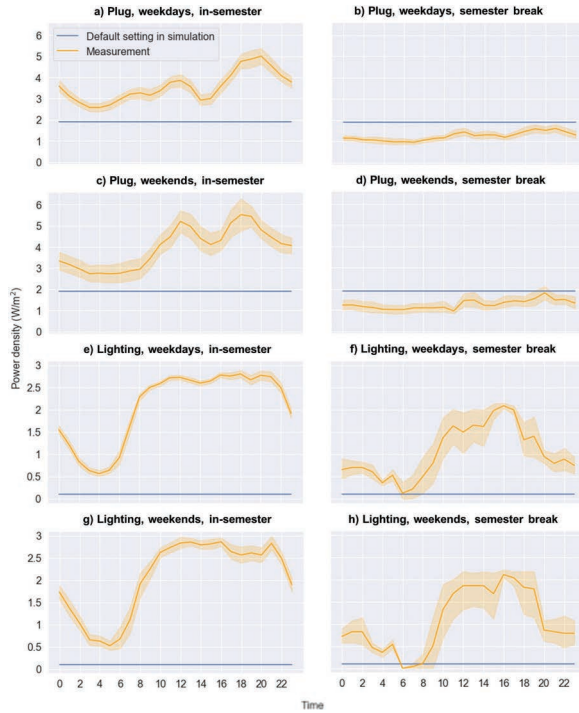

Figure 11.45 Power density of electrical appliances on (a) weekdays, in-semester, (b) weekdays, semester break, (c) weekends, in-semester and (d) weekends, semester break and lighting on (e) weekdays, in-semester, (f) weekdays, semester break, (g) weekends, in-semester and (h) weekends, semester break. The uncertainty bounds represent the standard deviation. Semester: August 2019 to November 2019, March 2020; Semester break: December 2019 to February 2020.

increased and reached the first peak (3.9 W/m^2) at 12h00 (lunchtime). Then after another reduction (12h00 to 14h00) and growth (14h00 to 20h00), the power density reached the second peak (5.2 W/m^2) at 20h00 (suppertime). The two peaks could be attributed to the cooking and corresponding energy demand related to kitchenware (e.g., microwave oven and cooktop). During the weekends, the electrical appliances were found to consume more energy than on weekdays (Figure 11.45c). The power density reached 5.2 and 5.5 W/m^2 at 12h00 (first peak) and 18h00 (second peak). The higher energy consumption during the weekends can be related to the fact that students did not have any courses during this period and could spend more time cooking. During the semester break, no significant difference in the power density of electrical appliances was observed between weekdays and weekends due to high vacancy.

There was no discernible discrepancy in the lighting power density between in-semester weekdays and weekends, despite the increased vacancy during the weekends (see the previous section). Considering the utility expense was amalgamated into the fixed rent, some vacant studio rooms might have had the lights left on during the weekends by less energy-conscious occupants. During the weekdays (Figure 11.45e), the power density of the lighting diminished from 1.6 to 0.6 W/m^2 between 00h00 and 4h00, as students fell asleep and turned off the lights. Then the value rose to 2.7 W/m^2 at noon with occupants getting up. After that, the power density fluctuated between 2.6 and 2.8 W/m^2 until 21h00, which was likely because individuals (who were not responsible for the energy bills) preferred to keep the lights on. After 21h00, the occupants began to rest, and the value dropped again. A similar profile was observed during the weekends (Figure 11.45g). No obvious variation was discovered in the lighting power density between weekdays and weekends during the semester break. It should be noted that considering the lights in the communal spaces were always on during the daytime, the lighting power density was observed to exceed 1 W/m^2 even during the semester break.

11.5.4.3 Thermal Comfort

The thermal comfort results based on the TM52 method are displayed in Table 11.11. It is worth mentioning that this table only shows data for five months (November 2019 to March 2020), which covered the non-heating season in the southern hemisphere. The remaining months were not in the scope of the TM52 analysis.

Although the PHPP simulation tool reported no overheating risk in the case study building, all 12 selected spaces were observed to have overheating

Table 11.11 TM52 analysis result summary

Room number	*TM52 method*			*Overheated (at least two criteria failed)*
	H_e *(%)*	*Annual max We (°C-h)*	*Annual max_ΔT (°C)*	
103	0	0	0	No
108	0	0	0	No
309	0.17	40	5	Yes
314	0.08	56	5	Yes
324	0.08	64	4	Yes
327	0.15	76	6	Yes
332	0.09	28	5	Yes
609	0.12	32	7	Yes
614	0.08	27	4	Yes
624	0.04	25	4	Yes
627	0.13	50	8	Yes
632	0.12	29	5	Yes

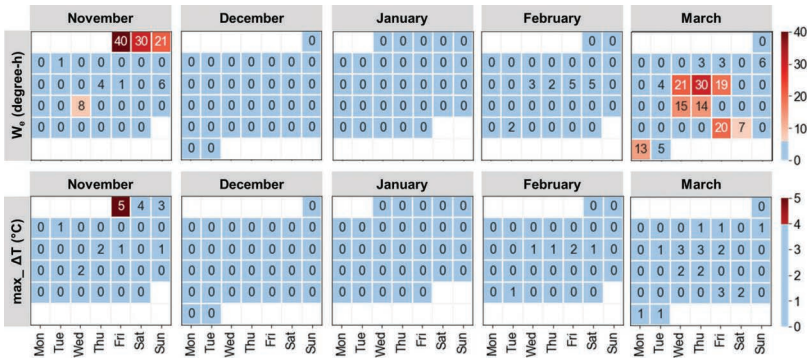

Figure 11.46 Daily weighted exceedance (W_e) and daily maximum exceedance (max_ ΔT) of room 309 between November 2019 and March 2020 in the southern hemisphere.

problems with the annual overheating frequency above 10%. Additionally, all the selected spaces on the third and sixth floors were classified as overheated based on TM52 analysis, as they failed both Criterion 1 and Criterion 2. Some occupants in the case study building also reported overheating problems. The overheating problem is likely because the PHPP recommended inputs underestimated the heat emitted from electrical appliances and lighting. As shown in Figure 11.46, the daily weighted exceedance (W_e) of room 309 was found to be higher than the threshold specified by the TM52 method (6°C-h) during the semester (i.e., November and March), likely because the in situ energy consumption for electrical appliances (with an average of 3.6 W/m^2, see Figure 11.45a and c) and lighting (with an average of 2.1 W/m^2, see Figure 11.45e and g) was much higher than that considered in the PHPP (1.9 W/m^2 for electrical appliances and 0.1 W/m^2 for lighting). The uncertainty in weather could also be a contributor. The maximum exceedance (max_ΔT) of room 309 was observed to reach 5°C, higher than the TM52 threshold (4°C), on the 1st of November (see Figure 11.46). In the PHPP software, the average monthly outdoor temperature in November was assumed to be 17.1°C (see Table 11.9) and a fixed value (10°C) was applied to represent the diurnal temperature fluctuation. In contrast, the maximum outdoor temperature recorded on the 1st of November reached 34°C. The maximum outdoor temperature measured on-site higher than that simulated in the PHPP software could be the main reason contributing to the high exceedance (ΔT) of room 309 on the 1st of November. Similar trends were observed in all the other selected rooms.

11.5.4.4 Recommendations to Improve the PHPP Software

The following strategies are proposed to reduce the performance gap of the Passivhaus case study building:

- The monthly quasi-steady state method in the PHPP software could be substituted by a dynamic building simulation model. The dynamic simulation could consider the variation of outdoor temperature and human interaction with plug load and lighting on an hourly basis. Thus, it could deliver more accurate simulation outcomes than the monthly calculation method. Additionally, the incorporation of dynamic simulation with the TM52 model could provide opportunities to better predict the overheating problems of the case building.
- A feedback loop could be integrated into the PHPP software to bring the predicted outcomes closer to reality. It is because the feedback mechanism could enable the incorporation of variations in occupant behavior and different building electrical appliance profiles into the PHPP simulation tool. The feedback loop could be used to better inform building design by identifying common mistaken assumptions. This process could be supported by various advanced methods, such as low-cost sensing techniques and post-occupancy evaluation.

11.5.5 Concluding Remarks

To summarize, the performance of a recently constructed Passivhaus student accommodation in the operational stage was compared to the corresponding PHPP simulation in the design stage to develop an in-depth understanding of occupant behavior in large Passivhaus buildings. The temporal schedule of occupancy, the human interaction with electrical appliances and lighting, and thermal comfort were analyzed and discussed.

The PHPP simulation assumed that spaces were always occupied, but this simplification does not work well, as evident by the fluctuating occupancy fraction. Discernible variation can be found between in-semester and semester breaks and between weekdays and weekends. The fluctuation of the occupancy fraction can be attributed to the discrepancy in occupants' activities. The design prediction underestimated the use of electrical appliance and lighting. The use frequency defined by the Passivhaus authority would have been a valid assumption for small family dwelling cases but not for the examined student accommodations. In addition, the occupants of the student accommodation may have been less energy-conscious with their appliance and lighting use since the utility expense was amalgamated into the fixed rent. There were also serious overheating issues that had not been identified in the design stage. The increased heat emission from electrical appliances and lighting and uncertainty in weather data contributed to the discrepancy in thermal comfort assessment.

Considering the limitation of the classical PH design applied in this study, adopting a dynamic building simulation model and feedback loop to recognize the context-dependent features of human behavior is suggested. Future occupant-centric building design should also consider the energy-consciousness of occupants, as it is a factor that can significantly affect occupant-building interactions and, consequently, building performance

11.6 Case Study 5: Redwood City, USA

Andrew Sonta, Thomas Dougherty, Rishee Jain

11.6.1 Summary

This case study considers the question of leveraging information on occupant behavioral patterns to optimize a commercial building's layout in terms of seat assignments in an effort to save energy. The case-study building is a three-story commercial office building located in Redwood City, California, USA, in a warm-summer, Mediterranean climate. Real-time data collected from one floor of the building was used to establish a correlation between zone-level lighting energy consumption and diversity in occupant behavior, where *diversity* refers to the level of differences in space use among occupants within a particular building zone. A data-driven surrogate simulation model was used to estimate lighting energy consumption as a result of changes to the building's layout. Both clustering-based and genetic algorithm optimization routines were introduced to find the layout that reduced lighting energy as much as possible. Through simulation, it was found that optimizing the building's layout can reduce lighting energy consumption by 5% compared to the existing layout. This study demonstrates the ability to use low-cost ambient sensing infrastructure to reconsider the layouts of existing buildings based on the past behavioral patterns of its occupants.

11.6.2 Building Description

This case study building is a three-story commercial office building located in Redwood City, California (Figure 11.47). The building is owned and operated by Stanford University and largely houses university operations staff. The building was completed in 2019. Plug load energy sensors were installed at each workstation on the third floor of the building (164 workstations) in June 2019, just before occupancy began (see sensor details in "Plug load energy sensors" below).

These plug load energy sensors enabled analysis of occupancy patterns. Workers were each assigned their own workstation, which did not change over the study period. The office design can be characterized as open plan, with large, shared office spaces in addition to meeting rooms of various sizes. Generally, occupants used the spaces during standard, but flexible, business hours: 7h00–19h00 Monday through Friday. Through the building management system's application programming interface (API), the energy consumption of the lighting system (see details in "Lighting system and zones" below) was also collected. The lighting system is controlled with infrared sensors by zone; 11 of the lighting zones service the 164 workstations in this office building. The data-collection period spanned August 1, 2019 to February 29, 2020. Due to sensor outages at the beginning of data collection, data collected between August 1 and September 30, 2019, was

Figure 11.47 Stanford case study building.

discarded. Data collected between December 16, 2019, and January 4, 2020, was also discarded due to irregularities during the university's winter holiday break. The analysis therefore included 132 full days of data. The collection of highly granular occupancy data alongside lighting energy data enabled analysis of the relationship between occupant behavior and energy consumption.

11.6.2.1 Plug Load Energy Sensors

Installed at each workstation on the third floor of the building were Zooz SmartPlugs, which communicated using Z-Wave technology to a Samsung SmartThings hub. A schematic of the sensing strategy is shown in Figure 11.48. The sensors reported power consumption values any time the power consumption varied by more than 0.1 W. Consistent with previous work (Sonta *et al.*, 2018; Sonta and Jain, 2020), the power consumption was aggregated to 15-minute intervals. This 15-minute scale offered insight into occupant behavioral patterns while reducing noise.

11.6.2.2 Lighting System and Zones

The building is equipped with an automated lighting system that operates using infrared occupancy sensors, daylighting sensors, and schedules. This system is controlled by zone (as shown in Figure 11.49). The occupancy sensors turn on the lights in the zone if they sense any motion in the past

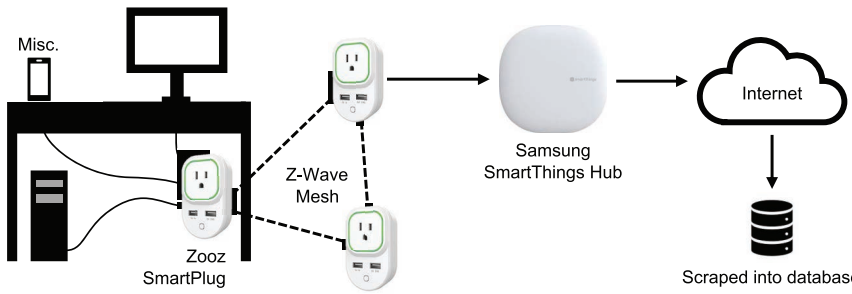

Figure 11.48 Schematic of plug load sensing data collection.

Figure 11.49 Floorplan diagram, with open office areas shown in white, workstations and meeting rooms in blue, and the ten lighting zones servicing workstations in red.

20 minutes (10 minutes on the weekends). Eleven of the lighting zones service all 164 workstations. There are other lighting zones that service the small, shared spaces of the building (e.g., meeting rooms, break areas), but analysis was restricted to the zones that service workstations, as this study focused on how workstation space use impacts lighting energy for those spaces. This lighting energy data were scraped for each fixture at one-hour intervals.

11.6.3 Methodology

This section describes the methodology for optimizing the layouts of existing buildings by leveraging individualized occupancy data, that is, data ascribed to each individual occupant (as outlined in Figure 11.50). First, the time series plug load energy data at each workstation was used to model occupancy schedules. The methodology introduced by Sonta *et al.* (2018)

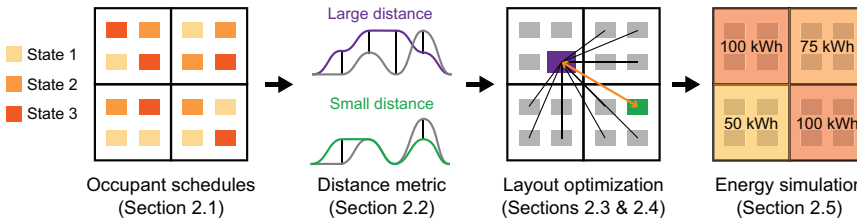

Figure 11.50 Methodology overview: Occupant schedules were used to measure zone diversity, which enabled layout optimization. Energy simulation was used to estimate the impact of layout optimization.

was leveraged to abstract the raw time series data into activity states, which describe patterns of space use and individual schedules. A distance metric, referred to as zone diversity, was introduced to describe the level of differences among the occupants' schedules within each lighting zone. This metric allowed the characterization of the relationship between zone diversity and empirical energy data, which has been theorized in the literature to be a positive relationship (Yang *et al.*, 2016). Given this theoretical relationship, two optimization routines were developed to rearrange the occupants' seat assignments. One optimization spatially clustered occupants in a manner that reduced zone diversity. The other, a genetic algorithm, leveraged a data-driven surrogate model for simulating energy consumption based on the layout. This surrogate model used both the occupant layout and the individualized occupant behavior data to estimate the energy consumption of the building's lighting system.

11.6.3.1 Individualized Occupant Schedules from Plug Load Energy Data

This section briefly describes the process for abstracting data streams from plug load monitoring devices into individualized occupant schedules. The key insight that enabled this process was that time series plug load energy signatures provide information about how occupants are interacting with their workstations. For example, higher energy consumption indicates that occupants are interacting with the electronic equipment at their workstations and are therefore likely to be actively using their workspaces. Lower energy consumption indicates that occupants have stopped interacting with this equipment and are likely away from their workstations. In this case study, the time series plug load data was defined as $\mathbf{X}_{i,\ d}$, where i is the occupant index and d is the day index. Each entry in $\mathbf{X}_{i,\ d}$ is a vector $\{x_1,..., x_T\}$ where T is the number of time steps during the day (here, $T = 96$). The method described in detail in Sonta *et al.* (2018) was used to map this raw

data onto the abstracted occupant schedules: $\mathbf{X}_{i,\,d} \rightarrow \mathbf{S}_{i,\,d}$. This mapping leveraged a variational Bayesian Gaussian Mixture Model to cluster the raw time series data into discrete states. As in Sonta *et al.* (2018), a two-step process was used, whereby the data for each occupant for each day was first clustered into two components, effectively clustering out the low-energy data (data near 0 W). The higher energy data was then clustered again, as this data generally maintains higher variability. As in past work, the higher energy data was clustered into two further components, giving three components in total: low energy, medium energy, and high energy ($\mathbf{X} \rightarrow \mathbf{S}$, where $s^{t}_{i,\,d} \cdot \in \cdot \{1,2,3\}$). Hereafter, these time series of clustered states are referred to as occupant schedules.

11.6.3.2 Zone Diversity

Given these individualized occupant schedules, a method was adapted from the building operation literature for characterizing the similarities and differences in the behavioral patterns of all occupants within a zone. These similarities and differences are referred to as *zone diversity*, with a higher zone diversity indicating a greater level of differences in behavior. Based on the work of Yang *et al.* (2016), this diversity metric was computed as the Euclidean distance among all vectors containing the occupant schedule data. It should be noted that other distance metrics could have been used (e.g., Manhattan distance, cosine similarity), but it was found that the specific distance metric did not have a meaningful impact on the analysis. With the schedule data defined as $\mathbf{S}_{i,\,t}$, where i is the occupant index and t an arbitrary time index, the distance between any two occupants i and j was computed via Equation (11.7):

$$d_{i,\,j} = \sqrt{\sum_{t=0}^{T} \left(\mathbf{S}_{i,\,t} - \mathbf{S}_{j,\,t}\right)^2} \tag{11.7}$$

The distances between all pairs of occupants were computed within each zone, which formed a distance matrix. This matrix was normalized by the total number of entries (excluding the diagonals, because the distance between occupants and themselves is 0). This normalized value is the overall *zone diversity*. Then, zone diversity computed over the course of a single day (i.e., $T = 96$) was compared to the energy consumption of the lighting system summed over a single day.

11.6.3.3 Optimizing Layouts: Naïve Clustering

The zone diversity metric quantifies the level of differences in occupant dynamics within each building zone. Given that higher zone diversity can be expected to cause more energy consumption, a clustering algorithm was

developed to change the occupant layout in an effort to reduce the diversity. A challenge in working with time series data is that the dimension of the vectors used for the distance calculation can grow quickly (e.g., 35,000 signals per year per occupant in our case). Distance metrics are known to be costly to compute and to potentially lose meaning when applied to data of such high dimensionality—often referred to as the curse of dimensionality. Therefore, singular value decomposition (SVD) was used in this study to reduce the dimensionality of the occupancy data without losing valuable information. SVD was applied to the occupant schedule data matrix $\mathbf{S}$, which has dimension $I \times D \cdot T$. The user can choose the number of dimensions d retained, up to I (in this case, 151), so that the resulting matrix is $I \times d$ with $d \leq I$. It should be noted that the zone diversity metric can be computed for either the unreduced data or the reduced data.

The data in $\mathbf{S}$ (reduced or otherwise) can then be used to cluster occupants. The next paragraphs describe the stochastic optimization routine used in this study for reducing zone diversity based on past occupancy data. This particular clustering problem had the real-world constraint that each building zone had a predefined size (i.e., number of workstations). Therefore, the resulting cluster sizes needed to match the sizes of the zones, which prevented the use of standard clustering algorithms such as *k*-means. The clustering algorithm simulated occupant "swaps", whereby two individuals swap locations, and then the resulting zone diversity was calculated.

Figure 11.51 outlines the algorithm. First, a random occupant, with replacement, was selected. Then, the effect on overall zone diversity across all building zones was simulated when the selected occupant was swapped with all other occupants in the building. The swap that produced the largest reduction in overall zone diversity was completed. This swap could include the null action of swapping the occupant with itself. The process was repeated by manually setting an iteration limit, beyond which no further improvement in overall zone diversity was seen. It should be noted that this stopping criterion could be automated if desired.

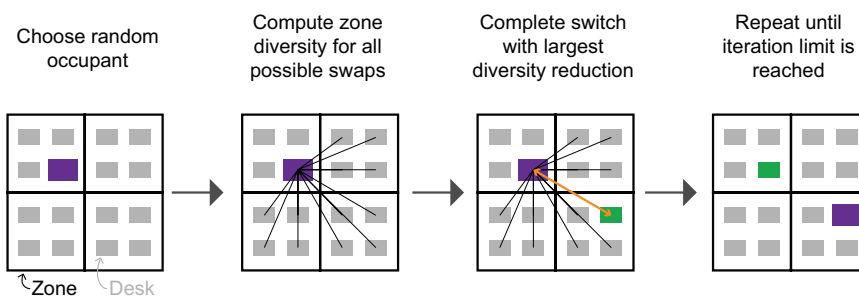

Figure 11.51 Occupant clustering algorithm.

11.6.3.4 Optimizing Layouts: Genetic Algorithm

The spatial optimization problem considered in this case study has an extremely large solution space. In an effort to fully explore the solution space and gain confidence in our clustering approach, an optimization routine that made direct use of our expected energy outcomes was also implemented. The clustering approach was designed to reduce zone diversity efficiently, but it does not explicitly consider energy consumption of building systems. It assumes that reducing zone diversity will have the effect of reducing energy consumption because these two concepts are hypothesized to be related. However, in this study, to optimize explicitly for energy, a simulation engine was required for predicting energy as new layouts are produced. The genetic algorithm optimization approach used to explicitly optimize for energy reduction is described here, and the data-driven surrogate simulation model is described in the following subsection.

Genetic algorithms belong to a class of evolutionary optimization algorithms originally inspired by the process of natural selection. They make use of a fitness function, which in our case study was expected energy consumption. This study's genetic algorithm routine started with a set of random design points x—in this case, occupant layouts—in an initial population **P**. The energy consumption of each design point was evaluated, and the **B** best performing designs were chosen as well as **R** random designs in order to maintain diversity. A key step in genetic algorithms is the recombination of selected designs in order to produce a new generation of designs based on the previous generation. For a pair of selected designs, this recombination was done c times. The first step is crossover, whereby a random selection of the two occupants in the two "parent" designs was selected for each desk location. The next step in recombination is mutation, which occurred with probability m. If mutation did occur, a random occupant in each zone was swapped with a random occupant in another random zone. This recombination was repeated until a new generation was formed. This overall process repeated G times. Figure 11.52 represents the algorithm and a visual summary of the crossover and mutation steps.

11.6.3.5 Data-Driven Surrogate Energy Simulation Model

To evaluate the impact of the occupant layout on energy consumption, a simulation engine that considers the key features of occupant layout and historical occupant schedule data was implemented. There are two major categories of building energy simulation: physics-based thermodynamic models (e.g., EnergyPlus), and data-driven "surrogate" models. Thermodynamic models can be particularly helpful when modeling heat flows, such as in the case of HVAC systems. However, these models are also quite complex and can be prohibitively time-intensive when evaluating many different

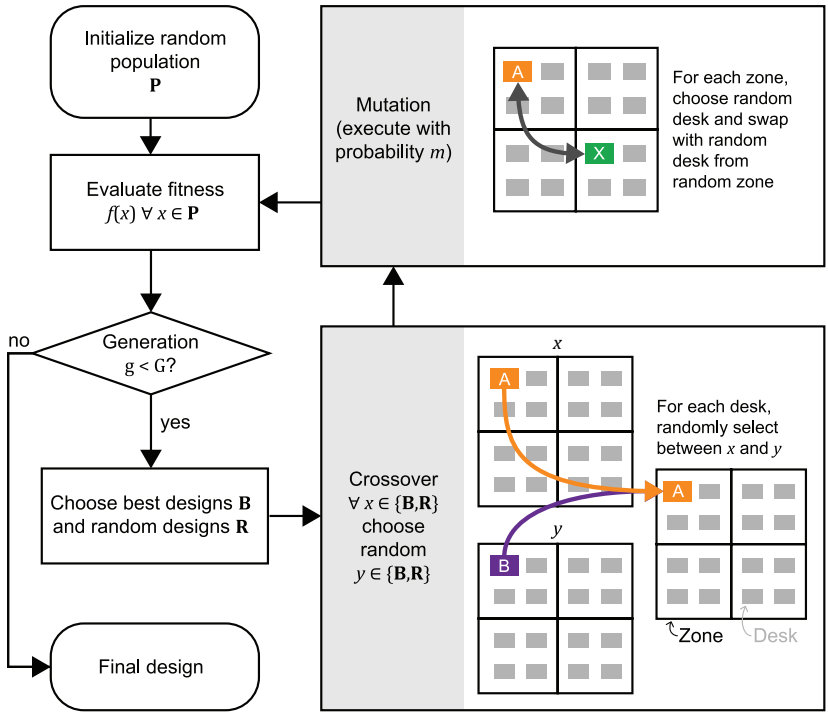

Figure 11.52 Genetic algorithm adapted for building layout optimization.

alternatives. Data-driven simulation models are growing in popularity for a variety of tasks and significantly reduce the time cost of prediction.

Because the present case study considers the lighting system, which is controlled through simple on/off sensors, a data-driven surrogate model was chosen for simulation. This surrogate modeling approach amounted to a machine learning problem that considered the study's key features (layout and schedules) to predict lighting energy consumption. We tested several models—multiple linear regression (MLR), support vector regression (SVR), random forests (RF), and artificial neural networks (ANN)—to determine the most robust model for the study's purpose. Each of these models has been applied to energy prediction tasks in the past (Ekici and Aksoy, 2009; Jain *et al.*, 2014; Ahmad *et al.*, 2017; Wang *et al.*, 2018). Key aspects of the surrogate modeling tests are listed below.

- **Features:** Seven specific features for this prediction task were identified:
  - s_1, s_2, s_3: the occupant energy states as described above, for each occupant in each zone.
  - Hour of day (0–23)

- Day of week (0–6)
- Weekend/weekday indicator (0 or 1)
- Zone number (0–number of zones)

It should be noted that the inclusion of both the day or week feature and the weekend/weekday feature can introduce multicollinearity. While this may reduce confidence when conducting hypothesis testing, it does not negatively impact the power of the machine learning algorithms. For the non-tree-based models (i.e., MLR, SVR, and ANN), the day of week and zone number features were one-hot encoded. For these models, the hour-of-day feature was also transformed using sine and cosine transformations to preserve cyclicity. Lastly, the state count features were transformed using a sigmoid function, as there are diminishing returns to having increasing occupants in each state. All features were scaled to fall between 0 and 1. These transformations are not required for the RF model, as the decisions on the trees in the model are invariant to this scaling.

- **Training and testing:** The data was split into a training set and a test set, using fivefold cross validation on the training test for model development. The training/test split was 80%–20%, and the choice was made to preserve the time-series order in this split so that the time-series nature of the predictions could be visualized.
- **Hyperparameter tuning:** For the high-performing models, any hyperparameters were tuned using fivefold cross validation on the training set. The specific hyperparameters for the high-performing models are discussed in "Data-driven prediction of energy consumption" below.

With this surrogate modeling approach defined and the layout optimization routines discussed above, simulation-based results from layout optimization can be analyzed.

11.6.4 Results and Discussion

This section describes the key results from the case study analysis and discusses their significance for occupant-centric design. The results are broken down into three sections: (1) analysis of zone diversity and energy consumption, (2) data-driven surrogate model performance, and (3) analysis of occupant layout optimization.

11.6.4.1 Energy Consumption versus Zone Diversity

A regression analysis was completed between the lighting energy consumption and the zone diversity metric. The analysis involved each of the 11 zones using energy and diversity data aggregated by day over the data-collection period. Zone diversity was computed using the Euclidean distance of the 96-dimensional vectors for each zone for each day, and the average lighting

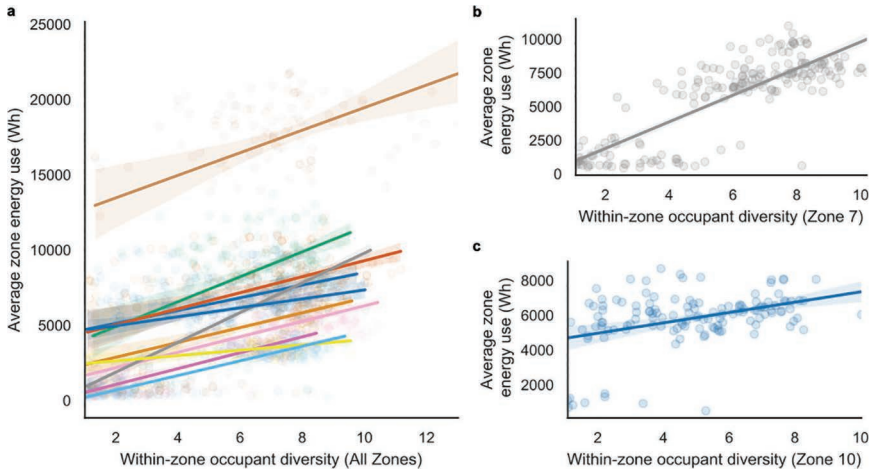

Figure 11.53 Relationship between zone diversity metric and energy consumption along with regression fits and confidence intervals for (a) all zones—with colors representing different zones, (b) zone with the largest regression coefficient (zone 7), and (c) zone with the smallest regression coefficient (zone 10).

consumption was computed across lighting fixtures within each zone. The regression analysis found that there exists a positive relationship between energy consumption and zone diversity for each zone, with the p-values for the t-statistics being significant at the 0.001 level for all zones. Figure 11.53 shows the data along with the regression lines for (a) all zones, (b) the zone with the strongest relationship in terms of the regression coefficient (zone 7), and (c) the zone with the weakest relationship (zone 10).

This result suggests that reducing zone diversity would be a means to reduce the energy consumption of the lighting system. The following sections present the results for simulating energy consumption based on occupant schedules as well as optimizing building layouts in order to reduce this energy consumption.

11.6.4.2 Data-Driven Prediction of Energy Consumption

The four models described above (MLR, SVR, RF, and ANN) were tested using the fivefold cross-validation methodology. Table 11.12 shows the performance of each model, as estimated through cross validation, using standard metrics, as well as the time required for both training and prediction in this case. The RF model performed the best in terms of MAE, while the ANN performed the best in terms of MSE and R^2. Therefore, these two models were chosen for hyperparameter tuning. Again, fivefold cross

Table 11.12 Energy prediction model results on fivefold cross-validation

Model	*Mean absolute error (MAE)*	*Mean squared error (MSE)*	*Explained variance (R^2)*	*Time for training (s)*	*Time for prediction (s)*
Multiple linear regression	9.55	141	0.534	0.0311	0.00198
Support vector regression	7.13	118	0.614	30.9	4.38
Random forest regression	6.11	98.2	0.678	2.82	0.0983
Artificial neural network	6.29	88.7	0.710	54.8	0.0105

Table 11.13 Energy prediction model results after hyperparameter tuning on both fivefold cross-validation and final test set

Model	*Errors on CV*			*Errors on test set*	
	Mean absolute error (MAE)	*Mean squared error (MSE)*	*Explained variance (R^2)*	*Explained variance (R^2) Hourly*	*Explained variance (R^2) Daily*
Tuned random forest regression	6.27	87.1	0.715	0.740	0.834
Tuned artificial neural network	6.28	88.5	0.710	0.734	0.817

validation was performed, and these parameters were tuned using a grid search. The final parameters for each model were as follows:

- ANN: single hidden layer of size 100, tan*h* activation function, Adam solver, learning rate of 0.01.
- RF: 200 trees, minimum split size of 50, minimum samples per leaf of 2, maximum depth of 300, bootstrap used in model training.

Model performance after training is shown in Table 11.13. The RF model outperformed the ANN model after hyperparameter tuning. In addition to calculating R^2 for hourly lighting energy prediction values, the data by day was also aggregated and the R^2 for these daily values computed. Prediction improved for both models, especially the RF model, after this aggregation.

Figure 11.54 shows the actual vs. predicted energy consumption (using the tuned RF model) for the first seven days in the test set for zone 1. The model, while not perfect, accurately captured the major jumps between low energy and high energy consumption. One of the benefits of the RF model is that

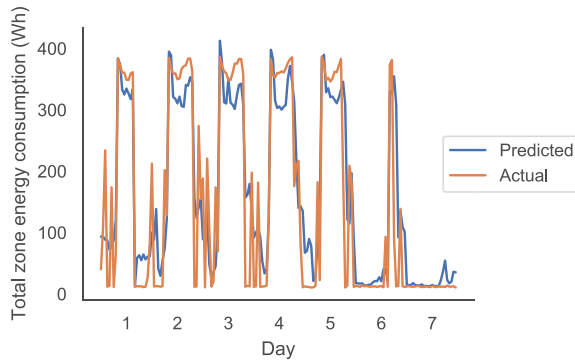

Figure 11.54 Example predicted (using tuned RF model) versus actual energy consumption data for the first seven days of data in the test set for zone 1.

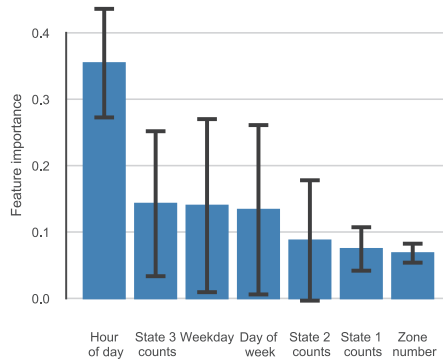

Figure 11.55 Feature importance for the final tuned random forest regression model.

it is quite interpretable in that the importance of each feature in the model can be quantified. The feature importance was calculated using the Gini importance metric, which can be interpreted as the relative number of times tree decisions involved a particular metric (see Figure 11.55). The number of occupants in state 3, the high-energy state, was the second most important feature. This finding may explain why the jumps between high and low energy consumption were accurately captured in the simulation model: the presence of occupants causes the lights to turn on, and this was accurately captured in the model.

11.6.4.3 Occupant Layout Optimization

The surrogate simulation model was leveraged to estimate the energy consumption of the lighting system for the existing occupant layout using the full

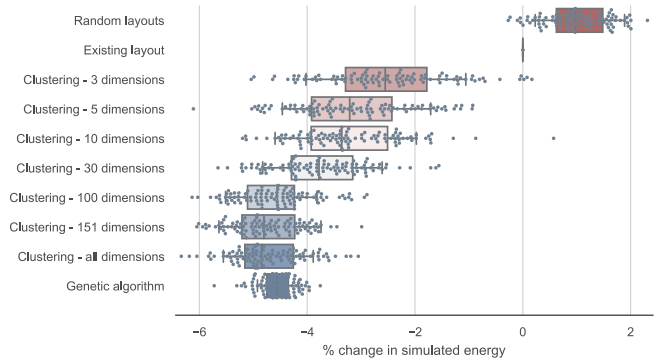

Figure 11.56 Simulated energy consumption (expressed as % change from the existing layout) for random and optimized building layouts.

132 days of data, which serves as a baseline. One hundred random occupant layouts were also produced and energy consumption was estimated again. Then, the clustering-based algorithm was applied using increasing dimensionality (3, 5, 10, 100, 151, and full dimensionality without reduction). The genetic algorithm was also implemented, which explicitly used the surrogate model in its optimization. For each optimization option, the algorithm was executed 100 times to produce 100 layouts, and the expected energy consumption was simulated for each. The results are shown in Figure 11.56. The 100-dimension clustering, 151-dimension clustering, full-dimension clustering, and the genetic algorithm all performed very similarly, resulting in a 5% reduction in expected energy compared to the existing layout and a 6% reduction compared to random layouts. An important result to highlight is that the distance-based clustering algorithm performed about the same as the genetic algorithm, which suggests that high-performance layouts can be generated without designing an optimization routine that explicitly considers energy consumption.

It is interesting to note that the random layouts performed slightly worse than the existing layout. There are many possible explanations for this. One likely explanation is that people tend to align their behavior to those around them, as documented in previous work (Chartrand and Bargh, 1999). In other words, individuals' actions could be influenced by what they see their physical neighbors doing. For example, a particular occupant might be inspired to take a coffee break when they see their neighbor doing so instead of going at a random time, which would have the effect of reducing the zone diversity metric. This possibility has notable implications for the interpretation of this study's results because the results were based on the assumption that occupants' behavior would not change when their seat assignments changed. While this possibility is unlikely to be completely

true (and is therefore a limitation of this study's approach), an important question is what the direction of the impact would be if individuals did in fact change their behavior. If occupants tend to assimilate their behavior to those around them, as this study's random versus existing results suggested, then it is quite possible that given new layouts, people will again assimilate to those around them, and thus an even further reduction in energy consumption might be expected. It is also possible that people would change their behavior after reassignment in other ways. Therefore, future work is recommended to test the empirical effects of true layout changes in office buildings.

11.6.5 Concluding Remarks

This case study demonstrated how capturing data on individualized occupant dynamics within existing buildings can be helpful for improving spatial design throughout the building's use phase. Using ambient plug load energy sensors at the desk level, individual schedules of behavior were captured. Higher diversity (i.e., more differences) in behavior within individual lighting zones correlated with higher energy consumption of the zone's lighting system. Two novel optimization methods were applied: (1) a naïve clustering approach that used only the occupant schedule data, and (2) a genetic algorithm that actively made use of a data-driven energy simulation engine. For this surrogate model, a random forest model was able to accurately predict the lighting system's energy consumption. Both spatial optimization routines could reduce lighting energy consumption by 5% compared to the existing layout and 6% compared to a random layout. Overall, this case study demonstrated the added value of reconsidering commercial buildings' spatial designs after occupancy has begun. This approach offers new opportunities for achieving sustainable energy targets in existing buildings and ensuring that buildings perform well throughout their life cycle.

11.7 Case Study 6: Niederanven, Luxembourg

Ghadeer Derbas, Karsten Voss, Tugcin Kirant Mitic

11.7.1 Summary

This case study presents the methodology and key findings of a field study conducted on a mid-rise office building located in Niederanven, Luxembourg. The study focused on the building's automated shading system activation and the interaction between occupants and the shading system with the aim of identifying occupant-centric rules for optimal shading design solutions. The study included a design investigation, data monitoring statistical analysis, a questionnaire, and a simulation-based analysis. The design investigation included an interview with the building designer to

better understand the shading system design characteristics and selection criteria. The data monitoring was performed under summer conditions in 2019, and the questionnaire was conducted in 2021 under similar conditions. Finally, the simulation-based analysis evaluated the daylighting and energy performance of the shade control strategy.

Contrary to expectations and previous studies' findings (Reinhart and Voss, 2003, Meerbeek *et al*., 2014), the present study found relatively few interactions between the occupants and the shading system, though more interactions occurred when the occupant was located closer to the button for manual shade adjustment. Building orientation, social constraints, and time of day were found to influence the manual activation of shading systems. The statistical analysis of the monitoring data showed the low performance of a regression model and the superior performance of data mining techniques. The main takeaways from this study for designers and researchers include: (1) the use of internal/external shading systems can lead to optimal results (i.e., fewer override actions), (2) the definition of control thresholds is essential, and (3) the deployment of lighting sensors is beneficial. On the operation level, simple and robust shade control strategies are recommended.

11.7.2 Building Description

The case study building was the new Headquarters Goblet Lavandier, a five-story office building located in Niederanven, Luxembourg. The building received DGNB (Deutsche Gesellschaft für Nachhaltiges Bauen) Platinum certification in 2018. The building is located in a temperate oceanic climate (Cfb) with a mild marine winter and warm summer with no dry season. The building is a quadrilateral concrete structure (25 m × 25 m) with a galvanized metal sheet façade (see Figure 11.57). It consists of three underground parking floors, a ground floor, and four upper floors (the fourth floor is rented). The building core includes circulation and washrooms and creates a naturally daylit office zone and passive night cooling. The moderate use of transparent surfaces (fenestration) in combination with external Venetian blind and inner textile screen play a central role in the energy efficiency and daylight concepts of the building design. Table 11.14 provides further details about the building.

11.7.2.1 Monitored Offices

Forty-seven offices were monitored over 66 working days from June to mid-September 2019. The majority of the offices are located along the quadrilateral perimeter facing one of the four cardinal directions (see Figure 11.58). The offices are situated on three floor levels and are occupied by an average of two to six workers per office (see Figure 11.59). The offices' windows are the same in width and height. Each window is equipped with a double

Figure 11.57 Perspective view of Luxembourg building, Christian Bauer & Associés Architects.
Source: Jürgen Leick from Goblet Lavadier.

shading system with an external Venetian blind (type Warema E80) and an inner textile screen operated manually to avoid glare discomfort.

11.7.2.2 Configuration of Automated Shading System

The automated external blinds combined with inner glare protection are a reflection of design considerations such as more individual workplace control and passive solar gains in winter. Due to the extra cost, this "double system approach" (see Figure 11.60) is not common. The designer was interviewed and the design briefs and architectural documents were investigated in-depth in order to define the design characteristics and selection criteria of the shading systems (more details in "Design Investigation" below).

The shading control strategy was developed based on the designer's experience. The external shading system is operated automatically based on light and temperature control thresholds. Occupants can override the blind position and tilt the slat angle to different positions (horizontal slat equal to 0°, 60°, and 80°). Any manual interventions disable the automated

Table 11.14 Luxembourg building general characteristics (Lichtmess, 2018)

Item	*Description*
Net floor area (NFA)	2,600 m^2
Area-to-volume ratio	0.31 m^{-1}
Window-to-wall ratio (WWR)	43% per façade
No. of employees in offices	138 employees (30–40 employees during the COVID-19 pandemic, July and August 2020)
Year of completion	2018
Thermal insulation	U-walls: 0.13 W/m^2 K, U-roof: 0.13 W/m^2 K, U-floor: 0.17 W/m^2 K
Windows	U-value: 0.75 W/m^2 K, g-value (SHGC): 0.49, color rendering: 96%
Ventilation	11,000 m^3/h total air volume control depending on CO_2 concentration, individual air volume control in meeting rooms. Highly efficient heat recovery 80.8%
Shading systems	• External Venetian blind (upper threshold if irradiance on the façade exceeds 400 W/m^2, lower threshold 250 W/m^2), g-tot = 0.07 • Inner textile screen (T_s = 8%, R_s = 12%, A_s = 80%)
Cooling system	• Passive night cooling to cover 20% of the cooling energy demand • Passive ground cooling to cover 80% of the rest of the cooling demand • A heat pump can be switched on only in hot weather
Heating system	Geothermal heat pump with an array of vertical probes (i.e., liquid-filled tubes installed in the drilled hole)
Electricity demand and generation	23.7 kWh/(m^2 a), PV = 14.5 kWh/(m^2 a)

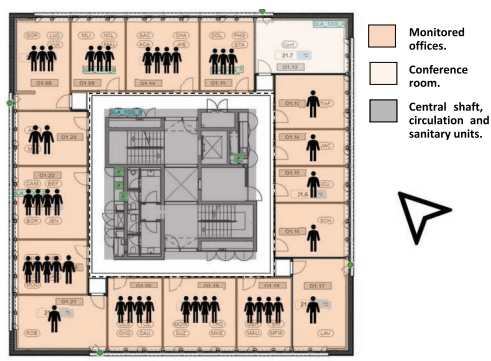

Figure 11.58 Typical offices plan view (Goblet Lavandier & Associés Navigation).

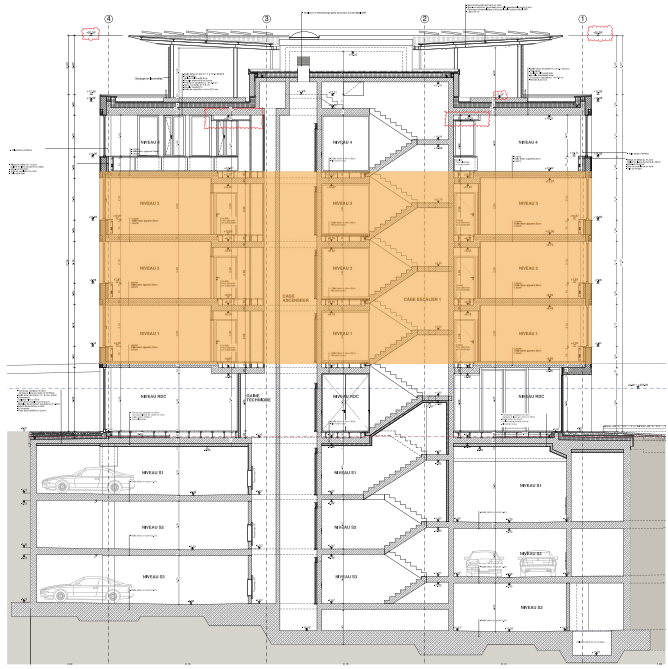

Figure 11.59 Section view of the building, where shaded areas indicate monitored offices (Goblet Lavandier & Associés Navigation).

system until it resets at 11h00 and 15h00. The KNX Elsner sensor controls the blinds in each facade. The blinds are automatically raised (closed) when wind speed exceeds 12 m/s. The blinds are lowered when the irradiance on the façade exceeds 120 W/m^2, and the outdoor temperature is above 5°C without any delay time. When the irradiance is below 50 W/m^2, the blinds are retracted after 60 minutes. During the operation phase, the established thresholds were modified. The lowering threshold is set up to 250 W/m^2 with a horizontal slat position to maximize the view to the outside. When the irradiance exceeds 400 W/m^2, the slat angle inclines up to 15° instead of 80° to provide sufficient daylight. Thresholds values can also be increased (e.g., a temporary cloudy sky) for less disruptive blind movements.

11.7.3 Methodology

Figure 11.61 outlines the methodology of the study. This study began with a design investigation via a written interview with the designer who was involved during the design and operation phase of the shading systems. Then,

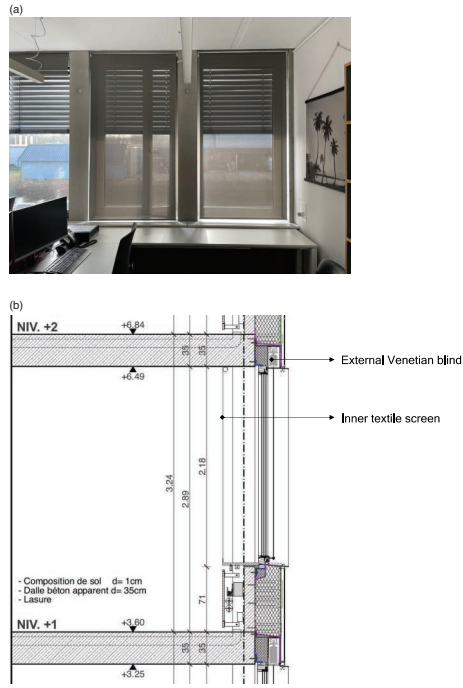

Figure 11.60 The double shading system approach. Left: Interior view. Right: Section view.
Source: Jürgen MÜLLER, https://www.golav.lu/.

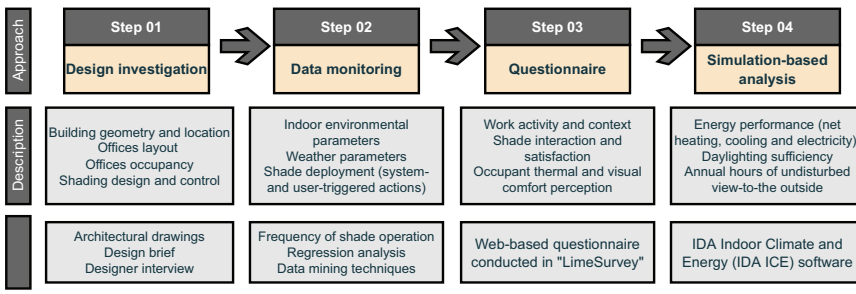

Figure 11.61 Methodology of the study.

a post-occupancy evaluation (POE) was performed using data monitoring and data collection (via a web-based questionnaire) to explore occupants' interaction, satisfaction, and preferences regarding the shading systems. Finally, a simulation-based analysis was performed. Each of these steps is presented and described in the sections that follow.

11.7.3.1 Design Investigation

A written, structured interview with the building's designer was conducted via email to explore if any of the questions below were considered during the shading system design. To streamline the interview, potential responses were provided for many of the questions (in brackets below).

a *Which solar shading scenarios were proposed before the final shading design selection?* (Internal roller shades, fixed, dynamic, vertical, complex, combined).
b *Which selection criteria were considered during the shading design?* (Environmental and climatic parameters, energy concern, aesthetics, safety, privacy, cost, user comfort, codes, etc.).
c *What was the basis for the selection of shading control strategy?* (Codes, guidelines, literature, design brief, designer experience).
d *Which occupant assumptions were considered during the shading design?* (Number of occupants, demographic, occupancy, work activities, preferences, etc.).
e *Did the simulation specialist consider any simulation-based evaluation for the selection of the optimal shading design? If yes, which metrics were used?*
f *Was there any cooperation between stakeholders (designer, client, energy modeler, etc.) with regard to shading selection and design?*

The designer's feedback provided clarity on the shading system design process and selection criteria and a better understanding of the quantitative findings of the monitoring study and the questionnaire analysis.

11.7.3.2 Data Monitoring

Monitored datasets were extracted from the building's KNX-based building management system (BMS). Data preprocessing was performed on the raw datasets, including cleaning, removing outliers, interpolation, and normalization (rescale a variable to have a value between 0 and 1).

The monitored weather parameters included global irradiance (I_{gl}, W/m^2), outdoor vertical illuminance (E_{out}, lux), air temperature (T_{out}, °C), solar azimuth, and altitude. The outdoor parameters were measured using a weather station mounted on the rooftop of the building. Indoor parameters included air temperature (T_{in}, °C), relative humidity (RH%), and CO_2 concentration (ppm). The indoor parameters were measured with Netatmo data loggers distributed in 11 workspaces throughout the building. Shading system-triggered actions and user-triggered actions were recorded as event-based measurements. The external Venetian blind position—activated by the automated system—was expressed as 0% fully open and 100% fully closed. The datasets were resampled every five minutes using an Excel tool

(i.e., HisKNX_V1_2_17_BETA.xlsb, developed by Jürgen Leick from Goblet Lavadier) to unify intervals. For analysis purposes, the range of data was limited to daytime work hours, between 6h00 and 20h00.

The study analyzed two shade deployment datasets using statistical analysis methods: (1) system-triggered datasets and (2) occupant-triggered datasets. The preliminary behavioral patterns were analyzed in terms of the "rate of change" of blind use. The "rate of change" was defined as the number of user-shade override adjustments (UOAs) per day per office. Logistic regression was applied to the given datasets to identify associations between the physical measurements and user-shade interactions and predict the likelihood of UOAs. Alternatively, clustering analysis and association rules mining (ARM) were used on the given dataset to allow more accurate assumptions on complex and diverse behavior in big office buildings. Clustering analysis was used to obtain distinct behavioral patterns using *K*-means algorithm. The frequent pattern growth algorithm (FP growth) was employed to mine the association rules. Both regression and clustering analysis were performed in IBM *SPSS* (version 21.0) software, while Rapid Minor, an open-source data mining program, was used for the ARM analysis.

11.7.3.3 Questionnaire

A cross-sectional web-based questionnaire using LimeSurvey was distributed to the building's occupants to examine subtle and non-physical triggers behind blind adjustments and better understand the findings of the monitored datasets. The questionnaire was distributed in the summer of 2021 to ensure that occupants had experienced the same thermal and visual conditions as those studied during the monitoring period. The questionnaire was distributed via email to the building's occupants on July 30, 2021, and followed by a reminder three weeks later. The questionnaire included questions about participants' demographic details, mood, work activity, contextual environment (e.g., window orientation, size, location), thermal and visual discomfort, and interaction with the shading systems, and their satisfaction and preferences regarding shading system performance. A total of 32 participants (25% of the population) working in single-occupancy offices completed the questionnaire. Employees who were working from home due to the COVID-19 pandemic were excluded from the population sample.

11.7.3.4 Simulation-based Analysis

Daylighting and energy performance of the automated shading control strategy was evaluated using a simulation-based analysis using IDA Indoor Climate and Energy (IDA ICE) software. Annual heating, cooling, and lighting demand (kWh/m^2) were calculated under five shading control strategies, including low (S01: irradiance on the façade exceeded 100 W/m^2), and high (S03: irradiance exceeded 450 W/m^2), S02 was the established design

lowering threshold (irradiance exceeded 250 W/m^2), S04 (fully closed) and S05 (fully open) were added to the analysis for benchmarking. Useful daylight illuminance (UDI) was used for the daylighting performance assessment. Achieved UDI% is defined as the annual occurrence of illuminances across the work plane where the illuminance is within the range of 300–3,000 lux (Nabil and Mardaljevic, 2005).

11.7.4 Results and Discussion

The main findings of the study are presented and discussed in the following sections.

11.7.4.1 Design Investigation

According to the designer's interview responses, the external and internal shading systems were proposed from the early stages of the building design. The design of the systems was based on different environmental and climatic parameters, thermal and visual comfort, energy concerns, aesthetics, safety and maintenance, budget restrictions, and building codes and standards. A simulation-based analysis had been conducted by the designer to find the optimal shading control strategy in terms of thermal and visual comfort as well as energy performance. However, according to the designer, occupant assumptions were not considered in their analysis.

The designer indicated that the intention of the shading design was to maximize users' satisfaction and comfort in their workspaces, which aligns with the notion of occupant-centric design, that is, placing occupants and their well-being as a top priority throughout the building life cycle. The designer's details about the shading design were helpful in better understanding the quantitative results of the monitoring and questionnaire analysis, described below.

11.7.4.2 Data Monitoring

Shade patterns are explored in terms of system- and user-triggered actions to differentiate their behavior regarding office orientation and shade control strategies.

11.7.4.2.1 SYSTEM BEHAVIOR

A total of 576 system-triggered actions (287 fully raising actions and 289 fully lowering actions) were recorded—an average of 8.72 blind changes per day. Figure 11.62 shows that the highest frequency of system-triggered actions was in west-facing offices, while the lowest was in east-facing offices. In contrast, the highest frequency of UOAs was in the east-facing offices, while the lowest was in the west-facing offices. The high rate of system-triggered

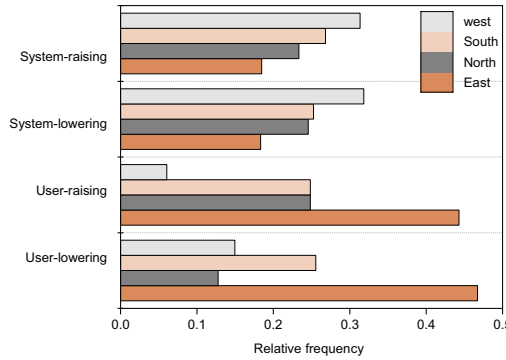

Figure 11.62 Relative frequency of system- and user-triggered actions for each façade.

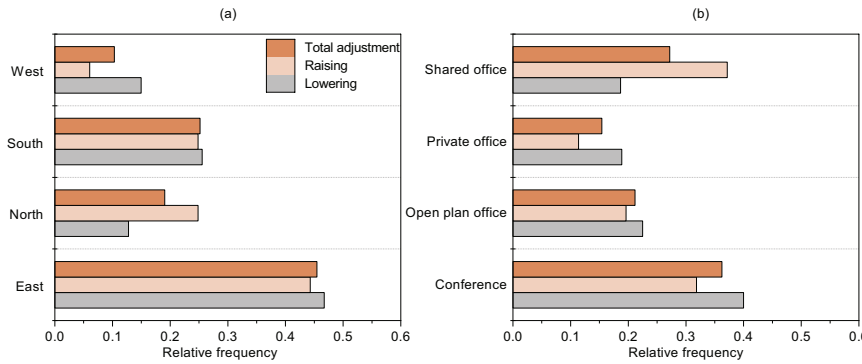

Figure 11.63 Relative frequency of UOAs in terms of (a) office orientation and (b) occupancy level.

actions in the west and south elevations can be explained by (a) the average daily high irradiance on the facade (above 400 W/m^2) and (b) the users (i.e., occupants) occasionally correcting the system.

11.7.4.2.2 USER BEHAVIOR

A total of 1,148 blind position changes were recorded over the 66 working days in the 47 monitored offices. The users triggered approximately 49% of the blind movements (fully and intermediate), 274 lowering actions, and 298 raising actions. The average daily rate of blind use was 0.184 per office. Figure 11.63a shows that the highest rate of UOAs was in the east elevation, where an average of 3.93 adjustments per day occurred. Fewer interactions were observed in the west and north elevations compared to the east and

south. This result can be explained by the significant variations of global irradiance and indoor work plane illuminance in offices in different elevations. To reduce the visual discomfort and blind-triggered actions in the east and south elevations, smaller window size and fixed shading could be adapted in the building envelope design, as suggested by O'Brien and Gunay's (2015) robust design strategies.

Figure 11.63b shows a higher frequency of UOAs observed in shared offices, with an average of 0.19 changes per day per office compared to single-occupancy and open-plan offices. Most of the shared offices are located in north-east elevation close to a nearby building. This result is not in agreement with O'Brien *et al.* (2013), who found that, due to social pressure and constraints, occupants tend to be more reluctant to control their environment if others are present.

Figure 11.64 shows that the shades in the east and south facades were adjusted more frequently in the morning than during the rest of the day, while the opposite occurred in west-facing offices. This result is in line with previous studies (Inoue *et al.*, 1988; Haldi and Robinson, 2010b) that found that occupants interact more with blinds immediately upon arrival to the space. In north-facing offices, occupants tended to raise the blinds all day and in the evening.

Overall, the daily rate of change of UOAs was relatively low compared to the findings of previous studies. For comparison, Reinhart and Voss (2003) reported a mean of 3.7 blind movements per day per office over 174 weekdays in 10 south-facing offices, which is 20 times the present study's findings. In another study by Meerbeek *et al.* (2014), an average of 0.86 blind adjustments per day per office were recorded over 100 working days in 40 offices, which is five times this study's findings. Considering these studies were conducted in temperate climate zones same as the present case study, the difference in

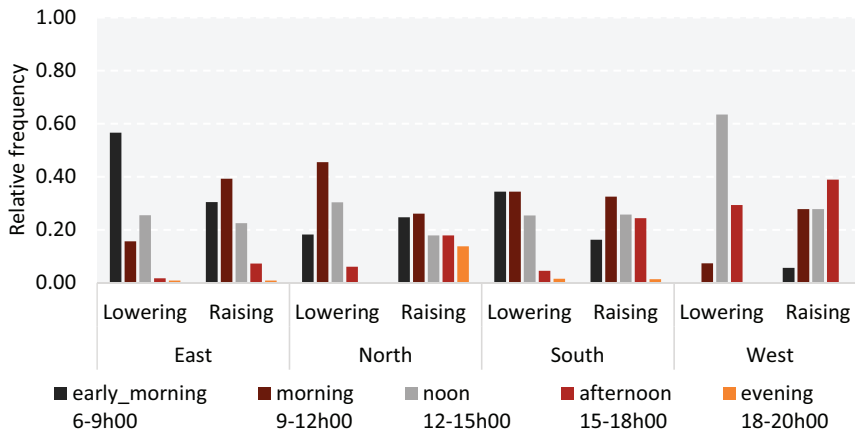

Figure 11.64 Relative frequency of UOAs during the day per façade.

findings may be explained by the case study building having both (a) appropriate and acceptable shade control thresholds and high-quality light sensor performance, and (b) additional inner glare protection, which requires less effort to prevent glare. Additionally, the daily profile of CO_2 concentration was analyzed in nine offices in the case study building to estimate occupancy presence; based on the results, the offices were occupied approximately 97% of the study period. Thus, the low rate of blind use is unlikely to be related to occupant absence. Instead, the findings suggest that the automation system performance met occupants' preferences and expectations.

11.7.4.3 Regression Analysis

The initial aim of the present study was to derive occupant behavior models, as a high rate of shades adjustments was expected based on previous studies (Reinhart and Voss, 2003, Meerbeek *et al*., 2014). Thermal and visual stimuli were identified by earlier research as influencing blind use (Haldi and Robinson, 2010a; Mahdavi *et al*., 2008). Accordingly, this study used logistic regression to predict the probability of UOAs as a function of several explanatory variables:

$$\begin{aligned}\text{Logit} = {} & \beta_0 + \beta_1\left(E_{\text{out}}\right) + \beta_2\left(I_{\text{gl}}\right) + \beta_3\left(T_{\text{out}}\right) + \beta_4\left(\tan\_d\right) \\ & + \beta_5\left(T_{\text{in}}\right) + \beta_6\left(\text{Rh}\right) + \beta_7\left(\text{CO}_2 \text{ concentration}\right) \\ & + \beta_8\left(\text{AOV\%}\right) + \beta_9\left(\theta_{\text{slat angle}}\right) + \beta_{10}\left(\text{time of the day}\right)\ldots\end{aligned} \tag{11.8}$$

where tan_*d* is the tan of solar profile angle, AOV% is the average occlusion value of the blind (0% fully open and 100% fully closed), $\theta_{\text{slat angle}}$ is the slat angle degree (0°, 60°, 80°), β_0 is the intercept, and β_n is the variable coefficient.

Separate analyses were conducted to predict the probability of UOAs (lowering and raising actions) for each façade (E, S, N, W), including eight sub-models. The forward regression method was used to select the explanatory variables that have a statistically significant influence on the value of the dependent variable (p-value < 0.05). Further details about the statistical analysis process are available in Derbas and Voss (2021).

The regression results had a considerably low Nag. R squared (in other words, the proportion of the variance for a dependent variable was close to zero) of all sub-models for shade lowering and raising actions. Moreover, a weak relationship between the model predictions and the physical parameters was found. The developed sub-models were all incapable of predicting UOAs. The limitations of the monitored parameters such as indoor work plane illuminance and glare probabilities, which are the primary triggers behind blind use, may explain why the models could not accurately explain the actions. Based on these results, it can be concluded that in this case, this commonly used modeling approach was not successful for explaining

occupant behavior. This limitation justified an alternative approach for analyzing the observed patterns, as discussed in the next section.

11.7.4.4 Data mining Analysis

Data mining techniques, including clustering analysis and association rules mining, were considered an alternative methodology to provide more accurate assumptions of complex and diverse individual behavior in big office buildings and overcome the limitations of the regression models. The results of the two techniques are described in turn below.

11.7.4.4.1 CLUSTERING ANALYSIS

First, interactivity patterns clustered occupant behavior based on the frequency of UOAs per day. The user-control ratio was calculated by dividing the number of user-triggered adjustments per office by the total number of adjustments (system- and user-triggered actions) for that office. The activity ratio was calculated by dividing the total number of user-shade override adjustments for an office by the average number per 47 offices. Figure 11.65 shows 47 offices labeled by numbers and plotted, where the x-axis indicates the activity ratio and the y-axis represents the user-control ratio. The following interactivity behavioral patterns were clustered in the given dataset:

- Passive adjustments [C01]: 66% of offices assigned (range of 0–0.17 times per day).
- Neutral adjustments [C02]: 21% of offices assigned (range of 0.18–0.36 times per day).
- Active adjustments [C03]: 13% of offices assigned (range of 0.44–0.58 times per day). The offices assigned to this cluster have common design features: they are all shared offices and face north-east.

Second, motivational patterns clustered the factors that drive users to override the automated shading systems. Three clusters of shade-lowering actions and two clusters of shade-raising actions were defined (see Figure 11.66a and b). The clusters were based on each variable's impact factor (regression coefficients) that influenced the UOAs. Accordingly, logistic regression was performed to define the most statistically significant variables in each office. Patterns of user-shade lowering were clustered in 25 offices, and user-shade raising was clustered in 30 offices. The rest of the offices were excluded since they had the lowest frequency of UOAs.

Based on the motivational patterns, five clusters were induced as follows:

- Shade lowering cluster 01 [C01_L]: 12% of offices were assigned and associated with the time of the day (early morning and morning) and outdoor weather conditions (T_{out}, tan_d).

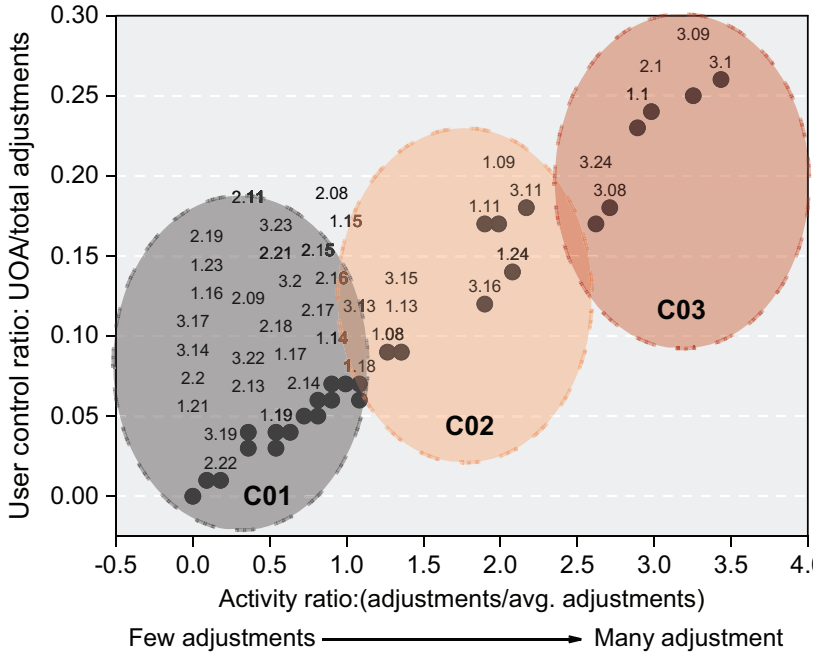

Figure 11.65 User-shade clusters based on interactivity patterns.

- Shade lowering cluster 02 [C02_L]: 24% of offices were assigned and associated to the time of the day (early morning until afternoon) more than physical drivers.
- Shade lowering cluster 03 [C03_L]: 64% of offices were assigned and appeared to be more influenced by slat angle position than physical and time-related drivers.
- Shade raising cluster 01 [C01_R]: 63% of offices were assigned and appeared to be more influenced by the slat angle position and time of the day (noon and afternoon) than physical drivers.
- Shade raising cluster 02 [C01_R]: 37% of offices were assigned and associated to the time of the day and indoor air temperature.

The clustered patterns constitute a base for association rules classifying the building occupants into typical office user profiles as described in the next section.

11.7.4.4.2 ASSOCIATION RULES MINING (ARM)

Based on the 20 rules mined, two working user profiles (user β, user μ) were drawn in this study:

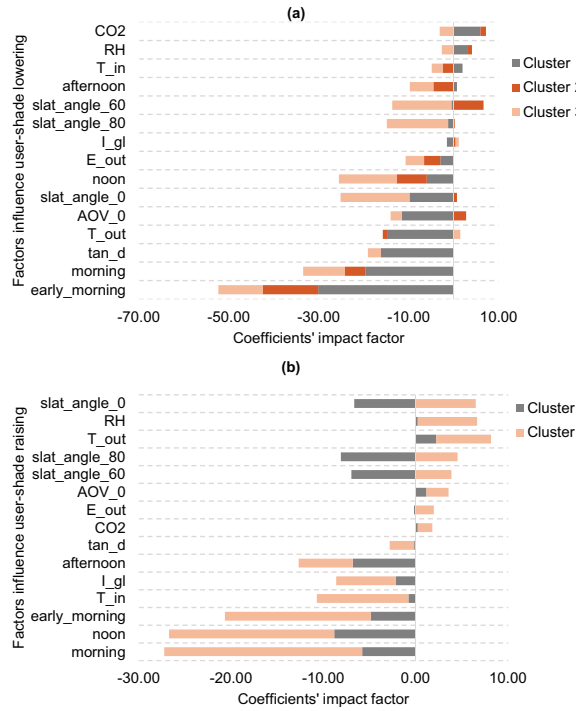

Figure 11.66 User shade (a) lowering and (b) raising clusters based on motivational patterns.

- User type (β) represents the passive user who tends to override the automated shading system on average 0.09–0.17 times per day (passive adjustments). User β is mainly influenced by the time of day and the current blind state for both lowering and raising adjustments.
- User type (μ) represents the medium user who tends to override the automated shading system on average 0.18–0.36 times per day (neutral adjustments). User μ is mainly influenced by the time of day and the current blind state only for raising adjustments.

11.7.4.5 Questionnaire

In total, 32 of the case study building's occupants completed the questionnaire, 71.9% of whom identified as male and 28.1% as female. Regarding employee role, 68.8% of participants performed professional jobs (e.g., engineer, specialist planner), 18.8% were in managerial positions, and 12.5% were administrators. The main results of the questionnaire are presented and discussed in the sections that follow.

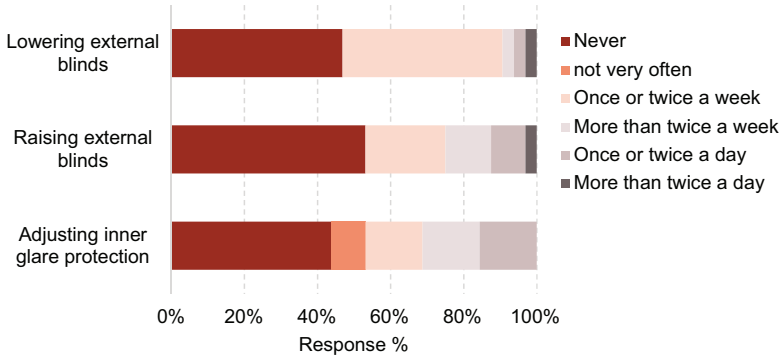

Figure 11.67 Relative frequency of user interactions with inner glare protection and external blinds.

11.7.4.5.1 USER-SHADE INTERACTION, SATISFACTION, AND PREFERENCES

About 75% of the participants reported never opening or adjusting the external blind once per week, whereas 10% closed the external blind a few times per day or week (see Figure 11.67). Overall, a low level of manual overrides to the automated shading system was observed, which is in line with the quantitative results from the study's monitoring analysis. More than half of the occupants indicated that there was no need to adjust the external blind, 20% reported that the blinds are fully open all the time, and 20% preferred the automatic position. Roughly 25% of the occupants chose to adjust only the inner glare protection because it is faster and easier to avoid glare (compared to waiting for the external blind to move). However, 34.4% of the occupants preferred the external blinds to the inner glare protection, while 28% liked both systems equally and 12% did not like either.

Approximately half of the occupants were satisfied with the performance of the automated shading system with an average of 3.68 on a 5-point scale (0 = very dissatisfied, 5 = very satisfied). Some participants explained that the automated shading systems are much more efficient than the glare protection and simple to operate via a push button. Most participants (93.8%) were satisfied with their ability to control both shading devices, that is, the "double approach", with an average satisfaction rating of 4.43 (see Figure 11.68).

11.7.4.5.2 INFLUENCE OF CONTEXTUAL FACTORS ON BEHAVIORAL PATTERNS

Figure 11.69 shows the relative frequency of shade lowering and raising actions in terms of floor level, office orientation, WWR, and window to a desk position. Few occupants (15%) whose offices are located on the first floor raised the external blind once or more per day. Fewer raising actions

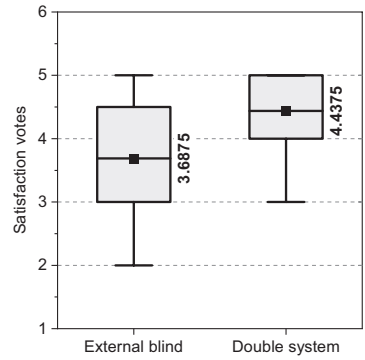

Figure 11.68 Satisfaction rating of the performance of external blind and the ability to control "double systems".

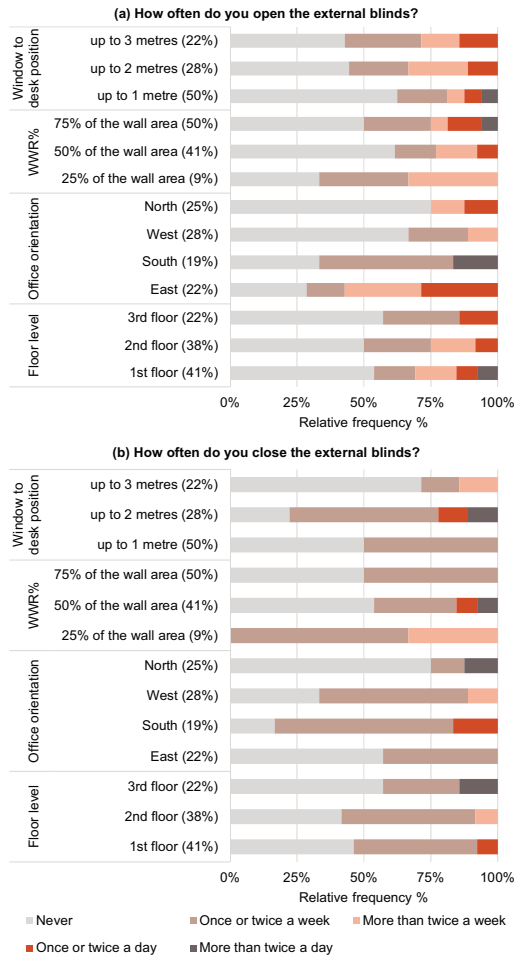

Figure 11.69 Influence of contextual factors on shade behavioral patterns.

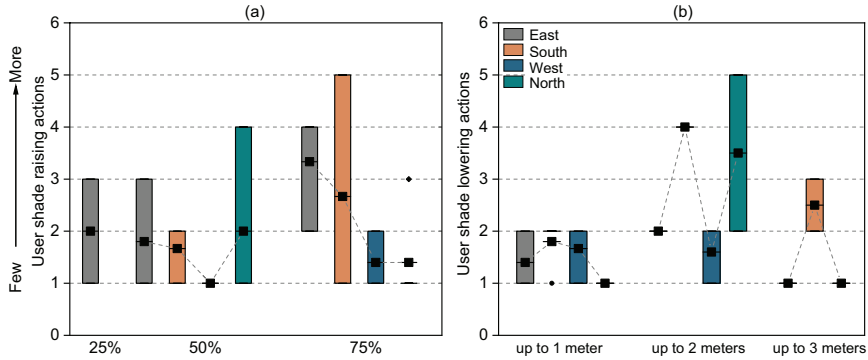

Figure 11.70 User shade raising action in terms of (a) WWR% and (b) window to desk position per each façade.

were noticed on the upper floors, while more closure actions occurred on the third floor. In the east- and south-facing offices, occupants opened the external blinds more frequently than in the north- and west-facing offices. This finding is in line with the findings from the data monitoring analysis.

In Figure 11.70a and b, considering that 0 on the *y*-axis refers to "never adjusted" and 5 refers to "more than twice a day", occupants who sit about 2 m from the window adjusted the external blinds more frequently than those sitting closer to the window. This difference could be due to (a) ease of access to the push button for the automatic blinds (next to the office door), and (b) most of these offices faced north (see Figure 11.70b). In the east- and south-facing offices with large window areas (WWR=75%), occupants opened the external blinds more frequently than those in offices with smaller windows (WWR=50% and 25%) (see Figure 11.70a). Therefore, moderate window size (50%) and desks farther from the window (more than 2 m) in east and west elevations may decrease UOAs. Based on these results, it is recommended that building designers set the first row of desks several meters back from the façade, such that the work planes will rarely receive direct solar radiation. Furthermore, moderately sized window areas are recommended in east and south elevations to decrease the number of shade interventions.

11.7.4.6 Simulation-based Analysis

The daylighting and energy performance of the different shading control strategies (based on irradiance threshold) were simulated. The impact of inner glare protection was ignored in the analysis since insufficient information about the usage of the system (e.g., number of lowering and raising actions) was known during the study period. Figure 11.71 demonstrates that UDI% values were the highest under S01 and S02 (original design) control

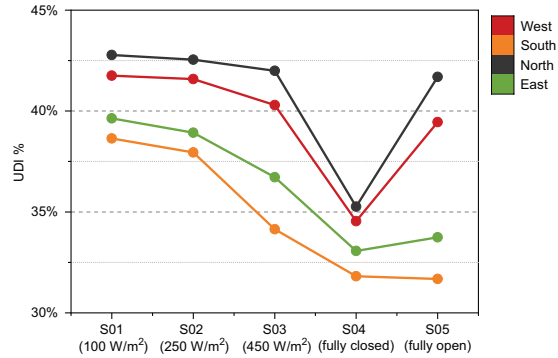

Figure 11.71 UDI% (300–3,000 lux) distribution on the work plane under different shading control strategies.

strategies in west- and north-facing offices with slight differences. This result is expected since the shade-lowering irradiance threshold exceeds 100 W/m^2 in S01 and 250 W/m^2 in S02. The lowest UDI% values were in the south elevation when irradiance thresholds exceeds 450 W/m^2 (S03), and the blind is fully closed or open.

Figure 11.72 shows the annual heating, cooling, and lighting demand in the building offices under different shading control strategies (S01–S05). Lighting demand was hardly affected by the different control strategies since the lighting was turned off if the work plane illuminance was above 500 lux. More significant differences were found in the heating demand, where the difference between the original design (S02) and the lowest demand (S05) reached up to 9.2 kWh/m^2. The total energy demand of S02 was higher than S01 by 43.74 kWh/m^2 and lower than S03 by 76.82 kWh/m^2. The main difference was in the cooling demand. Overall, the established shading control strategy seems to provide sufficient daylighting and views to the outside (note that the blind is closed 40% of annual working hours) as well as keep the energy use close to the minimum compared to other control strategies.

11.7.5 Concluding Remarks

The case study presented a successful example of automated shading system design and utilization. Based on the monitored datasets results, the daily rate of change of UOAs (i.e., occupants' interaction with the systems) was relatively low compared to previous studies (Reinhart and Voss, 2003; Meerbeek *et al.*, 2014). The regression analysis, a commonly used modeling approach, did not successfully explain the occupant behavior in this case. Using data mining techniques as an alternative methodology might be an improvement in terms of exploring occupant behavior patterns and

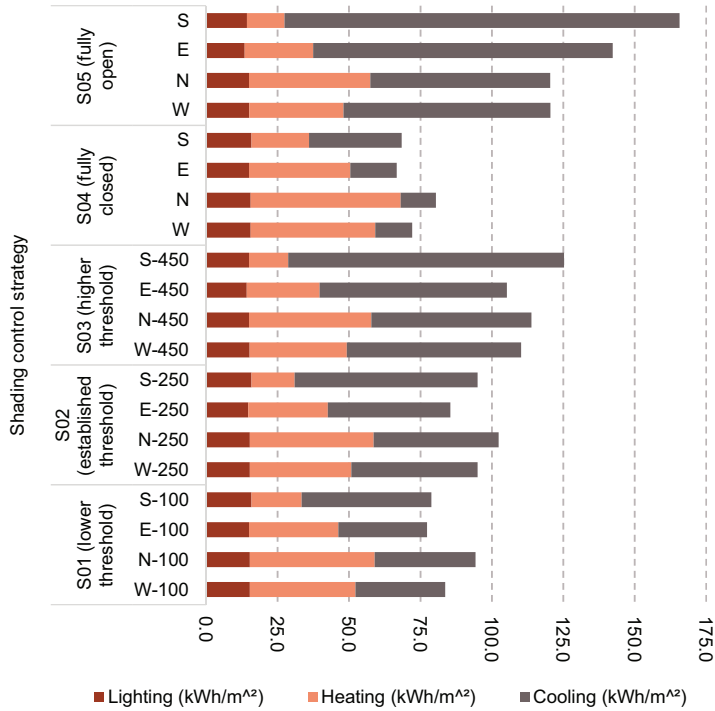

Figure 11.72 Annual heating, cooling, and lighting demand (kWh/m^2) using different shading control strategies.

allowing more accurate assumptions of complex and diverse behaviors in big office buildings. Similar results were found in the questionnaire analysis, where more than 50% of the occupants indicated that they rarely or never adjusted the automated external blinds.

This case study provides building designers and operators with potentially valuable insights about shading design features and operation strategies that may increase occupant comfort and satisfaction. Key insights include:

1 Use double shading system approach (internal/external).
2 Apply an acceptable range of established shade control thresholds. For instance, low irradiance thresholds (250–400 W/m^2) are recommended for shade control in south- and east-facing offices with moderate window size or fixed shades. In contrast, high irradiance-lowering threshold (above 400 W/m^2) can be adopted in north- and west-facing offices.
3 Use high-quality and accurate light sensors.
4 Quiet and infrequent movements while operating the automated shading systems can increase occupant satisfaction.

Further research is needed to develop comprehensive guidelines for occupant-centric shading design—for example, studies exploring various building types in different climatic zones and with long-term monitoring.

11.8 Case Study 7: Gothenburg, Sweden

Quan Jin, Holger Wallbaum

11.8.1 Summary

This case study, A-building, is a newly renovated office building in Gothenburg, Sweden. The building is certified Miljöbyggnad Silver (version 2.2), which aims to achieve both better indoor comfort and low energy use. This occupant-centric analysis focused on the operation phase and examined the indoor environmental performance predicted during design. The findings indicated both conformities and discrepancies between the designed performance and the actual performance as perceived by the occupants. On the one hand, the design enhanced the building's performance regarding, for example, daylight, ventilation, and energy savings. On the other hand, occupant surveys revealed that performance gaps exist between what was targeted and what was perceived regarding, for example, satisfaction with the indoor temperature and window screen and preference for daylight and indoor climate control. The findings of this study can contribute to closing performance gaps by examining how occupants perceive and experience the office environment.

11.8.2 Building Description

The A-building is an office building hosting the Department of Architecture and Civil Engineering on the Chalmers University campus in Gothenburg, Sweden (see Figures 11.73 and 11.74). The building was built in 1968 and extensively renovated in 2016 and 2017. A significant challenge during the building renovation was the preservation of the historical features of the building. The building was reoccupied in 2018 and is currently fully operational as of May 2022. It is located in the marine west coast climate zone according to the Köppen Climate Classification and features mild summers and cool but not cold winters.

The building consists of five stories with lecture halls and work studios on the first and second floors, staff and faculty offices on the third and fourth floors, and a kitchen and study rooms for students as well as a lunch and coffee room with a kitchen for employees on the fifth floor. In this case study, only the office floors (i.e., third and fourth floors) were the subject of analysis. The total floor area of the office floors is approximately 4,925 m^2. The study was conducted in 2018 after the building had been reoccupied for a year post-renovation.

Figure 11.73 Photo of the A-building exterior space.

Figure 11.74 Photo of the A-building interior office space.

The newly renovated A-building was certified as Miljöbyggnad Silver (version 2.2) by the Sweden Green Building Council. Miljöbyggnad is a Swedish system for the environmental certification of buildings (new and existing buildings as well as buildings in operation) that aims to provide comfortable and safe environments for people to work and live. The system certifies buildings at three levels—Bronze, Silver, and Gold—with regard to energy, indoor environment, and materials/chemicals. The case study building's Silver level is awarded when a building is designed to perform better than the reference values in the Swedish building regulation in terms of, for example, lower energy use, a higher daylight factor, and a lower predicted percentage of dissatisfied (PPD) value. The A-building specifically addresses low energy consumption, a comfortable indoor environment, and creative workspaces. The main energy-efficient features include sun shades, energy-efficient windows, a low U-value of wall, and a mechanical variable

air volume (VAV) ventilation system. Since the renovation of the A-building was so extensive, the certification process followed the (stricter) certification requirements required for new buildings.

11.8.3 Building Design Parameters

The focus of the renovation design was to create a building that contributed to different sustainable perspectives, including energy conservation and an improved indoor environment. The heating, cooling, and electricity are intended to be controlled based on internal load variations from people, equipment, and the outdoor climate. Table 11.15 shows the design parameters for the renovation of the A-building.

The building envelope was a classical brick-and-mortar double-wall with a cavity gap in between, as was very popular in Sweden in the 1960s. During the renovation, the building exterior was kept similar, and additional inorganic insulation was added from the inside. By adopting this strategy, the historical features of the building were preserved and better thermal performance of the exterior wall achieved by reducing the heat flows from the indoor to the outdoor environment.

The windows were also renovated. All the windows in the building were replaced with energy-efficient windows with a low thermal transmittance (U-value). The windows are now operable, triple-pane casement windows. Exterior screens (i.e., awnings, a sheet of canvas, or other material stretched on a frame and used to keep the sun off the windows) were also installed to further reduce solar heat gain and protect from glare. All sunlit rooms facing south, west, and east were provided with effective exterior screens. The screen is automatically controlled based on the solar radiation level and outdoor temperature. Curtains were also added on the inside of the windows to be controlled manually by occupants.

The ventilation system was replaced by a mechanical variable air volume (VAV) ventilation system with heat recovery. The ventilation system is controlled based on the presence of occupants in each room by adjusting the

Table 11.15 Design parameters for the renovation of the A-building

Exterior wall	*$U = 0.44$ W/m²K*
Window	Triple pane casement $U = 1.04$ W/m² K including window frame SHGC (g-value) = 0.4 Light transmission, 60%
Exterior screen	Awning, fabric g-value screen: 0.21–0.24
Ventilation	FTX with VAV Maximum four outlets × 5 m³/s in office room

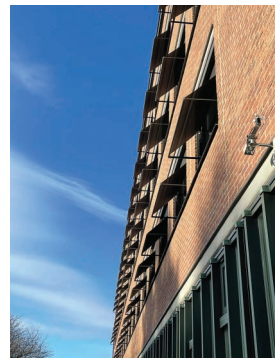

Figure 11.75 Photo of the A-building's exterior screens.

Figure 11.76 Photo of one of the A-building's triple pane windows and screens.

airflow rate according to the signal of presence as well as the indoor temperature. Figures 11.75–11.77 show each of the components mentioned above (exterior screens, windows, and ventilation).

11.8.4 Methodology

Energy performance is a topic frequently addressed in building renovations and green building design. However, there are still many newly renovated buildings that regularly receive complaints from their occupants, especially concerning the indoor environmental conditions (Lee *et al.*, 2019). In other words, there are often gaps regarding occupant satisfaction between the designed and the actual conditions. The purpose of the present case study was to examine the A-building's post-renovation performance in terms of indoor environmental quality (IEQ)—specifically, the extent to which the

Figure 11.77 Photo of the A-building's ventilation inlet.

building's design achieved the target of a comfortable indoor environment based on occupants' perceptions of the building's performance.

To achieve this purpose, the study included three parts. The first part involved reviewing the building's design parameters and simulation results of its energy performance and indoor comfort (thermal comfort and daylight). The second part was a post-occupancy evaluation (POE) based on the smart and sustainable office (SSO) User Insight Toolbox (Cordero *et al*., 2017; Jin *et al*., 2019) that collected occupant feedback on indoor environmental quality (IEQ) and behaviors related to indoor comfort and individual control over indoor climate. The third part was a comparison of the original building design and the occupant survey results and a reflection on the development of an occupant-centric design concept (see Figure 11.79). Each part is described in turn below.

11.8.4.1 Building Design Simulations

In this study, simulation was used in the early stage building design and to support the implementation of the Miljöbyggnad certification. There are 13 aspects and up to 16 indicators in the Miljöbyggnad certification that need to be rated individually and then aggregated to grade a building as Bronze, Silver, or Gold. The goal of the A-building renovation was to achieve Miljöbyggnad Silver. To achieve this goal, the renovation could not only focus on the energy performance but also needed to reach high-performance level of IEQ related to occupant comfort and health. This goal was achieved by performing comprehensive simulations of the building's energy demands, thermal comfort, and daylight. A detailed building model was created using the software IDA Indoor Climate and Energy (IDA ICE) to predict the building energy and indoor environment performance (see Figure 11.78). The results of this simulation were used for comparison with the results of the POE, described below.

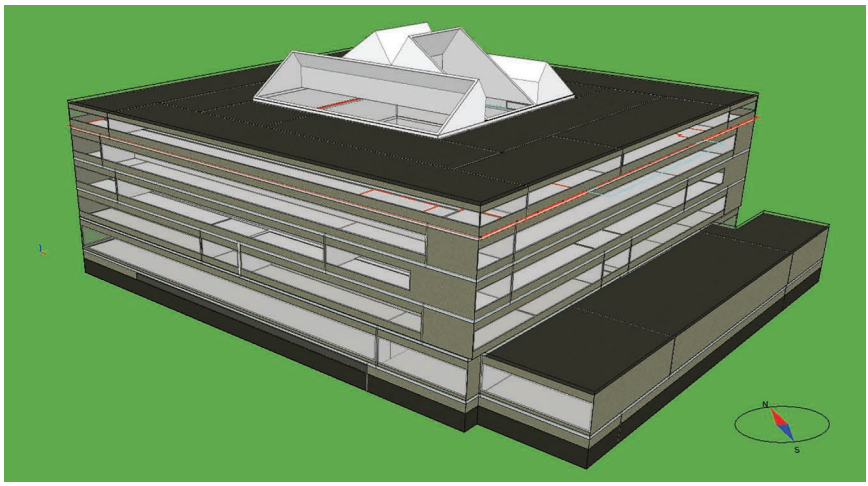

Figure 11.78 3D model for the structure of A-building.

Energy simulation was performed to ensure that the specific energy use, which refers to the supplied energy to building's service and energy system distributed over the floor area heated above 10°C, meet the requirement of 75% of the energy use of BBR (2017).

Indoor thermal comfort in winter and summer were simulated as well, and PPD index was calculated. To meet the Miljöbyggnad requirements, representative floors and worst cases were studied. The representative floor stands for the type of the entire building or a few floors (i.e., office or classroom). The worst cases are considered, such as lower floors for daylight simulation, the risk of overheating and cooling for thermal comfort in summer and winter, and full exposure toward north- and south-west. In this case, for the thermal comfort simulation, floor 4 was selected as the representative floor of office space, and for daylight simulation, floor 3 was selected as the representative floor, considering it bad for good daylight.

Occupant-related information and assumptions such as internal loads and occupancy were taken into account as they are of significance for the indoor climate. The basis of the set up for these parameters is based on the national guideline on determining the building energy use (BEN 2) and the default values provided by IDA ICE. The following Table 11.16 shows detailed information about these parameters.

11.8.4.2 Post-occupancy Evaluation

POE is frequently used to evaluate building performance and gather data from building occupants. When conducting POE, useful knowledge is

Table 11.16 Occupant-related parameters and setpoint (the third and fourth floors)

Cooling setpoint	23°C at presence, 25°C no presence
Heating setpoint	22°C at presence, 20°C no presence
Person heat	80 W/person
Clothing, activity	1.0 clo winter; 0.5 clo summer; 1.2 MET
Occupancy	Varying attendance between 7:00 and 17:00 Occupancy density: 0.07 person/m^2

assembled to improve the design and operation of both new and renovated buildings. POE is essential to examine and motivate occupant-centric building design. There are various ways to implement POE depending on the complexity and depth of evaluation. Surveys are a commonly used method to assess occupants' satisfaction levels—for example, the Building User Satisfaction (BUS) survey and UC Berkeley's Center for the Built Environment (CBE) survey on office IEQ satisfaction (Leaman and Bordass, 2001; Zagreus *et al*., 2004). These two surveys include detailed questions about occupants' comfort, health, and productivity.

For the preset case study, POE was conducted using the SSO User Insight Toolbox (Cordere *et al*., 2017; Jin *et al*., 2019). This toolbox relies on a holistic mixed methods approach based on qualitative and quantitative measures to capture a broad range of office occupants' comfort- and health-related factors, including current and general well-being. The empirical evidence can help identify implementation strategies for a new generation of user-oriented and resilient building design solutions for future offices. One of the main goals of the SSO User Insight Toolbox is to put users at the center of office design by collecting their experiences and needs—in this case, regarding the A-building's indoor environment, individual control, energy use, and social aspects of building use.

In addition to IEQ measurements, the SSO User Insight Toolbox includes the following tools:

- Web-based SSO Survey
- Web-based SSO Diary App
- Observation studies
- Individual and focus group interviews
- Reporting tool

The web-based survey (see Figure 11.79) is a tool to gain a holistic impression of a user's experience with the environment. The survey includes a series of questions around broad themes, such as general satisfaction, stress, and preferences, as well as more specific themes, such as mood and job and life satisfaction. Information about users' energy-related behavior, perceived health, and self-reported work performance is also gathered, as are details about individual contextual factors (e.g., nature of work). As the other tools

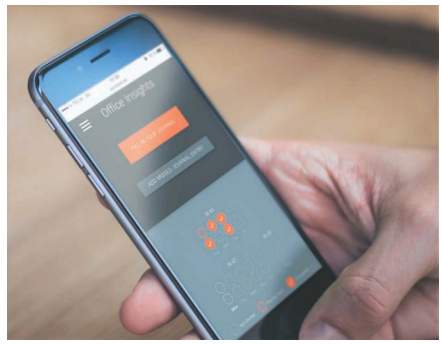

Figure 11.79 Image of the SSO User Insight Toolbox's web-based survey accessed via smartphone.

of the SSO User Insight Toolbox are not the focus of this chapter, the detailed description can be found in the study (Jin *et al*., 2019).

In the present study, a POE adapted from the SSO User Insight Toolbox focusing on the web-based survey was conducted over a two-week period in August and September 2019, one year after occupants' return post-renovation. In brief,

- A total of 283 permanent employees (i.e., long-term contracts) working in occupying offices on the third and fourth floors were invited to complete the web-based SSO survey; 160 (57%) participated in the survey, although around 40 chose not to answer all of the questions. Data were collected from occupant experience and satisfaction on IEQ, behavior, and individual control over indoor environment. The survey asked occupants a range of questions about their perceptions (i.e., experience and satisfaction) about the building's performance, including several factors of the indoor environment (glare, daylight, temperature, etc.) and adaptive behaviors for indoor comfort.
- Observations of the offices took place four times a day during three working days and three times a day during two working days to better understand how the spaces were used.
- A total of 46 in-depth individual interviews and two focus group interviews were conducted with a selection of the employees to gain a deeper understanding of individual needs.

For the purposes of this chapter, we will present and discuss only the survey findings because the study focuses on occupant perceptions of the actual indoor environments and the building design. See the study (Jin *et al*., 2020) for more results of the POE. The diary app and the reporting tool will be introduced in the future study.

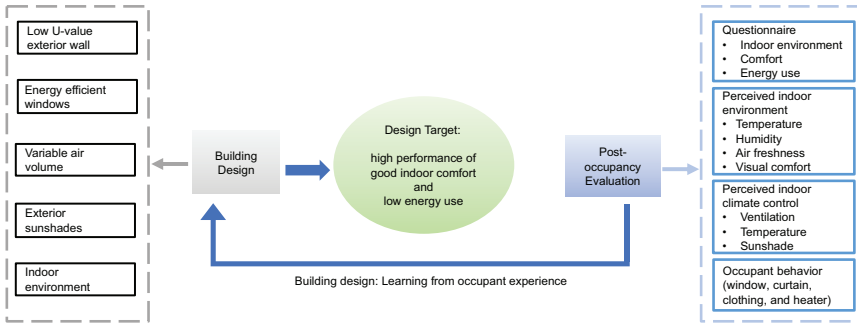

Figure 11.80 Building design concept: learning from occupant experience in the A-building.

11.8.4.2.1 COMPARISON OF THE BUILDING DESIGN AND SURVEY RESULTS

The target of the original building design is to achieve a high performance of good indoor environment and low energy use. The survey results from the study will be analyzed to examine the building's real performance and compare with the building design and simulation results. See Figure 11.80.

11.8.5 Results and Discussion

This section begins with the results of the building simulation from the early design phase, followed by key findings from the survey from the POE. Then, the simulation and survey results are compared and discussed alongside reflections on the development of an occupant-centric office design concept.

11.8.5.1 Building Simulation Results

The following sections describe the simulation results for the original model for the A-building's renovation, with a focus on energy performance, thermal comfort, and daylight.

11.8.5.1.1 ENERGY

Specific energy use intensity (EUI) for the whole building was calculated as 57.4 kWh/m^2 A_{temp} per year, which meets the requirement of Miljöbyggnad Silver (60 kWh/m^2 A_{temp} per year). The term A_{temp} defines the floor area for which the building's primary energy use is to be calculated. A_{temp} is the sum of the interior area for each floor, attic, or basement that is heated to more than 10°C. With the exterior screen installed, the solar heat load was reduced to less than 43 W/m^2 A_{temp}, which is rated as Miljöbyggnad Gold.

11.8.5.1.2 THERMAL COMFORT

The simulation results showed that the PPD in summer was lower than 10% in all simulated offices on the fourth floor. In the Miljöbyggnad rating system, this indicator of summer indoor climate was rated as Miljöbyggnad Gold. The simulation results also showed that the PPD in winter was lower than 10% in all simulated office spaces. This result means that the indicator of winter indoor climate was rated as Miljöbyggnad Gold as well. Figure 11.81 shows the PPD values on the fourth floor in a cold winter from the simulation by IDA ICE.

11.8.5.1.3 DAYLIGHT

The simulation results for daylight showed that the daylight factor (DF) was ≥1.2% for more than 21% of the total heated floor area on the third floor (see Figure 11.82). Only 3% of the total heated floor area was calculated with the DF of 1.0%. For all the office rooms on plan 3, most of the rooms were rated

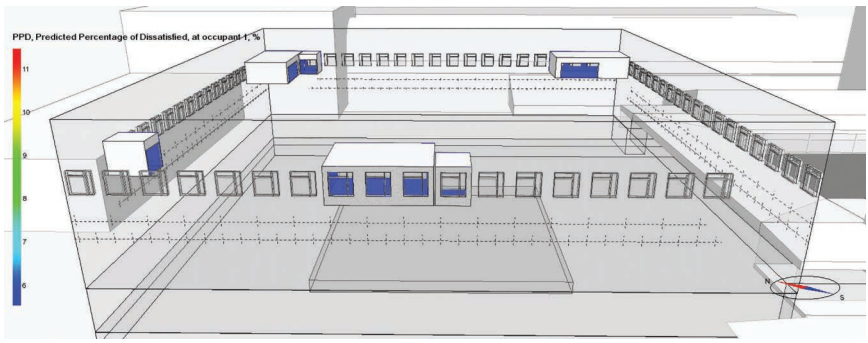

Figure 11.81 A selection of simulation result of the PPD on the fourth floor.

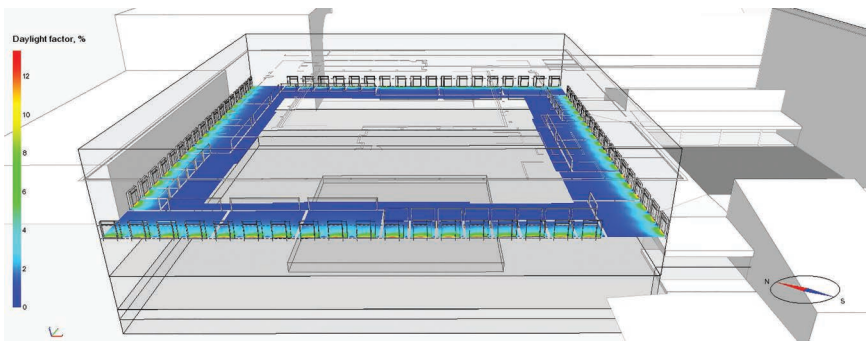

Figure 11.82 Simulation result of daylight factor on the third floor.

as Miljöbyggnad Gold, and one room was rated as Miljöbyggnad Bronze. The final grade for the DF was rated as Miljöbyggnad Silver.

11.8.5.2 Post-occupancy Evaluation Results

Figure 11.83 shows the levels and percentages of occupants' satisfaction with eight factors of the indoor office environment based on the survey results from the POE. In general, most of the factors were perceived as satisfactory by most of the occupants, except the screen and indoor temperature. The satisfaction rate for the overall indoor climate was about 70%. The amount of light and glare had a satisfaction rate higher than 80%, and other factors (air quality, daylight, air movement, and access to outside views) had a satisfaction rate of 70%. The most dissatisfactory factors were the air temperature and the screen.

Figure 11.84 shows occupants' satisfaction with the level of individual control of the indoor climate. In the survey, occupants were asked about their perceptions of daylight, ventilation, and indoor temperature since

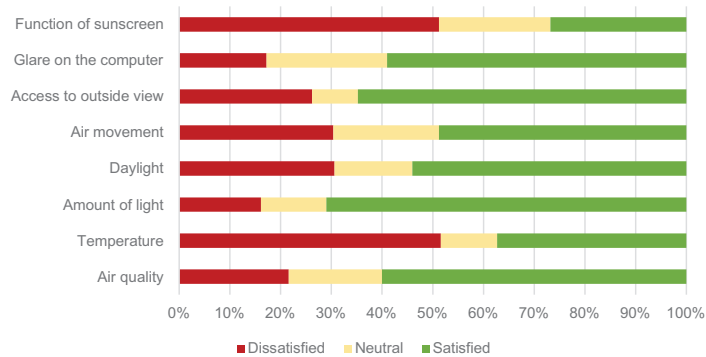

Figure 11.83 Percentage of occupant satisfaction with eight factors of the indoor environment.

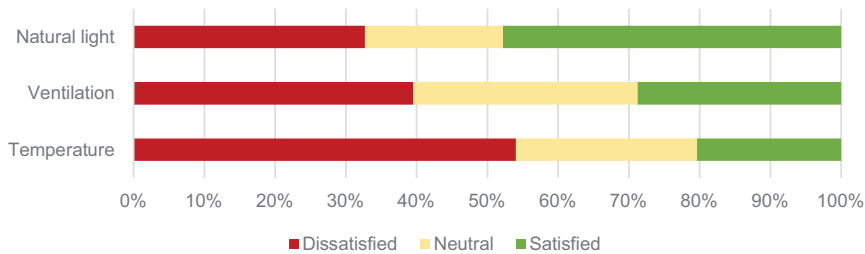

Figure 11.84 Percentage of occupant satisfaction for individual control of the indoor environment.

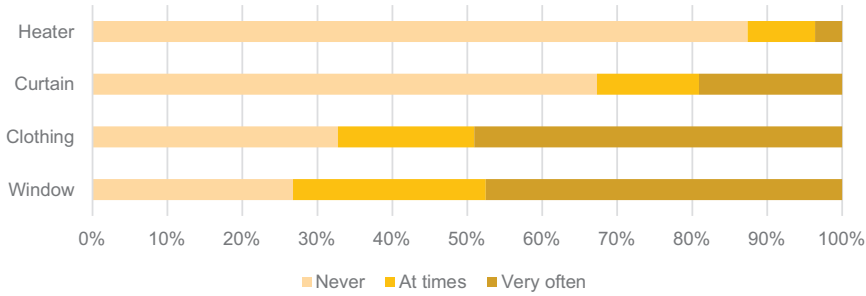

Figure 11.85 Frequency of occupant behavior for individual comfort.

these can be controlled to some extent by occupants. For example, glare/daylight can be blocked by a curtain, airflow can be controlled by either opening or closing a window, and indoor temperature can be controlled by operable windows. The screen cannot be operated manually by the occupants. In general, the satisfaction rates for all three components were relatively low, where more than 30% of occupants reported feeling dissatisfied. A majority of occupants expressed dissatisfaction with the control possibilities regarding indoor temperature.

Figure 11.85 shows the frequency of occupants' adaptive actions to improve comfort. It was observed that about half of the occupants reported operating the windows "Very often" in the office, and, in total, more than 70% of the occupants reported operating the windows at least "At times". Another factor related to occupant behavior was clothing: about 70% of the occupants reported adjusting their clothing to improve their thermal comfort.

11.8.5.3 Comparison of the Building Design Performance and the Perceived Performance

The original design for the renovation of the A-building met the design requirements of Miljöbyggnad Silver with a good indoor environment and low simulated energy consumption. In this case study analysis, the design information was collected and compared with data collected from occupant surveys. The results showed that the design enhanced the building's performance regarding daylight, ventilation rate, and energy saving, among others. Some indicators, such as daylight factor and PPD, were simulated and met the requirements for the Miljöbyggnad Gold level. Additionally, the exterior screen both reduced specific energy use in the A-building and contributed to high occupant satisfaction against the glare on their computer screens.

However, the survey results pointed to gaps between the designed performance and perceived building performance. Thermal comfort was not

perceived to be satisfactory by the majority of the occupants even though the PPD was simulated to be less than 10% with a thermal sensation around neutral. The majority of occupants indicated a preference for a warmer indoor environment. Simultaneously, 30% of the occupants were not satisfied with the air movement, as drafts were perceived in some rooms. Yet, the reported occupant satisfaction with perceived air quality was at a good level with VAV ventilation.

Furthermore, the function of the screen was not perceived to be satisfactory by more than half of occupants, where many occupants preferred more daylight and felt that the screen blocked daylight and outside views, and it cannot be operated manually. Thus, 30% of the occupants felt dissatisfied with daylight levels, even though the amount of light was sufficient according to the measured values (Jin *et al*., 2020). Likewise, occupants were not satisfied with the level of individual control of the indoor climate, such as room temperature, mechanical ventilation, and natural light.

These gaps may be because of design decisions and/or control strategies in the operation phase. For example, the airflow rate, which varies with presence, might be set too high and it cannot be controlled by occupants. Alternatively (or additionally), the setup value of solar radiation for daylight might be too low. The color and transparency of the screen material might be another influential factor.

When considering energy conservation in a building renovation, occupant demand and preference need to be addressed. In the A-building, the exterior screen was energy efficient; however, it reduced daylight and outside views. A better solution is needed to balance energy savings and visual comfort. Likewise, occupants' control of the indoor climate must be considered. With the possibility of ventilation and screen control, for example, occupant satisfaction might be improved.

11.8.6 Concluding Remarks

The A-building is an example of a building renovation that was designed to perform well in terms of indoor environment and low energy consumption. Energy-efficient solutions were applied, including high-performance windows, low U-value exterior walls, exterior screens, and a VAV with heat recovery. Yet, there were notable discrepancies between the A-building's designed and actual performance during operation and its occupants' perceptions of indoor comfort. Occupants' insights, collected through an extensive POE using the SSO User Insight Tool, included occupant satisfaction with IEQ, indoor climate control, and occupant behavior. The study found several instances of occupant dissatisfaction with the indoor environment that reinforce the need for more occupant-centric building design processes.

For example, in the A-building, opening windows happened frequently compared to other interventions, such as interactions with heaters and curtains. Enabling occupants to control the indoor climate, particularly the

temperature and the shading situation, may have significantly increased occupant satisfaction. However, these aspects were not sufficiently considered in the building design, nor are they considered in building regulations or building certification schemes. Early-phase design and building control strategies need to better consider occupants' indoor comfort and preferences alongside energy consumption. Conducting occupant surveys can increase stakeholders' awareness of occupant-centric building design and performance. A pre-intervention survey or POE should be conducted for building renovations as well as new building designs, and the collected information and feedback should be integrated into the building planning and design process.

The next step of this case study is to provide recommendations to the A-building owner and facility managers to further improve occupants' satisfaction regarding IEQ. A further point to make is for the office design of the future, we need to better understand not only the factors to negatively affect occupants' comfort and well-being but also the positive factors, for example, salutogenic design (health-promoting potential), drawing on sense of coherence (SOC) theory (Antonovsky, 1987; Eriksson and Lindström, 2006; Allen *et al*., 2019; Forooraghi *et al*., 2021).

11.9 Closing Remarks

In this chapter, we presented occupant-centric analyses of seven case study buildings to demonstrate the benefits of recognizing occupants and their behavior during the design process and throughout the building life cycle. The buildings were of different types and located in different countries and climates, and in different phases of the building life cycle. Likewise, the studies represented different design and analysis approaches including participatory design, parametric and sensitivity analysis, optimization, operational data analysis, and statistical modeling. Considering the lessons learned from each case study, we can conclude the chapter with the following:

- Undertaking occupant-centric design requires information to be shared effectively among design stakeholders. The traditional linear design process is problematic, as it can lead to discrepancies in design assumptions and, consequently, to suboptimal or overlooked design solutions.
- Assumptions about occupants can be influential when performing design parametric analysis. Different occupant-related assumption can lead to a different savings potential of ECM/DP. Additionally, occupant assumptions can influence the outcomes of the design optimization process.
- Occupant assumptions can also influence the comfort performance of buildings, as current comfort metrics used by practitioners do not consider comfort at the occupant and zone levels. New occupant-centric comfort metrics should be developed and used instead.
- Occupant participation in the design process (i.e., co-design) is beneficial in achieving a more accurate representation of occupants' presence

and activities. Co-design can reduce performance gaps and improve energy efficiency.
- Increasing occupants' consciousness of their energy-intensive behaviors is an important factor in achieving energy efficiency.
- Collecting occupant-related data on individualized occupant dynamics post-occupancy can be helpful for improving spatial design (i.e., optimized layouts) and energy efficiency. More broadly, such data collection is useful to understand performance gaps between predictions during design and actual performance.
- The analyses highlighted the importance of post-occupancy data collection through occupant surveys, sensing infrastructure, and interviews with building design stakeholders.

Note

Figures 11.50, 11.51, 11.52, 11.53, 11.54, 11.55, 11.56, and Tables 11.12, 11.13 reprinted from Energy and Buildings, Vol 238, Andrew Sonta, Thomas R. Dougherty, and Rishee K. Jain, Data-driven optimization of building layouts for energy efficiency, Copyright (2021), with permission from Elsevier.

References

ABUD Mérnökiroda Kft (2020), *Zugló E-CoHousing*, ABUD Mérnökiroda Kft, Budapest.

Abuimara T, O'Brien W, and Gunay B (2021), Quantifying the impact of occupants' spatial distributions on office buildings energy and comfort performance, *Energy and Buildings*, 233:110695, URL https://doi.org/10.1016/j.enbuild.2020.110695.

Abushakra B, Haberl JS, and Claridge DE (2004), Overview of existing literature on diversity factors and schedules for energy and cooling load calculations, in *2004 Winter Meeting – Technical and Symposium Papers, American Society of Heating, Refrigerating and Air-Conditioning Engineers*, 169–181, Anaheim, California.

Ahmad MW, Mourshed M, and Rezgui Y (2017), Trees vs neurons: comparison between random forest and ANN for high-resolution prediction of building energy consumption, *Energy and Buildings*, 147:77–89, URL https://doi.org/10.1016/j.enbuild.2017.04.038.

Allen C, Boddy J, and Kendall E (2019), An experiential learning theory of high level wellness: Australian salutogenic research. *Health Promotion International*, 34(5):1045–1054.

Antonovsky A (1987), *Unraveling the Mystery of Health: How People Manage Stress and Stay Well*, Jossey-Bass, San Francisco, CA.

Arditi D and Gunaydin HM (2002), Factors that affect process quality in the life cycle of building projects, *Journal of Construction Engineering and Management*, 124(3):194–203, URL https://doi.org/10.1061/(asce)0733-9364(1998)124:3(194).

Armstrong MM, Swinton MC, Ribberink H, Beausoleil-Morrison I, and Millette J (2009), Synthetically derived profiles for representing occupant-driven electric loads in Canadian housing, *Journal of Building Performance Simulation*, 2(1):15–30, URL https://doi.org/10.1080/19401490802706653.

ASHRAE (2017), *ANSI/ASHRAE Standard 55-2013: Thermal Environmental Conditions for Human Occupancy*, ASHRAE, Atlanta, GA.

ASHRAE (2019), *ANSI/ASHRAE/IES 90.1-2019: Energy Standard for Buildings Except Low-Rise Residential Buildings*, ASHRAE, Atlanta, GA.

Australian Passive House Association (2021), *PHPP software*, URL https://passivehouseaustralia.org/APHA/APHA/Shop/Software.aspx.

BBR (2017), *BFS 2017:6-BEN 2 the Swedish National Board of Housing, Building and Planning's Regulations on Amendments to the Regulations and General Advice (2016:12) on the determination of the building's energy use during normal use and a normal year*, URL https://www.boverket.se/contentassets/f3bf0ac62dc148438a007c987aeaea21/konsekvensutredning-bfs-2017-6-ben-2.pdf.

BCE (2012), *Méthode de Calcul Th-BCE 2012*, URL https://ingenierie.senova.fr/telechargements/Annexe-arrete-methode-de-calcul-TH-B-C-E-2012-CSTB.pdf.

CEN (2007), *Indoor Environmental Input Parameters for Design and Assessment of Energy Performance of Buildings addressing Indoor Air Quality, Thermal Environment, Lighting and Acoustics*, European Committee for Standardization, Brussels.

Chartered Institution of Building Services Engineers (2013), *The Limits of Thermal Comfort: Avoiding Overheating in European Buildings*, URL internal-pdf://70.171.143.68/CIBSE TM52 2013 The Limits of Thermal Comfort-.pdf. https://www.cibse.org/knowledge-research/knowledge-portal/tm52-the-limits-of-thermal-comfort-avoiding-overheating-in-european-buildings.

Chartrand TL and Bargh JA (1999), The Chameleon effect: the perception-behavior link and social interaction, *Journal of Personality and Social Psychology*, 76(6):893–910, URL https://doi.org/10.1037/0022-3514.76.6.893.

Cordero AC, Rahe U, Wallbaum H, Jin Q, and Forooraghi M (2017), Smart and sustainable offices (SSO): showcasing a holistic approach to realise the next generation offices, *Informes de La Construcción*, 69(548):e221.

Derbas G and Voss K (2021), Data-driven occupant-centric rules of automated shade adjustments: Luxembourg case study, *Journal of Physics: Conference Series*, 2042:12126, IOP Publishing.

Djunaedy E, Van den Wymelenberg K, Acker B, and Thimmana H (2011), Oversizing of HVAC system: signatures and penalties, *Energy and Buildings*, 43:468–475.

Ekici BB and Aksoy UT (2009), Prediction of building energy consumption by using artificial neural networks, *Advances in Engineering Software*, 40(5):356–362, URL https://doi.org/10.1016/j.advengsoft.2008.05.003.

Eriksson M and Lindström B (2006), Antonovsky's sense of coherence scale and the relation with health: a systematic review, *Journal of Epidemiology & Community Health*, 60(5):376–381.

Feist W (2012), *PHPP – Passive house planning package*, Passive House Institute, Darmstadt, Germany.

Fletcher MJ, Johnston DK, Glew DW, and Parker JM (2017), An empirical evaluation of temporal overheating in an assisted living Passivhaus dwelling in the UK, *Building and Environment*, 121:106–118, URL https://doi.org/10.1016/j.buildenv.2017.05.024.

Forooraghi M, Miedema E, Ryd N, and Wallbaum H (2021), How does office design support employees' health? A case study on the relationships among employees' perceptions of the office environment, their sense of coherence and office design, *International Journal of Environmental Research and Public Health*, 18(23):12779.

Haldi F and Robinson D (2010a), Adaptive actions on shading devices in response to local visual stimuli, no. October 2014:37–41, URL https://doi.org/10.1080/19401490903580759.

Haldi F and Robinson D (2010b), Adaptive actions on shading devices in response to local visual stimuli, *Journal of Building Performance Simulation*, 3(2):135–153, URL https://doi.org/10.1080/19401490903580759.

Hendron R, Burch J, and Barker G (2010), Tool for generating realistic residential hot water event schedules, *National Renewable Energy Laboratory, Golden, CO, Paper No. NREL/CP-550-47685*, October, URL http://energy.gov/sites/prod/files/2014/01/f6/47685.pdf.

Inoue T, Kawase T, Ibamoto T, Takakusa S, and Matsuo Y (1988), The development of an optimal control system for window shading devices based on investigations in office buildings, *ASHRAE Transactions*, 94:1034–1049.

International Organization for Standardization (2006), Ergonomics of the thermal environment – analytical determination and interpretation of thermal comfort using calculation of the PMV and PPD indices and local thermal comfort criteria, ISO Standard no. 7730:2006, issued 2006.

Jain RK, Smith KM, Culligan PJ, and Taylor JE (2014), Forecasting energy consumption of multi-family residential buildings using support vector regression: investigating the impact of temporal and spatial monitoring granularity on performance accuracy, *Applied Energy*, 123(June):168–178, URL https://doi.org/10.1016/j.apenergy.2014.02.057.

Jin Q, Wallbaum H, and Rahe U (2020), The influence of multi-disciplinary factors of indoor environment and workspace design on employees' comfort, health and work performance, in *The Second Transdisciplinary Workplace Research Conference*, Frankfurt, Germany.

Jin Q, Wallbaum H, Rahe U, and Forooraghi M (2019), SSO user insight toolbox for employees' health, well-being and productivity, *REHVA Journal*, 6:58–63.

Leaman A and Bordass B (2001), Assessing building performance in use 4: the probe occupant surveys and their implications, *Building Research & Information*, 29(2):129–143.

Lee J-Y, Wargocki P, Chan Y-H, Chen L, and Tham K-W (2019), Indoor environmental quality, occupant satisfaction, and acute building-related health symptoms in Green Mark-certified compared with non-certified office buildings, *Indoor Air*, 29(1):112–129.

Lichtmess M (2018), Neues Bürogebäude Energiekonzept Und Nachhaltigkeit Objektbericht, *Revue Technique Luxembourgeoise, Series 016* https://www.golav.lu/uploads/editor/files/HS_2018_02_-web_Copie.pdf.

Mahdavi A, Mohammadi A, Kabir E, and Lambeva L (2008), 'Occupants' operation of lighting and shading systems in office buildings, *Journal of Building Performance Simulation*, 1(1):57–65, URL https://doi.org/10.1080/19401490801906502.

Meerbeek B, te Kulve M, Gritti T, Aarts M, van Loenen E, and Aarts E (2014), Building automation and perceived control: a field study on motorized exterior blinds in Dutch offices, *Building and Environment*, 79(September):66–77, URL https://doi.org/10.1016/j.buildenv.2014.04.023.

Nabil A and Mardaljevic J (2005), Useful daylight illuminance: a new paradigm for assessing daylight in buildings, *Lighting Research & Technology*, 37(1):41–57.

National Resources Canada (2011), *Survey of house energy use – detailed statistical report*, Ottawa.

O'Brien W, and Gunay HB (2015), Mitigating office performance uncertainty of occupant use of window blinds and lighting using robust design, *Building Simulation*, 8:621–636, Tsinghua University Press, URL https://doi.org/10.1007/s12273-015-0239-2.

O'Brien W, Kapsis K, and Athienitis AK (2013), Manually-operated window shade patterns in of Fi Ce buildings : a critical review, *Building and Environment*, 60:319–338, URL https://doi.org/10.1016/j.buildenv.2012.10.003.

Oliveira S and Marco E (2018), Architects' approaches to early stage design energy modelling-an organisational perspective, in *4th Building Simulation and Optimization Conference*, 511–518, Cambridge, UK.

Passive House Institute (2015), *Passive House Planning Package (PHPP) Version 9 (2015): The Energy Balance and Design Tool for Efficient Buildings and Retrofits*, Passive House Institute, Darmstadt, Germany.

Reinhart C and Voss K (2003), Monitoring manual control of electric lighting and blinds, *Lighting Research & Technology*, 35(3):243–258, URL https://doi.org/10.1191/1365782803li064oa.

Richardson I, Thomson M, and Infield D (2008), A high-resolution domestic building occupancy model for energy demand simulations, *Energy and Buildings*, 40 (8):1560–1566, URL https://doi.org/10.1016/j.enbuild.2008.02.006.

Richardson I, Thomson M, Infield D, and Clifford C (2010), Domestic electricity use: a high-resolution energy demand model, *Energy and Buildings*, 42(10):1878–1887, URL https://doi.org/10.1016/j.enbuild.2010.05.023.

Rouleau J and Gosselin L (2018), Assessing the risk of overheating in high-performance social housing buildings with the use of regression analysis, in *ASHRAE 2018 Annual Conference*, ASHRAE, Houston TX.

Rouleau J and Gosselin L (2020), Probabilistic window opening model considering occupant behavior diversity: a data-driven case study of Canadian residential buildings, *Energy*, 195:116981.

Rouleau J, Gosselin L, and Blanchet P (2018), Understanding energy consumption in high-performance social housing buildings: a case study from Canada, *Energy*, 145(April):677–690, URL https://doi.org/10.1016/j.energy.2017.12.107.

Rouleau J, Gosselin L, and Blanchet P (2019), Robustness of energy consumption and comfort in high-performance residential building with respect to occupant behavior, *Energy*, 188(December), URL https://doi.org/10.1016/j.energy.2019.115978.

Rouleau J, Ramallo-González AP, Gosselin L, Blanchet P, and Natarajan S (2019), A unified probabilistic model for predicting occupancy, domestic hot water use and electricity use in residential buildings, *Energy and Buildings*, 202(April):109375, URL https://doi.org/10.1016/j.enbuild.2019.109375.

Sonta AJ, Simmons PE, and Jain RK (2018), Understanding building occupant activities at scale: an integrated knowledge-based and data-driven approach, *Advanced Engineering Informatics* 37(April):1–13, URL https://doi.org/10.1016/j.aei.2018.04.009.

Sonta A and Jain RK (2020), Learning socio-organizational network structure in buildings with ambient sensing data, *Data-Centric Engineering*, 1(October):e9, URL https://doi.org/10.1017/dce.2020.9.

Tabatabaei S, Masoud S, Gaterell M, Montazami A, and Ahmed A (2015), Overheating investigation in UK social housing flats built to the Passivhaus standard, *Building and Environment*, 92:222–235, URL https://doi.org/10.1016/j.buildenv.2015.03.030.

UK NCM (2018), *UK NCM Database*, URL https://www.uk-ncm.org.uk/filelibrary/NCM_Databases_v5.6.a.zip.

Wang Z, Wang Y, Zeng R, Srinivasan RS, and Ahrentzen S (2018), Random forest based hourly building energy prediction, *Energy and Buildings*, URL https://doi.org/10.1016/j.enbuild.2018.04.008.

Whitmore J and Pineau P-O (2021), *État de l'énergie Au Québec – Édition 2021,* Chaire de gestion du secteur de l'énergie, HEC Montréal.

Yang Z, Ghahramani A, and Becerik-Gerber B (2016), Building occupancy diversity and HVAC (heating, ventilation, and air conditioning) system energy efficiency, *Energy*, 109(August):641–649, URL https://doi.org/10.1016/j.energy.2016.04.099.

Zagreus L, Huizenga C, Arens E, and Lehrer D (2004), Listening to the occupants: a web-based indoor environmental quality survey, *Indoor Air*, 14:65–74.